NASA TECHNICAL NOTE

NASA TN D-8512

NASA TN D-8512

THEORETICAL AND EXPERIMENTAL ANALYSIS OF LONGITUDINAL AND LATERAL AERODYNAMIC CHARACTERISTICS OF SKEWED WINGS AT SUBSONIC SPEEDS TO HIGH ANGLES OF ATTACK

James M. Luckring

Langley Research Center

Hampton, Va. 23665

NATIONAL AERONAUTICS AND SPACE ADMINISTRATION • WASHINGTON, D. C. • DECEMBER 1977

98

1. Report No.
NASA TN D-8512

2. Government Accession No.

3. Recipient's Catalog No.

4. Title and Subtitle
THEORETICAL AND EXPERIMENTAL ANALYSIS OF LONGITUDINAL AND LATERAL AERODYNAMIC CHARACTERISTICS OF SKEWED WINGS AT SUBSONIC SPEEDS TO HIGH ANGLES OF ATTACK

5. Report Date
December 1977

6. Performing Organization Code

7. Author(s)
James M. Luckring

8. Performing Organization Report No.
L-11230

10. Work Unit No.
505-06-14-01

9. Performing Organization Name and Address
NASA Langley Research Center
Hampton, VA 23665

11. Contract or Grant No.

13. Type of Report and Period Covered
Technical Note

12. Sponsoring Agency Name and Address
National Aeronautics and Space Administration
Washington, DC 20546

14. Sponsoring Agency Code

15. Supplementary Notes

16. Abstract
This paper presents a theoretical and experimental analysis of the aerodynamic characteristics of low-aspect-ratio skewed (oblique) wings having separation-induced vortex flows along leading and side edges. The purposes of this investigation were to determine the effects of sweep and aspect ratio on the longitudinal and lateral-directional aerodynamic characteristics of these wings and to compare experimental results with asymmetric, separated, vortex-flow theory. The theoretical analysis used the vortex-lattice method for estimating attached-flow aerodynamic characteristics and the leading-edge suction analogy of Polhamus for estimating separation induced vortex-flow effects. The experimental results were obtained in the Langley high-speed 7- by 10-foot tunnel at a low-subsonic Mach number.

17. Key Words (Suggested by Author(s))
Longitudinal aerodynamic characteristics
Lateral aerodynamic characteristics
Skewed (oblique) wings
Subsonic speeds
High angles of attack
Vortex lift

18. Distribution Statement
Unclassified - Unlimited

Subject Category 02

19. Security Classif. (of this report)	20. Security Classif. (of this page)	21. No. of Pages	22. Price*
Unclassified	Unclassified	96	$5.00

* For sale by the National Technical Information Service, Springfield, Virginia 22161

THEORETICAL AND EXPERIMENTAL ANALYSIS OF LONGITUDINAL AND LATERAL AERODYNAMIC CHARACTERISTICS OF SKEWED WINGS AT SUBSONIC SPEEDS TO HIGH ANGLES OF ATTACK

James M. Luckring
Langley Research Center

SUMMARY

This paper presents a theoretical and experimental analysis of the aerodynamic characteristics of low-aspect-ratio skewed (oblique) wings having separation-induced vortex flows along leading and side edges. The purposes of this investigation were to determine the effects of sweep and aspect ratio on the longitudinal and lateral-directional aerodynamic characteristics of these wings and to compare experimental results with asymmetric, separated, vortex-flow theory. The theoretical analysis used the vortex-lattice method for estimating attached-flow aerodynamic characteristics and the leading-edge suction analogy of Polhamus for estimating separation induced vortex-flow effects. The experimental results were obtained in the Langley high-speed 7- by 10-foot tunnel at a low-subsonic Mach number.

In general, the effects of sweep on the longitudinal aerodynamic characteristics of the skewed wings were small. The effects of aspect ratio were consistent with simple wing theory; that is, an increase in aspect ratio increased lift-curve slope and decreased drag due to lift. The effects of sweep and aspect ratio on the lateral-directional aerodynamic characteristics were more significantly pronounced. When either sweep or aspect ratio was increased, the magnitude of the lateral-directional coefficients increased.

Total lift and drag were well estimated by the theoretical method employed. Pitching moments and, to a lesser degree, rolling moments were also well estimated as long as substantial amounts of vortex growth and subsequent inboard movement of the vortex core with increasing angle of attack were not encountered. This growth of the vortex and the subsequent inboard movement of the vortex core were documented in a series of oil-flow photographs and account for discrepancies between theoretical and experimental moments.

INTRODUCTION

The oblique-wing concept has undergone considerable study in recent years as a potential means of drag reduction (refs. 1 and 2). Although this concept was originally applied to high-aspect-ratio configurations such as transonic transport airplanes, recent application studies (refs. 3 and 4) indicate that there is an interest in low-aspect-ratio skewed (oblique) wing configurations which may be applied to advanced fighter-aircraft concepts. These studies dealt with configurations designed to exhibit attached-flow characteristics up

to stall. In addition, the theoretical effort emphasized the analysis of low-angle-of-attack aerodynamic characteristics by attached-flow linear theory. However, the flow over skewed wings at maneuver conditions (as is true for swept wings) can contain separation-induced vortex flows which, because of their asymmetry, can significantly affect the aerodynamic characteristics of the skewed wing in ways not encountered by conventional (symmetric) swept wings. Very little information is available on this type of asymmetric flow.

The present investigation was conducted to determine and compare theoretical and experimental, nonlinear aerodynamic characteristics, up to high angles of attack, of several low-aspect-ratio skewed wings having separation-induced vortex flows along their leading and side edges. The configurations were untapered planforms (parallelograms) with side edges aligned in the free-stream direction and with no twist or camber. The geometric parameters altered in this study were leading-edge sweep and aspect ratio. The theoretical investigation was performed by using a computer program developed, as part of this study, for the analysis of asymmetric flow conditions including both fully attached flows and separation-induced vortex flows. This method, briefly described in reference 5, is an extension of the vortex-lattice method for estimating subsonic aerodynamic characteristics of complex planforms (refs. 6 and 7) and applies the leading-edge suction analogy of Polhamus (refs. 8 to 10) for the analysis of the separation-induced vortex-flow effects. The wings were tested in the Langley high-speed 7- by 10-foot tunnel at a low-subsonic Mach number of 0.12, which corresponded to a Reynolds number of 2.46×10^6/m (0.75×10^6/ft). Angles of attack were varied from approximately -4° to 24°, and angles of sideslip were varied from approximately -10° to 10°.

SYMBOLS

Physical quantities are presented in the International System of Units (SI) with the equivalent values in U.S. Customary Units given parenthetically. The measurements and calculations were made in U.S. Customary Units. All data are referenced to the stability axis system. In addition, the tabulated values of the rolling-moment and yawing-moment coefficients are referenced to the body axis system. The comparisons of theoretical with experimental rolling-moment coefficients are also referenced to the body axis system. The quarter-chord point measured at the wing center line was designated as the moment reference point.

A	aspect ratio, b^2/S
b	wing span, cm (in.)
C_D	drag coefficient, $\mathrm{Drag}/q_\infty S$
$C_{D,o}$	experimental drag coefficient at zero lift
C_L	lift coefficient, $\mathrm{Lift}/q_\infty S$
$C_{L,o}$	lift coefficient at zero angle of attack

C_l	rolling-moment coefficient, Rolling moment/$q_\infty Sb$
C_m	pitching-moment coefficient, Pitching moment/$q_\infty S\bar{c}$
$C_{m,o}$	pitching-moment coefficient at zero lift
C_N	normal-force coefficient, Normal force/$q_\infty S$
C_n	yawing-moment coefficient, Yawing moment/$q_\infty Sb$
$C_{S,le}$	leading-edge suction-force coefficient, $K_{v,le}\lvert\sin\alpha\rvert \sin\alpha$
$C_{T,le}$	leading-edge thrust-force coefficient, $C_{S,le} \cos\Lambda$
C_Y	side-force coefficient, Side force/$q_\infty S$
$C_{Y,i}$	elemental side-force coefficient
$C_{Y,le}$	leading-edge side-force coefficient, $C_{S,le} \sin\Lambda$
$\Delta C_{L,v}$	increment of C_L associated with augmented-vortex lift
$\Delta C_{Y,se}$	contribution to side-edge side-force coefficient from elemental spanwise strip
c	streamwise chord, cm (in.)
$\bar{c}$	reference chord, cm (in.)
$\tilde{c}$	characteristic length used in computing $K_{v,\overline{se}}$
c_l	section lift coefficient
c_s	section suction-force coefficient, Section suction force/$q_\infty c$
c_t	section thrust-force coefficient, Section thrust force/$q_\infty c$
c_y	section side-force coefficient, Section side force/$q_\infty c$
K_p	$= \partial(C_{N,p})/\partial(\sin\alpha \cos\alpha)$
$K_{v,le}$	$= \partial(\text{Leading-edge suction force}/q_\infty S)\big/\partial(\sin^2\alpha)$
$K_{v,se}$	$= \partial(\text{Tip suction force}/q_\infty S)\big/\partial(\sin^2\alpha)$
$K_{v,\overline{se}}$	augmented-vortex lift factor, $(K_{v,le}/b \sec\Lambda)\tilde{c}$
$K_{v,tot}$	$= K_{v,le} + K_{v,se}$
L.E.	leading edge
M_∞	free-stream Mach number

q_∞ free-stream dynamic pressure, Pa (lbf/ft^2)

R Reynolds number

S reference area, m^2 (ft^2)

s horseshoe-vortex semiwidth

U_∞ free-stream velocity, m/sec (ft/sec)

x distance along wing center line, positive downstream of leading edge, cm (in.)

y spanwise distance, m (ft)

α angle of attack, deg

β angle of sideslip, deg

ζ nondimensional spanwise distance (see fig. 3)

η $= 2y/b$

Λ leading-edge sweep angle, deg

λ taper ratio

Subscripts:

av average

c centroid

le leading edge

p potential

r root

se side edge

tot total

v vortex

vle vortex effect at leading edge

vse vortex effect at side edge

$v\overline{se}$ augmented-vortex effect

β partial derivative of quantity subscripted with respect to β, $\partial(\;)/\partial\beta$, per degree

Superscript:

* parameter is computed for one semispan only

THEORETICAL ANALYSIS

Method

A technique has been documented (refs. 6 and 7) for the analysis of both fully attached and separation-induced vortex-flow situations for symmetric configurations having symmetric loads. With this method, the attached-potential-flow solution is computed using the vortex-lattice method while the separation-induced vortex-flow solution is computed using the suction analogy. A computer program was developed as part of this study to compute potential-flow solutions about arbitrary, thin, asymmetric configurations by use of the vortex-lattice method. (The capabilities of this program are described briefly in ref. 5.) Once the asymmetric potential-flow solution had been determined, the suction analogy was used to compute the vortex-flow solution. This resulted in the following formulation for theoretical, force and moment coefficients:

$$C_{L,tot}^{*} = \overbrace{K_p^{*} \sin\alpha \cos^2\alpha}^{C_{L,p}^{*}} + \overbrace{K_{v,le}^{*}|\sin\alpha| \sin\alpha \cos\alpha}^{C_{L,vle}^{*}}$$

$$+ \overbrace{K_{v,se}^{*}|\sin\alpha| \sin\alpha \cos\alpha}^{C_{L,vse}^{*}} \qquad (1a)$$

or

$$C_{L,tot}^{*} = K_p^{*} \sin\alpha \cos^2\alpha + K_{v,tot}^{*}|\sin\alpha| \sin\alpha \cos\alpha \qquad (1b)$$

$$C_D^{*} = C_{D,o} + C_L^{*} \tan\alpha = C_{D,o} + K_p^{*} \sin^2\alpha \cos\alpha + K_{v,tot}^{*} \sin^3\alpha \qquad (2)$$

$$C_{m,tot}^{*} = \overbrace{K_p^{*} \sin\alpha \cos\alpha \frac{x_{c,p}^{*}}{\bar{c}}}^{C_{m,p}^{*}} + \overbrace{K_{v,le}^{*}|\sin\alpha| \sin\alpha \frac{x_{c,le}^{*}}{\bar{c}}}^{C_{m,vle}^{*}}$$

$$+ \overbrace{K_{v,se}^{*}|\sin\alpha| \sin\alpha \frac{x_{c,se}^{*}}{\bar{c}}}^{C_{m,vse}^{*}} \qquad (3)$$

$$C_{l,tot}^{*} = \overbrace{K_p^{*} \sin\alpha \cos\alpha \frac{y_{c,p}^{*}}{b}}^{C_{l,p}^{*}} + \overbrace{K_{v,le}^{*}|\sin\alpha| \sin\alpha \frac{y_{c,le}^{*}}{b}}^{C_{l,vle}^{*}}$$

$$+ \overbrace{K_{v,se}^{*}|\sin\alpha| \sin\alpha \frac{y_{c,se}^{*}}{b}}^{C_{l,vse}^{*}} \qquad (4)$$

In equations (1) to (4), the asterisks indicate that the particular parameter was computed for each semispan individually (in the presence of the other semispan). Later in this section, this method for computing the loads will be shown to be useful for making comparisons of the loads on a swept wing with those on a skewed wing. The x_c and y_c terms in these equations represent the chordwise and spanwise distances, respectively, between the appropriate centroid and the reference point (defined as the quarter-chord point of the mean geometric chord). Since the suction analogy does not provide a prediction of the rate of inboard movement of the center of vortex lift with increasing angle of attack, the reattached vortex loads were assumed to act at the centroid of the corresponding edge-force distribution as has been done in previous investigations (ref. 11). Hence, no angle-of-attack effects on the location of the vortex loads were represented. This assumption is valid as long as the vortex core remains in the vicinity of the edge from which the corresponding vortex sheet is being generated.

In addition to the edge-vortex factors $K_{v,le}$ and $K_{v,se}$, the augmented-vortex lift factor $K_{v,\overline{se}}$ was included in the formulation to account for the effect of the leading-edge vortex which persists over the aft portion of the wing (ref. 12). Figure 1 illustrates the concept of augmented-vortex lift applied to a skewed wing (ref. 5). By applying the method of reference 12 to the skewed wing, the leading-edge-vortex lift factor $K_{v,le}$, developed along the leading-edge length $b \sec \Lambda$, persists over a portion of the wing aft of

the leading edge $\tilde{c}$, herein taken to be the tip chord. This results in the additional vortex lift factor

$$K_{v,\overline{se}} = \left(\frac{K_{v,le}}{b \sec \Lambda}\right)\tilde{c}$$

and the additional vortex lift quantity

$$\Delta C_{L,v} = K_{v,\overline{se}}|\sin \alpha| \sin \alpha \cos \alpha$$

It should be noted that, for a skewed geometry, augmentation occurs only on the tip of the sweptback (downwind) semispan. Recent investigations have demonstrated that the distance over which the vortex persists and, hence, the extent of the augmented effect, is angle-of-attack dependent (ref. 13). This is due to the well established fact that as angle of attack is increased the vortex tends to grow and its core moves inboard, away from the edge where the vortex sheet is being generated. Hence, the distance $\tilde{c}$ which gives rise to the augmented-vortex lift will change as angle of attack is increased. For a skewed planform, $\tilde{c}$ will decrease as angle of attack is increased; however, as with the edge-vortex terms, no angle-of-attack effects on the location of the vortex and, hence, on the extent of $\tilde{c}$, are represented in the present theoretical method. Therefore, the present method should tend to overpredict the augmented-vortex lift at high angles of attack. Since the chordwise centroid of side-edge-vortex lift distribution is generally near the midpoint of the tip chord, the centroid of the augmented-vortex lift term is assumed to be the midpoint of the downstream tip chord. Because the actual center of vortex lift moves inboard as angle of attack is increased, this assumption about the centroidal location of the augmented-vortex lift is expected to result in overpredictions of moments due to augmentation at high angles of attack.

Theoretical Results

The theoretical methods just described were used in calculating the effects of wing sweep and aspect ratio on the magnitudes and centroids of the load quantities K_p, $K_{v,le}$, and $K_{v,se}$ for the skewed wing. Since the augmented-vortex lift term is geometrically related to the leading-edge-vortex term, it is not included in this presentation. The quantities are presented for each planform semispan. Hence, the total lift factor for a skewed wing configuration is the sum of the factor associated with the sweptback (downwind) semispan and the factor associated with the sweptforward (upwind) semispan. Similarly the total lift factor for the swept wing (symmetrical) configuration is twice the value shown.

The effects of sweep angle on the potential lift factor K_p and on the vortex lift factors $K_{v,le}$ and $K_{v,se}$ are presented in figure 2 for the semispans of both a swept wing and a skewed wing, each having an aspect ratio of one. The full span skewed wing is seen to develop slightly less total potential-flow lift, to maintain essentially the same amount of total leading-edge-vortex lift, and to develop substantially less total side-edge-vortex lift than a full span swept wing with the same sweep. For all three lift fac-

tors, the sweptforward semispan becomes unloaded over the range of configurations shown because of the change in the upwash field, as shown later. The reduction in side-edge suction on the sweptforward semispan is also due to the effect of forward sweep on side-edge suction (ref. 5). In the computation of side-edge-vortex lift by the method of reference 11, the portion of the wing inboard of the side edge is assumed to contribute to the side forces acting on the side edge. For sweptback wings, the region of the wing inboard of the leading edge (which might be considered as contributing to a leading-edge side force) and the region of the wing inboard of the side edge are mutually exclusive. Moreover, in the case of sweepback, the leading-edge side force and the side-edge side force are acting in the same direction. However, in the instance of forward sweep such as for a skewed wing as illustrated in the upper left part of figure 3, the leading-edge side force and the side-edge side force on the sweptforward semispan act in opposition to one another across an elemental spanwise strip. A more detailed illustration of the sweptforward semispan is presented in the upper right portion of figure 3. Here the leading-edge and side-edge side forces are seen to oppose one another along a representative elemental spanwise strip; as a result, there is a region of positive elemental side force and a region of negative elemental side force. The distribution of elemental side-force coefficient along the representative spanwise strip is shown in the lower right part of figure 3.

The change of sign of the elemental side force tends to imply that the positive elemental side forces act on the side edge while the negative elemental side forces act on the leading edge. A comparison of the leading-edge side-force coefficient distribution (computed by integrating the negative elemental side-force coefficients on the sweptforward semispan) with the side component of the leading-edge thrust coefficient on the sweptforward semispan is presented in the lower left part of figure 3. The agreement tends to substantiate the implication that the negative elemental side forces are in actuality the side-force components of the leading-edge thrust. The present method takes this force into account by computing the leading-edge thrust and using the secant relationship of the leading-edge sweep to compute the resultant leading-edge suction. Accordingly, only the positive elemental side forces inboard of the side edge are integrated to compute the side-edge force on the sweptforward semispan properly.

The effects of sweep on the spanwise centroids of the potential and leading-edge-vortex lift factors are presented in figure 4 for both the swept and the skewed wings. The nondimensional spanwise centroid of the side-edge-vortex lift term is assumed to be one (at the tip). For the skewed wing configuration, the centroids of the sweptback semispan loadings are further outboard than the centroids of the loadings on the sweptforward semispan. In each case, however, the centroids are further inboard for the skewed wing geometry than for the swept wing geometry.

The effects of aspect ratio on the potential and vortex lift factors are presented in figure 5 for swept and skewed wings, each with 30° of sweep. Over the aspect-ratio range shown, the overall effect of the skewed geometry on the potential and vortex lift factors is similar to that observed for the wings with aspect ratio of one (fig. 2). For the aspect-ratio range shown, a full span skewed wing is seen to develop slightly less total potential-flow lift, to

maintain essentially the same amount of total leading-edge-vortex lift, and to develop substantially less total side-edge-vortex lift than a full span swept wing of the same aspect ratio. The spanwise centroids of these loadings show (fig. 6) that, as in the variation of leading-edge sweep (fig. 4), the spanwise centroids on the sweptback semispan remain further outboard than the spanwise centroids on the sweptforward semispan. These centroids are further inboard, however, than the centroids for the swept wing configuration. Also shown is a reduction in the difference between swept and skewed wing potential centroid at lower aspect ratios and leading-edge-vortex centroids at higher aspect ratios.

The spanwise distributions of the theoretical, potential-span-load and leading-edge section suction coefficients are presented in figure 7 for both a swept and skewed wing ($\Lambda = 45^\circ$, $A = 1.0$). Comparisons of the two configurations illustrate the change in the upwash field as well as the shift of the potential and vortex loads to the sweptback semispan for the skewed wing planform. For a given angle of attack, the complete theoretical span load distribution could be computed from these two figures by applying the appropriate constants and angle-of-attack terms to each distribution of coefficients and then summing the results.

EXPERIMENTAL INVESTIGATION

Description of Models

A total of six, thin, flat wings were tested, each having streamwise tips and symmetrically beveled sharp leading and side edges. The trailing edge of each model was unbeveled. Sharp edges were selected to assure completely developed vortex flows in accordance with the purpose of this study. The trailing edge was left unbeveled because of the manner in which aspect-ratio variation was achieved. The geometric parameters pertinent to these models are given in table I. Figure 8 presents a representative drawing of the wings. Figures 9(a), (b), (c), and (d) are photographs of models I, II, III, and VI, respectively. Models IV and V were obtained by cutting off the aft portion of model I, at the appropriate chordwise station, parallel to the trailing edge to achieve the desired aspect ratio. Model VI consisted of a 113.03-cm- (44.5 in.) long ogive cylinder, 14.605 cm (5.75 in.) in diameter, with a nose fineness ratio of 1.57, mounted symmetrically about model II. (See fig. 8(b).) The nose of the fuselage was situated 48.46 cm (19.08 in.) ahead of the moment reference point. Number 80 transition grit was applied to upper and lower surfaces of each wing approximately 2.54 cm (1 in.) behind the wing leading edge and 2.54 cm (1 in.) inboard of the wing side edges (ref. 14). The typical wind-tunnel installation is shown in figure 10.

Apparatus Tests and Corrections

The models are depicted in figures 8 to 10 and have dimensions given in table I. The tests were conducted in the Langley high-speed 7- by 10-foot tunnel (ref. 15) at $q_\infty = 957.6$ Pa (20 psf), $M_\infty = 0.12$, and $R = 2.46 \times 10^6$/m (0.75×10^6/ft). All models were tested at angles of attack from approximately -4° to 24° at zero sideslip. For the purpose of computing β-derivatives, mod-

els I, II, and III were also tested over the same angle-of-attack range at sideslip angles of -4° and 4°. In addition, model I was tested in sideslip from approximately -10° to 10° at fixed angles of attack of approximately 6° and 12°. This sideslip investigation was conducted to verify the approximation of the β-derivative by a linear finite difference between the runs at $\beta = 4^{\circ}$ and -4°. Finally, oil-flow studies were conducted for models I, II, and III at angles of attack of 5°, 10°, and 15° at zero sideslip.

A bolt-on balance housing was mounted beneath the models. In addition, a dummy balance housing could be mounted on the upper surface symmetrically with respect to the balance housing. The dummy housing was used to cancel the camber caused by the balance housing and hence minimize the interference effects of the housing apparatus on the experimental data. Since it was not clear whether the dummy balance housing mounted on the upper surface of the wing would increase or decrease the interference loads due to vortex interaction with the housing apparatus, all tests, except for the wing-fuselage model, were conducted both with and without the dummy balance housing. Table II provides a matrix of test parameters for each model.

Angles of attack have been corrected for the effects of balance and sting deflections due to loads. All drag data have been corrected to a condition of free-stream static pressure acting on the base of the balance housing, on the base of the dummy housing, in the balance chamber, and, for the wing-fuselage model, on the base of the fuselage. No corrections have been applied for jet-boundary or blockage effects. These effects were small because the models were small compared to the test section, the test section was slotted, and the tests were conducted at low speeds.

Presentation of Experimental Results

Experimental results in the form of tabulated data are presented in tables III and IV. In addition to the tabulated data, results are presented graphically in figures 11 to 25. Unless otherwise stated, the results are for the configuration without the dummy balance housing. An outline of the contents of these figures follows:

	Figure
Flow visualization:	
$\Lambda = 30^{\circ}$	11
$\Lambda = 45^{\circ}$	12
$\Lambda = 55^{\circ}$	13
Sketches of wing-fuselage flow field	14
Longitudinal aerodynamic characteristics:	
Sweep effect	15
Aspect-ratio effect	16
Dummy-balance-housing effect	17
Fuselage effect	18
Lateral-directional aerodynamic characteristics:	
Sweep effect	19

Flow visualization.- Surface oil-flow studies were conducted in order to better understand the nature of the asymmetric vortex flows. The effects of angle of attack are shown for models I ($\Lambda = 30^{\circ}$), II ($\Lambda = 45^{\circ}$), and III ($\Lambda = 55^{\circ}$) (figs. 11, 12, and 13, respectively). The pertinent features of the flows are as follows:

(1) For each model at 5° angle of attack, the vortex was well formed and situated near the edge from which it was being generated.

(2) At the higher angles of attack, the vortex grew and moved substantially inboard from the generating edge. As the sweep angle was increased, the extent which the vortex moved inboard with increasing angle of attack was decreased.

(3) At 15° angle of attack, the vortex on the wing with 30° sweep appears to be very weak. The strength of the vortex increased as the sweep angle was increased. Based on results of previous investigations of symmetrical wings (ref. 16), the bursting point of the vortex is probably well above each wing at 15° angle of attack.

(4) The region of the wing outboard of the leading-edge vortex showed little evidence of attached or reattached flows. The extent of this region was decreased by increasing sweep. This outboard region is where the secondary vortex[1] would be expected to form. This vortex did not produce visible evidence for one of the following reasons: (a) it did not form to any great extent; (b) it did form, but it was too weak to disturb the surface oil; or (c) it did form, but it was raised off the surface of the wing enough to prevent the oil from being visibly disturbed.

(5) The side-edge region of the sweptforward semispan showed visible evidence of the side-edge vortex. The side-edge vortex is not usually seen on a sweptback semispan because of the persistance of the leading-edge vortex along the side edge.

Additional oil-flow studies were conducted at 20° angle of attack. These studies showed little evidence of attached or vortex flow on most of the left

[1]The secondary vortex is a counter-rotating vortex induced by the primary vortex and is situated in the region between the primary vortex and the edge from which the primary vortex is being generated.

semispan for the wing with aspect ratio of 1.0 and sweep of 30°. As the sweep angle was increased, the left semispan showed more evidence of attached and vortex flow at this angle of attack. Sketches of the surface oil-flow patterns for the wing-fuselage configuration at a low and a high angle of attack are presented in figure 14. The primary feature of this configuration was the formation of a separate leading-edge vortex on the sweptback semispan. The apex of this vortex was situated at the juncture of the fuselage and the leading edge. As angle of attack was increased, the leading- and side-edge vortex system on the sweptback (downwind) semispan moved inboard (toward the fuselage), whereas the leading-edge vortex on the sweptforward (upwind) semispan moved outboard (away from the fuselage) toward the side-edge vortex. The skewed wing configurations without the fuselage encountered extensive inboard movement of the vortex system with increasing angle of attack. This movement was decreased for the skewed wing configuration with the fuselage by fixing the apex of the additional leading-edge vortex at the wing-fuselage juncture.

Longitudinal aerodynamic characteristics.- The effects of variation in leading-edge sweep ($\Lambda = 30^\circ$, 45°, and 55°) on the longitudinal aerodynamic characteristics of a skewed wing configuration with aspect ratio of one at Mach 0.12 are presented in figure 15. Variation of the leading-edge sweep angle had little influence on lift or drag. However, for angles of attack less than approximately 16° an increase in sweep resulted in a more nose-down pitching moment, while for angles of attack greater than approximately 16° an increase in sweep resulted in a less nose-down pitching moment. For swept or skewed wings, an increase in leading-edge sweep results in an increase in leading-edge suction. As shown theoretically (figs. 2 to 6), the potential and vortex loads on the sweptback semispan were greater and situated further outboard, hence further aft, than loads on the sweptforward semispan. In addition, an increase in sweep resulted in an aft movement of the leading-edge-vortex centroids (fig. 4). Consequently, an increase in sweep at lower angles of attack not only increased the load on the sweptback semispan relative to the sweptforward semispan but also increased the pitching-moment arm which resulted in the observed trend. At higher angles of attack, the sweptback semispan was beginning to stall which resulted in the less nose-down pitching moment.

The effects of variation in aspect ratio ($A = 1.0$, 1.5, and 2.0) on the longitudinal aerodynamic characteristics of a skewed wing with leading-edge sweep of 30° are presented in figure 16. An increase in aspect ratio caused a slightly negative shift in C_m/C_L up to moderate angles of attack and, consistent with simple wing theory, increased lift-curve slope and decreased drag due to lift. In addition, the angle at which the wing began to stall decreased as aspect ratio was increased. This resulted in a reduced maximum lift coefficient. Small shifts in $C_{L,o}$ and $C_{m,o}$ also occurred as aspect ratio was increased. These shifts were caused by the increased size of the housing apparatus relative to the wing chord which was reduced to achieve the higher aspect ratios.

The effects of the dummy balance housing on the longitudinal aerodynamic characteristics (presented in fig. 17) were found to be generally small. Since the camber attributable to the balance housing was canceled by that of the dummy balance housing, the measured pitching moment at zero lift and the lift at zero angle of attack more closely approximated the expected values of zero.

The effects of the cylindrical fuselage on the longitudinal aerodynamic characteristics are presented in figure 18. In this figure, a comparison is made between the wing-fuselage model and the wing-alone model, both with and without the dummy balance housing. In general, the fuselage had little influence on the longitudinal aerodynamic characteristics. The influence of the fuselage was comparable in magnitude to the influence of the dummy balance housing.

Lateral-directional aerodynamic characteristics.- Because of the asymmetric geometry, the skewed wing can develop large rolling- and yawing-moment coefficients at zero sideslip angle and moderate angles of attack. These coefficients become extremely nonlinear at higher angles of attack. For wings designed to promote attached flow, these nonlinearities can be attributed to an asymmetric, spanwise stall, with the sweptback semispan showing the first evidence of separated flow (ref. 3). For wings which exhibit separation-induced vortex flow, these nonlinearities still occur at high angles of attack (shown in fig. 19) and can be attributed to the combination of an asymmetric, spanwise stall and the asymmetric nature of the vortex system.

The skewed wings at low to moderate angles of attack had positive rolling-moment coefficients C_l and negative yawing-moment coefficients C_n due to the increased loads on the sweptback semispan. An increase in sweep at these angles of attack increased the magnitude of the rolling-moment and (to a lesser degree) yawing-moment coefficients but had little effect on the side-force coefficients C_Y up to a moderate angle of attack. The skewed wings at high angles of attack had negative rolling-moment coefficients and positive yawing-moment coefficients, because the loads had shifted to the sweptforward semispan. An increase in sweep caused a negative increment in the side-force coefficient and had little discernible effect on the rolling-moment and yawing-moment coefficients at high angles of attack. At zero angle of attack, these wings had nonzero yawing-moment and side-force coefficients. This was thought to be due to a slight misalignment of the balance housing. However, the main lateral-directional parameter of interest was the rolling moment, and the housing apparatus did not seem to influence this coefficient at zero angle of attack to any great degree.

The effects of changes in aspect ratio on the lateral-directional aerodynamic characteristics are shown in figure 20. An increase in aspect ratio at low to moderate angles of attack increased the rolling-moment and side-force coefficients but had little effect on the yawing-moment coefficient. At higher angles of attack, the rolling- and yawing-moment coefficients changed sign as they had in the study of sweep variation. An increase in aspect ratio at the higher angles of attack caused a negative increment in the rolling-moment coefficient and a positive increment in the yawing-moment and side-force coefficients. In addition, the angle of attack at which the data became highly nonlinear decreased as aspect ratio was increased. This trend was due to the earlier development of stall on the higher-aspect-ratio wings. These wings had nonzero yawing-moment and side-force coefficients at zero angle of attack, probably because of the misaligned balance housing discussed previously.

As expected, the dummy balance housing had little influence on the lateral-directional aerodynamic characteristics at low to moderate angles of

attack, while the effects of interference between the leading-edge vortex and the dummy balance housing were evident at higher angles of attack (fig. 21).

The lateral-directional aerodynamic characteristics of the wing-fuselage configuration are compared (fig. 22) to the lateral-directional aerodynamic characteristics of the $\Lambda = 45^{\circ}$, $A = 1.0$ wing with and without the dummy balance housing. The most notable effects of the fuselage at high angles of attack were to prevent the rolling-moment coefficient from changing sign and to cause large negative yawing-moment and side-force coefficients. As evidenced by additional oil-flow studies, these effects could be attributed to the formation of the separate leading-edge vortex with an apex situated at the juncture of the fuselage and the leading edge of the sweptback semispan (fig. 14). The rolling-moment characteristics of the wing fuselage were linearized at high angles of attack because, due to the fixed location of the apex of the additional leading-edge vortex, the extensive inboard movement of the vortex system with increasing angle of attack encountered by the models with no fuselage was substantially reduced for the model with the fuselage. The large, negative, yawing-moment and side-force coefficients can be attributed to the manner in which the left and right leading-edge vortices move with increasing angle of attack as well as to the ensuing stall. The leading- and side-edge vortices on the sweptback (downwind) semispan moved inboard from their respective edges toward the wing-fuselage juncture as angle of attack was increased. At the same time, the leading-edge vortex on the sweptforward (upwind) semispan moved outboard from a position near the leading edge, where it impinges upon the fuselage, to a position near the side edge, where it had little interference with the fuselage. The wing-fuselage configuration at high angles of attack showed visible evidence of stall outboard of each vortex, in the vicinity of the wing tip on the sweptback semispan and in the vicinity of the fuselage on the sweptforward semispan. The asymmetric stall, as well as the relative locations of the leading-edge vortices with respect to the fuselage, tends to account for the observed trends in the yawing-moment and side-force coefficients. It should be noted that, at zero angle of attack and zero sideslip angle, the yawing-moment and side-force coefficients for the wing-fuselage configuration were approximately equal to zero, as expected. Since the fuselage completely enclosed the housing apparatus, these results tend to substantiate the assumption that the nonzero values of yawing-moment and side-force coefficients for the other configurations at zero angle of attack and zero sideslip angle were caused by a slight misalignment of the housing apparatus.

The effects of sideslip angle β on rolling-moment, yawing-moment, and side-force coefficients for the $A = 1.0$, $\Lambda = 30^{\circ}$ skewed wing are shown (fig. 23) for angles of attack of approximately 6° and 12°, both with and without the dummy balance housing. The dummy balance housing is seen to have little effect on the lateral-directional coefficients at the lower angle of attack. At the higher angle of attack, the dummy balance housing has a more pronounced influence on the level of the lateral-directional coefficients and a slight influence on the slopes of the data at $\beta = 0^{\circ}$. However, the data for both angles of attack exhibit an approximately linear relationship with sideslip angle in the vicinity of $\beta = 0^{\circ}$. This linear relationship validates the method which approximates the partial derivative of the lateral-directional coefficient by finite difference using the runs having $\beta = 4^{\circ}$ and -4°.

The effects of leading-edge sweep variation on the lateral-directional stability derivatives are presented in figure 24. An increase in sweep decreased the magnitude of C_{l_β} and increased the magnitude of C_{n_β}, although the level of C_{n_β} for these wings is very low relative to conventional configurations. The more highly swept wings showed a strong unstable break in C_{l_β} at approximately 12°. All three configurations were very stable directionally throughout the angle-of-attack range investigated. The sweep change had little effect of level of C_{Y_β}.

The effects of the dummy balance housing on the lateral-directional stability derivatives are presented in figure 25. In general, there was little effect up to an angle of attack of 12°. Above this angle, the interference effects were significant and resulted in more nonlinear characteristics which became increasingly destabilizing as leading-edge sweep angle was increased.

COMPARISONS BETWEEN THEORY AND EXPERIMENT

A theoretical analysis of the lift, drag, pitching moment, and rolling moment has been performed by use of the technique presented in the theoretical method section of this paper. A lattice of 6 chordwise and 40 spanwise singularities was used for this analysis. The data presented in this comparison are for the configurations with the dummy balance housing.

A comparison of theoretical and experimental lift, drag, and pitching moments is presented in figures 26 and 27. The very large effects of the separation-induced vortex flow can be seen by comparison of the experimental results with the attached-flow theory. Application of the suction analogy provides reasonable predictions of the vortex lift contributions. For example, the lift and drag were well predicted up to a C_L of approximately 0.8 when all the vortex lift terms, including the augmented term, were applied. Pitching moments were also well predicted by including the augmented term for all aspect ratios at $\Lambda = 30°$; however, C_m for the more highly swept wings was better predicted without the augmented term. Hence, application of the augmented-vortex lift concept for the prediction of pitching moments appears to be more sensitive to changes in sweep than to changes in aspect ratio. The overpredictions of the pitching-moment coefficient at high angles of attack emphasize the significance of the reduction in the augmented-vortex lift effect for these wings due to the reduction of $\tilde{c}$ and the forward shift of the centroid as the vortex moves inboard with increasing angle of attack. Since the augmented-vortex term consistently improved the lift (and, hence, drag) estimates by a small amount but did not consistently improve the prediction of the pitching-moment trends, the assumption about the centroidal location (and, hence, $\tilde{c}$) of these loads for a skewed wing configuration requires further study. This is also supported by flow-visualization results presented earlier. It is of interest to observe the significance of the side-edge-vortex loads by noting that the pitching moment predicted by using only the attached flow and the leading-edge-vortex theory has the opposite sign of the experimental pitching moments at high angles of attack. By including the contribution from the

side-edge vortices, reasonable correlation was achieved up to a moderate angle of attack. The overall forces and pitching moments for the configuration with the fuselage (fig. 27) were reasonably well predicted up to high angles of attack, with the augmented term resulting in a slight overprediction of lift and pitching-moment coefficients at the high angles of attack.

A comparison of the theoretical and experimental rolling-moment coefficients is presented in figures 28 and 29. Except for the wing-fuselage configuration, rolling-moment characteristics were well predicted only up to an angle of attack of approximately 6° and, at that, only by excluding the augmented-vortex term. Above this angle, the data depart from the theory and eventually change sign. (As with the pitching moments, the application of the augmented-vortex lift quantity at the assumed centroid resulted in overpredictions of the rolling moments.) This discrepancy between the theory and the data can be attributed to the vortex growth and subsequent inboard movement of the center of vortex lift as angle of attack was increased. While pitching moments were reasonably well predicted, the rolling moments were, as expected, overpredicted at moderate and high angles of attack as the actual center of vortex lift moved inboard.

The comparison of the theoretical and experimental rolling-moment characteristics of the wing-fuselage configuration are shown in figure 29. The rolling-moment characteristics for this configuration were well predicted up to an angle of atttack of approximately 16° by excluding the augmented-vortex contribution. As discussed in the flow visualization section, the fuselage caused a separate leading-edge vortex to form on the sweptback semispan with the apex of the vortex situated at the left-fuselage—leading-edge juncture and, hence, kept the vortex loads closer to the edges from which the vortices were generated. For this reason, the rolling moments were better predicted for this configuration than for the others by including the edge-vortex terms.

CONCLUSIONS

A theoretical and experimental analysis of the aerodynamic characteristics of several, thin, skewed wings having separation-induced vortex flows along the leading and side edges has been presented. The theoretical study was accomplished with a computer program that was developed for the analysis of asymmetric flow conditions including both fully attached flows and separation-induced vortex flows. The experimental tests were conducted in the Langley high-speed 7- by 10-foot tunnel at a Mach number of 0.12. The experimental tests included an additional configuration having a cylindrical fuselage mounted about one of the skewed wings. The purpose of the investigation was to determine the effects of sweep and aspect ratio on the longitudinal and lateral-directional aerodynamic characteristics of these skewed wings and to compare experimental with theoretical results. The results of this study are as follows:

1. For a given aspect ratio and sweep angle, the theoretical effect of the skewed planform was to shift the loads to the sweptback semispan. The skewed wing, compared with the swept wing, has slightly less potential-flow lift, approximately the same leading-edge-vortex lift, and substantially less side-edge-vortex lift.

2. The effect of sweep on the experimental longitudinal aerodynamic characteristics was, in general, small, while the effect of aspect ratio was consistent with simple wing theory; an increase in aspect ratio increased lift-curve slope and decreased drag due to lift. As aspect ratio was increased, the angle of attack at which the wing stalled was decreased which resulted in a reduced maximum lift coefficient. The fuselage had little influence on the longitudinal aerodynamic characteristics.

3. Experimental results indicated that the skewed wings exhibited relatively large values of rolling- and yawing-moment coefficients at moderate to high angles of attack and zero sideslip. An increase in either sweep or aspect ratio tended to increase the experimental rolling-moment coefficients at low to moderate angles of attack and zero sideslip, while at high angles of attack, the lateral-directional aerodynamic coefficients showed extreme nonlinearities (including change of sign) due to the asymmetric nature of the leading- and side-edge vortices. Addition of the fuselage to the skewed wing linearized the rolling moment throughout the angle-of-attack range investigated by causing a vortex to form on the sweptback semispan at the wing-fuselage juncture. Flow patterns seen in oil-flow photographs correlated with measured characteristics.

4. The measured lift and drag were consistently well estimated for all configurations, up to a lift coefficient of approximately 0.8, by the vortex-lattice-suction-analogy theory with both the edge-vortex and augmented-vortex terms included.

5. The measured pitching moments were not as consistently well predicted by including the edge-vortex and augmented-vortex terms as the lift and drag were. The assumption about the centroidal location of the augmented-vortex lift resulted in overpredictions for the wing-alone configurations with 45° and 55° sweep and requires further study.

6. Because the present theoretical method does not account for the inboard movement of the center of vortex lift with increasing angle of attack, the measured rolling moments were well predicted only up to an angle of attack of approximately 6° by the edge-vortex terms for the wing-alone configurations. Assumption of the centroidal location for the augmented-vortex lift resulted in substantial overpredictions of rolling moment throughout the angle-of-attack range investigated.

7. The measured lift and drag on the wing-fuselage configuration were well estimated up to a lift coefficient of approximately 0.8. Pitching moments were reasonably well estimated throughout the angle-of-attack range investigated, while rolling moments were well estimated with the leading- and side-edge vortex contributions up to an angle of attack of approximately 16°.

Langley Research Center
National Aeronautics and Space Administration
Hampton, VA 23665
October 17, 1977

REFERENCES

1. Jones, R. T.: Reduction of Wave Drag by Antisymmetric Arrangement of Wings and Bodies. AIAA J., vol. 10, no. 2, Feb. 1972, pp. 171-176.

2. Jones, Robert T.: New Design Goals and a New Shape for the SST. Astronaut. & Aeronaut., Dec. 1972, pp. 66-70.

3. Hopkins, Edward J.; Meriwether, Frank D.; and Pena, Douglas F.: Experimental Aerodynamic Characteristics of Low-Aspect Ratio Swept and Oblique Wings at Mach Numbers Between 0.6 and 1.4. NASA TM X-62,317, 1973.

4. Hopkins, Edward J.; and Leven, Alan D.: An Experimental and Theoretical Study of Low-Aspect Ratio Swept and Oblique Wings at Mach Numbers Between 0.6 and 1.4. AIAA Paper No. 74-771, Aug. 1974.

5. Luckring, James M.: Some Recent Applications of the Suction Analogy to Asymmetric Flow Situations. Vortex-Lattice Utilization. NASA SP-405, 1976, pp. 219-236.

6. Margason, Richard J.; and Lamar, John E.: Vortex-Lattice FORTRAN Program for Estimating Subsonic Aerodynamic Characteristics of Complex Planforms. NASA TN D-6142, 1971.

7. Lamar, John E.; and Gloss, Blair B.: Subsonic Aerodynamic Characteristics of Interacting Lifting Surfaces With Separated Flow Around Sharp Edges Predicted by a Vortex-Lattice Method. NASA TN D-7921, 1975.

8. Polhamus, Edward C.: A Concept of the Vortex Lift of Sharp-Edge Delta Wings Based on a Leading-Edge-Suction Analogy. NASA TN D-3767, 1966.

9. Polhamus, Edward C.: Charts for Predicting the Subsonic Vortex-Lift Characteristics of Arrow, Delta, and Diamond Wings. NASA TN D-6243, 1971.

10. Polhamus, Edward C.: Predictions of Vortex-Lift Characteristics by a Leading-Edge Suction Analogy. J. Aircraft, vol. 8, no. 4, Apr. 1971, pp. 193-199.

11. Lamar, John E.: Extension of Leading-Edge-Suction Analogy to Wings With Separated Flow Around the Side Edges at Subsonic Speeds. NASA TR R-428, 1974.

12. Lamar, John E.: Some Recent Applications of the Suction Analogy to Vortex-Lift Estimates. Aerodynamic Analyses Requiring Advanced Computers, Part II, NASA SP-347, 1975, pp. 985-1011.

13. Lamar, John E.: Summary of Some Recent Studies of Subsonic Vortex Lift and Parameters Affecting the Leading-Edge Vortex Stability. AIAA Paper No. 76-414, July 1976.

14. Braslow, Albert L.; Hicks, Raymond M.; and Harris, Roy V., Jr.: Use of Grit-Type Boundary-Layer-Transition Trips on Wind-Tunnel Models. NASA TN D-3579, 1966.

15. Schaefer, William T., Jr.: Characteristics of Major Active Wind Tunnels at the Langley Research Center. NASA TM X-1130, 1965.

16. Wentz, William H., Jr.; and Kohlman, David L.: Wind Tunnel Investigations of Vortex Breakdown on Slender Sharp-Edged Wings. NASA CR-98737, 1968.

TABLE I.- GEOMETRIC CHARACTERISTICS OF MODELS

Model number	Λ, deg	A	λ	Fuselage	b		c_r and $\bar{c}$		S		x^a	
					cm	in.	cm	in.	m^2	ft^2	cm	in.
I	30	1.0	1	Off	60.96	24	60.96	24	0.37	4.00	15.24	6
II	45	1.0	1	Off	60.96	24	60.96	24	.37	4.00	15.24	6
III	55	1.0	1	Off	60.96	24	60.96	24	.37	4.00	15.24	6
IV	30	1.5	1	Off	60.96	24	40.64	16	.25	2.67	10.16	4
V	30	2.0	1	Off	60.96	24	30.48	12	.19	2.00	7.62	3
VI	45	1.0	1	On	60.96	24	60.96	24	.37	4.00	15.24	6

[a]See figure 8(a).

TABLE II.- TEST PROGRAM MATRIX

Model number	$-4^\circ \leq \alpha \leq 24^\circ$			$-10^\circ \leq \beta \leq 10^\circ$	
	$\beta = -4^\circ$	$\beta = 0^\circ$	$\beta = 4^\circ$	$\alpha = 6^\circ$	$\alpha = 12^\circ$
I	X	X	X	X	X
II	X	X	X		
III	X	X	X		
IV		X			
V		X			
VI		X			

TABLE III.- CONFIGURATIONS

Run as listed in table IV	q_∞, Pa	Λ, deg	A	Dummy balance housing	α, deg	β, deg
1	958	45	1	Off	-4 to 24	0
3	958	45	1	On	-4 to 24	0
5	958	55	1	Off	-4 to 24	0
7	958	55	1	On	-4 to 24	0
9	958	30	1	On	-4 to 24	0
11	958	30	1	Off	-4 to 24	0
13	958	30	1	Off	-4 to 24	0
15	958	30	1	On	12	-10 to 10
17	958	30	1	Off	12	-10 to 10
19	958	30	1	Off	-4 to 24	4
21	958	30	1	On	-4 to 24	4
23	958	45	1	On	-4 to 24	4
26	958	45	1	Off	-4 to 24	4
28	958	55	1	Off	-4 to 24	4
30	958	55	1	On	-4 to 24	4
32	958	55	1	On	-4 to 24	-4
34	958	55	1	Off	-4 to 24	-4
36	958	45	1	Off	-4 to 24	-4
38	958	45	1	On	-4 to 24	-4
40	958	30	1	Off	-4 to 24	-4
42	958	30	1	On	-4 to 24	-4
44	958	30	1	Off	6	-10 to 10
46	958	30	1	On	6	-10 to 10
48	958	45	1	(a)	-4 to 24	0
50	958	30	1.5	Off	-4 to 24	0
52	958	30	1.5	On	-4 to 24	0
54	958	30	2	Off	-4 to 24	0
56	958	30	2	On	-4 to 24	0

[a]Model VI.

TABLE IV.- TABULATED RESULTS

The symbols used in the tabulated data are as follows:

RUN	run number (see table III)
ALPHA	angle of attack, deg
BETA	angle of sideslip, deg
Q	free-stream dynamic pressure, Pa
CL(SA)	lift coefficient, stability axis
CD(SA)	drag coefficient, stability axis
CPM(SA)	pitching-moment coefficient, stability axis
CRM(SA)	rolling-moment coefficient, stability axis
CYM(SA)	yawing-moment coefficient, stability axis
CSF(SA)	side-force coefficient, stability axis
CRM(BA)	rolling-moment coefficient, body axis
CYM(BA)	yawing-moment coefficient, body axis

RUN 1

ALPHA	BETA	Q	CL(SA)	CD(SA)	CPM(SA)	CRM(SA)	CYM(SA)	CSF(SA)	CRM(BA)	CYM(BA)
-.00	-.00	961.1110	-.0070	.0114	.0037	-.0001	-.0019	.0035	-.0001	-.0019
-2.06	-.01	961.0449	-.0891	.0147	.0042	-.0014	-.0013	.0009	-.0014	-.0012
-1.00	-.01	961.0449	-.0336	.0120	.0035	-.0009	-.0019	.0030	-.0009	-.0019
.04	-.00	961.7097	-.0060	.0115	.0040	-.0003	-.0019	.0032	-.0003	-.0019
1.07	.00	961.9171	.0224	.0117	.0043	.0001	-.0019	.0032	.0002	-.0019
2.10	.01	963.1729	.0538	.0125	.0045	.0009	-.0017	.0023	.0005	-.0016
3.16	.01	966.9300	.0858	.0141	.0040	.0011	-.0014	.0015	.0012	-.0013
4.23	.02	960.5126	.1237	.0170	.0038	.0016	-.0011	.0002	.0016	-.0010
5.32	.02	960.4461	.1646	.0227	.0029	.0027	-.0016	.0003	.0029	-.0014
6.44	.03	962.4415	.2137	.0312	.0008	.0038	-.0020	.0005	.0040	-.0016
7.56	.04	967.2966	.2639	.0416	-.0022	.0048	-.0024	.0002	.0050	-.0017
8.68	.04	959.5017	.3146	.0543	-.0053	.0053	-.0027	.0002	.0056	-.0019
9.81	.05	951.2673	.3717	.0701	-.0093	.0062	-.0033	.0003	.0067	-.0022
10.99	.05	957.4532	.4290	.0885	-.0134	.0069	-.0036	.0002	.0066	-.0024
13.31	.06	945.8129	.5433	.1327	-.0227	.0039	-.0037	-.0003	.0047	-.0027
15.71	.07	940.6909	.6669	.1907	-.0328	-.0011	-.0030	-.0009	-.0092	-.0032
17.97	.06	945.9460	.7738	.2587	-.0431	-.0085	-.0013	-.0010	-.0077	-.0030
20.23	.04	949.5370	.8706	.3236	-.0515	-.0184	.0016	-.0009	-.0178	-.0049
22.39	.01	965.3684	.9271	.3858	-.0564	-.0317	.0066	.0011	-.0318	-.0066
24.29	-.03	952.9316	.9880	.4509	-.0640	-.0424	.0118	.0026	-.0435	-.0067
.31	-.00	952.1170	-.0028	.0114	.0040	-.0001	-.0018	.0029	-.0001	-.0018

TABLE IV.- Continued

RUN 3

ALPHA	BETA	Q	CL(SA)	CD(SA)	CPM(SA)	CRM(SA)	CYM(SA)	CSF(SA)	CRM(BA)	CYM(BA)
.01	-.02	966.1016	.0040	.0114	-.0008	.0001	-.0016	.0032	.0001	-.0016
-2.97	-.01	960.0477	-.0820	.0146	-.0023	-.0010	-.0010	.0007	-.0011	-.0009
-1.02	-.01	959.3779	-.0229	.0122	-.0012	-.0002	-.0016	.0031	-.0002	-.0016
.00	-.00	963.1021	.0031	.0116	-.0008	-.0000	-.0016	.0032	-.0000	-.0016
1.03	-.02	963.3682	.0902	.0119	-.0006	.0001	-.0016	.0034	.0003	-.0016
2.06	.00	961.3729	.0658	.0128	-.0016	.0009	-.0013	.0026	.0010	-.0013
3.14	.01	959.1779	.0960	.0145	-.0013	.0012	-.0009	.0010	.0012	-.0009
4.20	.02	960.6412	.1325	.0176	-.0024	.0022	-.0008	-.0002	.0027	-.0006
5.29	.02	964.5650	.1725	.0728	-.0027	.0025	-.0050	-.0003	.0026	-.0007
6.40	.01	963.9669	.2219	.0315	-.0049	.0040	-.0014	-.0002	.0041	-.0016
7.51	.04	959.9771	.2691	.0414	-.0070	.0054	-.0020	-.0009	.0056	-.0013
8.63	.05	957.7148	.3184	.0520	-.0100	.0062	-.0029	-.0025	.0066	-.0016
9.75	.06	956.7937	.3716	.0665	-.0145	.0372	-.0029	-.0052	.0076	-.0016
10.91	.07	949.0680	.4260	.0826	-.0176	.0069	-.0030	-.0560	.0074	-.0017
13.26	.10	960.3887	.5433	.1266	-.0303	.0062	-.0021	-.0169	.0063	-.0006
15.61	.11	963.1021	.6477	.1790	-.0431	-.0014	.0018	-.0242	-.0018	.0013
17.79	.09	955.9148	.7277	.2275	-.0506	-.0115	.0056	-.0291	-.0176	.0016
19.99	.06	955.3258	.8070	.2883	-.0520	-.0241	.0091	-.0212	-.0257	.0006
22.15	.02	954.1229	.8763	.3508	-.0559	-.0347	.0126	-.0141	-.0369	-.0016
24.08	-.02	937.4270	.9320	.4144	-.0670	-.0401	.0142	-.0033	-.0426	-.0034
-.03	-.00	965.4759	.0034	.0114	-.0010	.0002	-.0013	.0026	.0002	-.0013

RUN 5

ALPHA	BETA	Q	CL(SA)	CD(SA)	CPM(SA)	CRM(SA)	CYM(SA)	CSF(SA)	CRM(BA)	CYM(BA)
.01	-.00	966.0919	-.0009	.0109	.0020	-.0003	-.0017	.0031	-.0003	-.0017
-3.10	-.01	965.9709	-.0881	.0130	.0042	-.0015	-.0008	-.1001	-.0016	-.0007
-.97	-.01	961.9686	-.0778	.0113	.0024	-.0052	-.0016	.0027	-.0003	-.0016
.04	-.00	961.3699	-.0020	.0111	.0021	.0001	-.0017	.0030	.0001	-.0017
1.67	.00	967.2226	.0290	.0115	.0013	.0058	-.0015	.0024	.0008	-.0015
2.10	.01	959.9066	.0565	.0125	.0005	.0014	-.0011	.0018	.0015	-.0011
3.16	.01	959.1086	.0871	.0145	-.0001	.0028	-.0008	.0005	.0020	-.0006
4.22	.02	960.5053	.1266	.0186	-.0017	.0033	-.0011	-.0001	.0034	-.0008
5.30	.03	961.0373	.1671	.0267	-.0048	.0051	-.0015	-.0006	.0052	-.0010
6.40	.03	958.9090	.2113	.0327	-.0089	.0069	-.0020	-.0006	.0077	-.0012
7.53	.04	957.7724	.2646	.0435	-.0135	.0084	-.0025	-.0008	.0086	-.0014
8.64	.05	957.7110	.3207	.0567	-.0192	.0101	-.0030	-.0013	.0104	-.0014
9.76	.06	955.4906	.3710	.0712	-.0226	.0105	-.0034	-.0017	.0109	-.0016
10.93	.06	957.7110	.4243	.0887	-.0276	.0105	-.0036	-.0024	.0110	-.0015
13.26	.07	948.6659	.5304	.1327	-.0367	.0075	-.0036	-.0035	.0081	-.0018
15.65	.07	947.4822	.6486	.1865	-.0385	-.0000	-.0027	-.0044	.0007	-.0026
17.98	.06	962.4341	.7554	.2406	-.0388	-.0109	-.0009	-.0043	-.0101	-.0042
20.20	.05	951.3266	.8472	.3158	-.0394	-.0217	.0019	-.0043	-.0210	-.0037
22.47	.02	964.2296	.9386	.3927	-.0435	-.0329	.0051	-.0031	-.0324	-.0079
24.32	-.01	965.0962	.9787	.4477	-.0421	-.0432	.0093	-.0016	-.0432	-.0093
.02	-.00	966.7617	.0019	.0107	.0021	.0000	-.0016	.0027	.0000	-.0016

RUN 7

ALPHA	BETA	Q	CL(SA)	CD(SA)	CPM(SA)	CRM(SA)	CYM(SA)	CSF(SA)	CRM(BA)	CYM(BA)
.00	-.00	965.8907	.0034	.0107	-.0024	.0004	-.0013	.0032	.0004	-.0013
-3.04	-.01	960.1045	-.0808	.0133	-.0010	-.0008	-.0009	-.0001	-.0009	-.0009
-.99	-.01	956.8900	-.0197	.0110	-.0028	.0004	-.0013	.0031	.0004	-.0013
.04	-.00	957.7101	.0093	.0109	-.0027	.0006	-.0013	.0033	.0006	-.0013
1.05	-.00	962.0332	.0321	.0113	-.0033	.0012	-.0011	.0028	.0012	-.0010
2.09	.01	961.6342	.0606	.0124	-.0048	.0022	-.0006	.0015	.0022	-.0005
3.14	.01	961.5676	.0900	.0144	-.0057	.0028	-.0002	.0002	.0028	-.0000
4.20	.02	963.3633	.1285	.0183	-.0070	.0040	-.0005	-.0008	.0040	-.0002
5.30	.03	957.2465	.1721	.0248	-.0101	.0056	-.0010	-.0006	.0057	-.0004
6.39	.03	957.6435	.2167	.0326	-.0142	.0075	-.0015	-.0013	.0076	-.0007
7.50	.05	956.6498	.2656	.0423	-.0176	.0088	-.0020	-.0031	.0090	-.0009
8.62	.06	960.9034	.3133	.0534	-.0218	.0104	-.0025	-.0054	.0104	-.0009
9.79	.07	959.7092	.3676	.0676	-.0257	.0115	-.0027	-.0093	.0118	-.0007
10.90	.09	954.0878	.4170	.0826	-.0286	.0116	-.0026	-.0132	.0116	-.0006
13.26	.12	960.9073	.5310	.1229	-.0355	.0105	-.0019	-.0240	.0106	.0006
15.61	.15	955.3156	.6419	.1725	-.0453	.0073	.0001	-.0360	.0071	.0020
17.85	.17	955.7149	.7407	.2309	-.0564	.0027	.0052	-.0465	.0011	.0037
20.13	.16	960.5698	.8380	.2952	-.0592	-.9109	.0080	-.0516	-.0130	.0038
22.24	.09	951.5906	.8790	.3607	-.0629	-.6307	.0140	-.0426	-.0337	.0013
.00	-.00	966.5909	.0043	.0106	-.0027	.0006	-.0012	.0029	.0006	-.0012

TABLE IV.- Continued

RUN 9

ALPHA	BETA	Q	CL(SA)	CD(SA)	CPM(SA)	CRM(SA)	CYM(SA)	CSF(SA)	CRM(BA)	CYM(BA)
.01	-.00	952.0694	.0040	.0125	-.0022	.0002	-.0014	.0024	.0002	-.0014
-2.06	-.01	958.1175	-.0555	.0137	-.0039	-.0000	-.0012	.0013	-.0001	-.0012
-.98	-.00	957.7194	-.0228	.0126	-.0033	.0002	-.0013	.0019	.0001	-.0013
.05	-.00	956.8539	.0044	.0124	-.0028	.0002	-.0013	.0023	.0002	-.0013
1.06	.00	961.7756	.0313	.0130	-.0013	.0006	-.0013	.0024	.0006	-.0013
2.13	.01	970.4217	.0654	.0143	-.0008	.0010	-.0012	.0021	.0010	-.0012
3.19	.01	961.9099	.0987	.0164	-.0008	.0014	-.0011	.0018	.0015	-.0010
4.25	.02	956.2591	.1356	.0194	-.0011	.0021	-.0009	.0007	.0022	-.0007
5.34	.02	957.7187	.1766	.0238	-.0011	.0023	-.0008	-.0003	.0023	-.0006
6.45	.03	956.3214	.2208	.0317	-.0011	.0023	-.0010	-.0003	.0024	-.0007
7.57	.03	964.3691	.2681	.0425	-.0024	.0030	-.0012	-.0000	.0032	-.0008
8.70	.04	964.3693	.3182	.0546	-.0043	.0031	-.0014	-.0007	.0032	-.0004
9.81	.05	953.7937	.3709	.0683	-.0076	.0032	-.0013	-.0025	.0034	-.0050
10.99	.06	963.1059	.4229	.0843	-.0115	.0029	-.0008	-.0052	.0030	-.0003
12.11	.07	954.3823	.4791	.1031	-.0177	.0032	-.0002	-.0060	.0031	.0005
15.63	.06	947.8738	.6449	.1781	-.0442	-.0042	[illegible]	-.0083	-.0051	.0025
17.83	.04	949.4781	.7334	.2357	-.0687	-.0119	[illegible]	-.0036	-.0128	.0021
20.02	.01	960.2457	.8182	.2992	-.0807	-.0177	.0002	.0019	-.0199	.0016
22.18	-.04	964.2358	.8835	.3611	-.1066	-.0223	.0111	.0069	-.0248	.0019
24.31	-.02	959.5824	.9737	.4410	-.1326	-.0219	.0127	.0077	-.0252	.0026
.01	-.00	959.5134	.0052	.0125	-.0022	.0004	-.0013	.0022	.0004	-.0013

RUN 11

ALPHA	BETA	Q	CL(SA)	CD(SA)	CPM(SA)	CRM(SA)	CYM(SA)	CSF(SA)	CRM(BA)	CYM(BA)
.00	-.00	957.7811	-.0031	.0128	.0025	.0001	-.0016	.0028	.0001	-.0016
-2.27	-.01	955.9107	-.0681	.0148	.0006	-.0002	-.0015	.0016	-.0003	-.0015
-.99	-.00	957.7018	-.0310	.0132	.0014	-.0000	-.0016	.0026	-.0000	-.0016
.05	-.00	951.5829	.0004	.0129	.0025	.0004	-.0016	.0027	.0004	-.0016
1.07	.00	969.6066	.0273	.0132	.0035	.0005	-.0016	.0027	.0007	-.0016
2.12	.01	975.6549	.0589	.0142	.0039	.0016	-.0014	.0020	.0011	-.0014
3.20	.01	959.2004	.0942	.0165	.0043	.0014	-.0013	.0020	.0014	-.0013
4.25	.02	957.7817	.1303	.0193	.0045	.0017	-.0011	.0010	.0018	-.0010
5.34	.02	954.3741	.1760	.0240	.0042	.0021	-.0010	.0002	.0022	-.0008
6.47	.03	963.2219	.2176	.0315	.0030	.0028	-.0012	-.0000	.0029	-.0009
7.58	.03	965.3629	.2659	.0420	.0020	.0027	-.0013	.0004	.0028	-.0010
8.70	.04	956.8370	.3182	.0547	.0002	.0027	-.0014	.0005	.0029	-.0010
9.82	.04	954.3761	.3705	.0699	-.0036	.0026	-.0015	.0007	.0028	-.0010
10.99	.04	950.6069	.4251	.0880	-.0086	.0019	-.0015	.0010	.0021	-.0012
13.32	.05	955.2458	.5416	.1327	-.0211	-.0005	-.0014	.0019	.0001	-.0015
15.72	.04	962.2008	.6579	.1891	-.0363	-.0063	-.0001	.0036	-.0060	-.0019
17.93	.02	968.0105	.7339	.2483	-.0536	-.0131	.0025	.0051	-.0132	-.0017
19.92	.00	964.4857	.8301	.3063	-.0717	-.0204	.0061	.0072	-.0213	-.0012
22.14	-.02	955.4400	.9006	.3739	-.1015	-.0251	.0100	.0108	-.0270	-.0002
24.26	-.03	975.9919	.9856	.4515	-.1314	-.0246	.0114	.0134	-.0271	.0003
.00	-.00	960.9617	-.0035	.0128	.0024	.0004	-.0015	.0022	.0004	-.0015

RUN 13

ALPHA	BETA	Q	CL(SA)	CD(SA)	CPM(SA)	CRM(SA)	CYM(SA)	CSF(SA)	CRM(BA)	CYM(BA)
.00	-.00	954.0421	-.0025	.0125	.0022	.0001	-.0014	.0019	.0001	-.0014
-2.61	-.01	957.3030	-.0827	.0145	.0009	-.0005	-.0012	.0005	-.0005	-.0012
-.98	-.00	955.1747	-.0309	.0126	.0017	-.0001	-.0014	.0018	-.0001	-.0014
.04	.00	954.9086	-.0029	.0124	.0028	.0001	-.0014	.0019	.0001	-.0014
1.08	.00	959.6979	.0276	.0127	.0038	.0004	-.0014	.0020	.0005	-.0014
2.12	.01	961.4931	.0585	.0138	.0045	.0007	-.0013	.0018	.0007	-.0013
3.20	.01	966.4811	.0947	.0155	.0047	.0010	-.0011	.0013	.0011	-.0011
4.26	.02	968.6098	.1322	.0182	.0045	.0019	-.0008	.0000	.0019	-.0006
5.34	.02	954.9751	.1711	.0227	.0045	.0021	-.0008	-.0004	.0022	-.0006
6.46	.03	954.6429	.2179	.0305	.0043	.0024	-.0010	-.0003	.0025	-.0007
7.58	.03	954.9769	.2682	.0410	.0030	.0025	-.0011	-.0002	.0026	-.0008
8.70	.04	956.3050	.3166	.0534	.0005	.0027	-.0012	.0001	.0028	-.0008
9.83	.04	954.9082	.3719	.0691	-.0020	.0015	-.0012	.0006	.0018	-.0009
11.03	.04	944.6650	.4336	.0886	-.0086	.0012	-.0013	.0012	.0014	-.0011
13.36	.04	957.7016	.5515	[illegible]	-.0216	-.0010	-.0014	.0026	-.0007	-.0015
15.75	.04	966.3479	.6659	.1906	-.0368	-.0068	.0001	.0040	-.0066	-.0017
17.97	.02	960.5614	.7677	.2520	-.0553	-.0149	.0031	.0058	-.0151	-.0016
20.10	-.01	957.0364	.8483	[illegible]	-.0762	-.0221	.0069	.0087	-.0231	-.0012
22.18	-.03	950.8963	.9149	.3786	-.1070	-.0255	.0105	.0119	-.0276	.0001
24.34	-.03	962.4901	1.0074	.4608	-.1356	-.0250	.0116	.0141	-.0276	.0003
.01	.00	965.0887	-.0030	.0125	.0026	.0004	-.0014	.0019	.0004	-.0014

TABLE IV.- Continued

RUN 15

ALPHA	BETA	Q	CL(SA)	CD(SA)	CPM(SA)	CRM(SA)	CYM(SA)	CSF(SA)	CRM(BA)	CYM(BA)
13.48	.02	961.0865	.5533	.1385	-.0282	-.0004	.0016	-.0085	-.0008	.0014
13.53	-3.83	956.3636	.5723	.1442	-.0350	.0104	-.0017	-.0047	.0086	.0007
13.53	-7.78	957.7604	.5875	.1473	-.0412	.0206	-.0049	-.0023	.0212	.0003
13.54	-9.76	952.0397	.5956	.1491	-.0446	.0249	-.0064	-.0007	.0237	-.0004
13.56	-10.27	949.7470	.5972	.1497	-.0453	.0257	-.0067	-.0006	.0266	-.0003
13.56	-9.74	963.4810	.5966	.1493	-.0447	.0246	-.0062	-.0012	.0234	-.0003
13.55	-8.74	966.4760	.5915	.1480	-.0428	.0227	-.0056	-.0019	.0234	-.0001
13.53	-7.73	962.2037	.5862	.1467	-.0408	.0202	-.0047	-.0023	.0208	.0001
13.53	-6.76	966.4122	.5834	.1461	-.0394	.0170	-.0041	-.0029	.0183	.0002
13.52	-5.77	962.7493	.5767	.1453	-.0378	.0151	-.0031	-.0036	.0154	.0005
13.51	-4.73	962.9501	.5735	.1443	-.0361	.0124	-.0022	-.0042	.0126	.0007
13.50	-3.82	961.2059	.5692	.1429	-.0340	.0106	-.0015	-.0052	.0106	.0010
13.49	-2.87	960.0087	.5656	.1420	-.0324	.0080	-.0008	-.0056	.0080	.0011
13.49	-1.91	960.0888	.5609	.1408	-.0313	.0048	.0001	-.0065	.0047	.0012
13.48	-.96	960.1553	.5556	.1392	-.0300	.0027	.0009	-.0080	.0023	.0015
13.48	.00	961.0281	.5526	.1380	-.0280	-.0002	.0016	-.0085	-.0006	.0015
13.46	.96	956.0979	.5471	.1362	-.0256	-.0029	.0024	-.0096	-.0034	.0017
13.46	1.91	958.0380	.5427	.1349	-.0238	-.0052	.0029	-.0104	-.0057	.0016
13.45	2.90	957.7611	.5356	.1333	-.0217	-.0081	.0034	-.0107	-.0087	.0015
13.47	3.81	964.4128	.5333	.1328	-.0198	-.0109	.0040	-.0111	-.0115	.0012
13.47	4.76	963.7476	.5279	.1317	-.0175	-.0137	.0045	-.0114	-.0144	.0012
13.48	5.71	968.6697	.5254	.1315	-.0156	-.0164	.0049	-.0111	-.0171	.0010
13.46	6.65	959.4900	.5177	.1300	-.0134	-.0189	.0053	-.0111	-.0197	.0008
13.47	7.55	964.4129	.5133	.1294	-.0115	-.0213	.0057	-.0112	-.0221	.0006
13.47	8.40	967.6056	.5079	.1287	-.0092	-.0241	.0061	-.0107	-.0249	.0003
13.49	.02	949.5887	.5514	.1369	-.0277	.0000	.0018	-.0094	-.0004	.0018

RUN 17

ALPHA	BETA	Q	CL(SA)	CD(SA)	CPM(SA)	CRM(SA)	CYM(SA)	CSF(SA)	CRM(BA)	CYM(BA)
13.52	.01	959.6909	.5588	.1468	-.0217	-.0029	-.0013	.0040	-.0025	-.0019
13.51	-3.81	935.8996	.5724	.1500	-.0312	.0057	-.0036	.0052	.0064	-.0021
13.53	-7.80	960.9549	.5848	.1533	-.0405	.0125	-.0053	.0064	.0136	-.0022
13.54	-9.79	958.1590	.5969	.1562	-.0462	.0160	-.0061	.0068	.0170	-.0022
13.53	-10.23	954.3698	.5968	.1553	-.0471	.0173	-.0064	.0069	.0183	-.0022
13.54	-9.77	962.9509	.5953	.1554	-.0460	.0158	-.0062	.0074	.0169	-.0023
13.54	-8.73	964.8796	.5909	.1543	-.0432	.0142	-.0057	.0066	.0151	-.0022
13.55	-7.75	966.2769	.5895	.1541	-.0411	.0123	-.0053	.0065	.0132	-.0023
13.54	-6.77	965.7443	.5860	.1533	-.0387	.0110	-.0049	.0058	.0118	-.0022
13.54	-5.79	967.7899	.5790	.1515	-.0358	.0092	-.0045	.0057	.0100	-.0022
13.53	-4.80	967.7399	.5759	.1507	-.0334	.0072	-.0040	.0058	.0079	-.0022
13.53	-3.83	966.0089	.5737	.1500	-.0311	.0051	-.0034	.0054	.0058	-.0021
13.53	-2.87	981.0606	.5703	.1484	-.0284	.0037	-.0030	.0050	.0043	-.0021
13.53	-1.91	966.2101	.5662	.1479	-.0263	.0016	-.0023	.0049	.0020	-.0021
13.53	-.96	970.6000	.5615	.1467	-.0239	-.0007	-.0016	.0045	-.0002	-.0020
13.54	.01	969.0702	.5602	.1460	-.0219	-.0030	-.0013	.0040	-.0027	-.0020
13.52	.97	964.0172	.5560	.1445	-.0196	-.0049	-.0008	.0039	-.0046	-.0019
13.52	1.91	958.6930	.5538	.1441	-.0180	-.0070	-.0003	.0037	-.0067	-.0019
13.52	2.87	959.4259	.5478	.1425	-.0154	-.0097	.0004	.0032	-.0095	-.0018
13.53	3.80	963.1505	.5456	.1419	-.0138	-.0123	.0011	.0031	-.0122	-.0018
13.53	4.75	964.0019	.5423	.1411	-.0117	-.0154	.0018	.0030	-.0154	-.0018
13.53	5.69	966.2768	.5357	.1395	-.0093	-.0181	.0025	.0026	-.0182	-.0018
13.54	6.61	969.2033	.5340	.1392	[illegible]	-.0205	.0031	.0021	-.0207	-.0017
13.54	[illegible]	967.2749	.5287	.1378	[illegible]	-.0229	.0039	.0016	-.0232	-.0016
13.55	8.45	971.0655	.5238	.1373	-.0038	-.0257	.0046	.0015	-.0260	-.0016
13.54	9.30	971.0051	.5191	.1357	-.0019	-.0286	.0053	.0010	-.0290	-.0015
13.53	.01	969.2719	.5572	.1448	-.0216	-.0027	-.0014	.0041	-.0023	-.0020

RUN 19

ALPHA	BETA	Q	CL(SA)	CD(SA)	CPM(SA)	CRM(SA)	CYM(SA)	CSF(SA)	CRM(BA)	CYM(BA)
-.00	4.00	963.9678	-.0039	.0118	.0023	-.0003	-.0013	.0011	-.0003	-.0013
-3.15	4.00	956.7866	-.0946	.0149	-.0006	.0015	-.0020	-.0011	.0015	-.0009
-1.00	4.00	957.7823	-.0301	.0116	.0010	.0002	-.0011	.0005	.0002	-.0011
.05	4.00	960.3097	-.0022	.0113	.0023	-.0003	-.0012	.0008	-.0003	-.0012
1.09	4.00	964.0323	.0244	.0117	.0039	-.0008	-.0012	.0004	-.0007	-.0012
2.12	4.00	964.3667	.0552	.0127	.0049	-.0013	-.0010	.0004	-.0013	-.0011
3.19	4.00	961.0794	.0870	.0144	.0056	-.0019	-.0008	.0003	-.0019	-.0009
4.26	4.00	964.2738	.1233	.0173	.0061	-.0024	-.0007	-.0002	-.0026	-.0007
5.34	3.99	961.5735	.1625	.0216	.0068	-.0033	-.0006	-.0010	-.0032	-.0007
6.37	3.98	963.7019	.2001	.0300	.0070	-.0040	-.0005	-.0006	-.0039	-.0010
7.36	3.98	960.2432	.2338	.0395	.0061	-.0046	-.0004	-.0003	-.0045	-.0010
8.74	3.97	962.0605	.3055	.0522	.0038	-.0049	-.0003	-.0003	-.0048	-.0010
9.80	3.96	990.4716	.3539	.0660	.0010	-.0060	-.0001	.0001	-.0059	-.0011
10.48	3.94	961.2409	.4101	.0838	-.0033	-.0069	.0001	.0007	-.0068	-.0012
13.37	3.91	967.0261	.5306	.1289	-.0142	-.0100	.0011	.0004	-.0100	-.0012
15.70	3.96	962.9030	.6471	.1851	-.0276	-.0160	.0031	.0018	-.0163	-.0014
19.01	3.00	963.3691	.7554	.2471	-.0421	-.0226	.0059	.0030	-.0235	-.0014
20.19	3.74	954.7224	.8437	.3130	-.0592	-.0297	.0096	.0052	-.0312	-.0013
22.42	3.65	968.0558	.9270	.3870	-.0803	-.0364	.0144	.0079	-.0392	-.0006
23.20	3.62	970.9509	.9521	.4133	-.0928	-.0384	.0166	.0094	-.0418	.0001
.01	4.00	960.9001	-.0035	.0111	.0023	-.0000	-.0011	.0008	-.0000	-.0011

TABLE IV.- Continued

RUN 21

ALPHA	BETA	Q	CL(SA)	CD(SA)	CPM(SA)	CRM(SA)	CYM(SA)	CSF(SA)	CRM(BA)	CYM(BA)
.00	4.01	954.4049	.0044	.0120	-.0014	.0001	-.0009	-.0011	.0001	-.0009
-3.10	4.00	954.8040	-.0932	.0190	-.0052	.0021	-.0006	-.0029	.0020	-.0007
-.98	4.01	964.2489	-.0219	.0122	-.0033	.0007	-.0017	-.0010	.0007	-.0010
.06	4.01	965.6503	.0064	.0121	-.0010	.0001	-.0010	-.0006	.0001	-.0010
1.05	4.00	959.1959	.0306	.0124	-.0018	-.0001	-.0011	-.0007	-.0001	-.0011
2.13	4.00	964.9814	.0620	.0136	.0002	-.0007	-.0010	-.0003	-.0006	-.0010
3.19	4.00	954.4044	.0962	.0156	.0010	-.0016	-.0007	-.0010	-.0016	-.0007
4.27	4.00	962.3866	.1334	.0187	.0013	-.0020	-.0005	-.0014	-.0020	-.0006
5.36	4.00	972.4209	.1727	.0235	.0017	-.0024	-.0004	-.0021	-.0024	-.0006
6.44	3.99	957.1089	.2143	.0315	.0021	-.0031	-.0004	-.0023	-.0030	-.0007
7.57	3.98	954.4049	.2646	.0426	.0012	-.0037	-.0006	-.0014	-.0036	-.0011
8.74	3.97	959.1959	.3140	.0551	-.0013	-.0050	-.0006	-.0016	-.0036	-.0011
9.84	3.96	954.8709	.3621	.0690	-.0034	-.0054	-.0008	-.0029	-.0053	-.0009
11.04	3.96	970.8999	.4283	.0863	-.0078	-.0071	.0009	-.0059	-.0072	-.0024
13.32	3.93	956.0013	.5273	.1250	-.0203	-.0093	.0037	-.0122	-.0090	.0014
15.69	3.86	956.9829	.6368	.1773	-.0369	-.0140	.0070	-.0137	-.0154	.0029
17.94	3.82	960.9247	.7392	.2370	-.0532	-.0223	.0108	-.0096	-.0246	.0034
20.02	3.75	951.9451	.8189	.2980	-.0700	-.0290	.0141	-.0629	-.0320	.0033
22.37	3.66	955.0729	.9033	.3736	-.0951	-.0338	.0176	.0059	-.0380	.0034
22.92	3.64	957.7906	.9252	.3934	-.1040	-.0347	.0186	.0029	-.0392	.0036
.00	4.01	952.8750	.0045	.0118	-.0019	.0002	-.0018	-.0011	.0002	-.0018

RUN 23

ALPHA	BETA	Q	CL(SA)	CD(SA)	CPM(SA)	CRM(SA)	CYM(SA)	CSF(SA)	CRM(BA)	CYM(BA)
.01	4.00	959.4494	.0029	.0113	.0001	-.0002	-.0013	.0003	-.0002	-.0013
-3.31	4.03	942.0953	-.0994	.0144	-.0023	.0011	-.0006	-.0029	.0010	-.0006
-.97	4.00	947.7495	-.0228	.0116	-.0007	-.0000	-.0012	-.0000	-.0001	-.0012
.04	4.00	954.4011	.0027	.0116	.0002	-.0003	-.0012	.0001	-.0003	-.0012
1.08	4.00	954.4011	.0294	.0121	.0009	-.0004	-.0011	-.0002	-.0004	-.0011
2.11	4.00	954.4011	.0567	.0133	.0017	-.0010	-.0009	-.0007	-.0009	-.0010
3.18	4.00	959.4562	.0890	.0154	.0017	-.0010	-.0007	-.0015	-.0009	-.0007
4.22	4.00	961.0979	.1223	.0185	.0023	-.0016	-.0004	-.0029	-.0015	-.0005
5.31	4.00	958.7244	.1611	.0230	.0025	-.0017	-.0005	-.0034	-.0016	-.0006
6.42	3.99	957.9937	.2071	.0321	.0010	-.0008	-.0008	-.0031	-.0007	-.0009
7.54	3.99	954.4009	.2535	.0422	-.0005	-.0007	-.0010	-.0035	-.0005	-.0011
8.66	3.99	954.4009	.3036	.0538	-.0025	-.0006	-.0010	-.0052	-.0004	-.0011
9.77	3.98	954.4009	.3498	.0667	-.0045	-.0008	-.0011	-.0069	-.0006	-.0012
10.97	3.98	965.3095	.4022	.0825	-.0065	-.0020	-.0009	-.0093	-.0018	-.0012
13.29	3.96	950.4764	.5154	.1226	-.0168	-.0039	.0002	-.0174	-.0040	-.0002
15.60	3.94	956.6073	.6333	.1744	-.0297	-.0078	.0037	-.0276	-.0085	.0014
17.96	3.90	954.9994	.7396	.2333	-.0423	-.0138	.0078	-.0339	-.0155	.0032
20.16	3.83	956.7288	.8258	.2965	-.0526	-.0240	.0121	-.0349	-.0268	.0036
22.30	3.74	950.4100	.8899	.3590	-.0563	-.0397	.0175	-.0309	-.0397	.0027
23.16	3.70	959.3321	.9118	.3845	-.0561	-.0411	.0209	-.0285	-.0457	.0022
.01	4.01	961.4919	.0022	.0110	.0002	-.0002	-.0010	-.0008	-.0002	-.0010

RUN 26

ALPHA	BETA	Q	CL(SA)	CD(SA)	CPM(SA)	CRM(SA)	CYM(SA)	CSF(SA)	CRM(BA)	CYM(BA)
.00	4.00	957.9291	-.0037	.0109	.0038	-.0007	-.0014	.0014	-.0007	-.0014
-3.44	4.00	948.5463	-.0980	.0148	.0017	.0009	-.0006	-.0012	.0005	-.0006
-.97	4.00	962.0489	-.0276	.0112	.0031	-.0005	-.0013	.0011	-.0005	-.0013
.03	4.00	962.7806	-.0023	.0111	.0037	-.0005	-.0015	.0015	-.0005	-.0015
1.07	4.00	960.7186	.0219	.0114	.0049	-.0011	-.0013	.0012	-.0011	-.0013
2.12	4.00	951.8070	.0520	.0125	.0057	-.0015	-.0010	.0006	-.0015	-.0011
3.18	4.00	955.4943	.0845	.0145	.0065	-.0021	-.0008	.0001	-.0020	-.0009
4.22	4.00	956.4619	.1161	.0175	.0064	-.0021	-.0006	-.0009	-.0021	-.0007
5.32	3.99	958.9903	.1544	.0228	.0061	-.0016	-.0007	-.0012	-.0016	-.0009
6.43	3.99	959.0651	.2019	.0310	.0054	-.0016	-.0010	-.0007	-.0014	-.0012
7.56	3.98	951.0762	.2519	.0416	.0033	-.0010	-.0012	-.0009	-.0009	-.0013
8.68	3.98	959.2579	.3017	.0539	.0010	-.0009	-.0014	-.0009	-.0007	-.0015
9.79	3.97	952.4049	.3511	.0680	-.0010	-.0014	-.0016	-.0009	-.0011	-.0017
11.00	3.96	955.6603	.4124	.0870	-.0047	-.0019	-.0016	-.0014	-.0016	-.0017
13.36	3.93	959.9880	.5280	.1309	-.0137	-.0047	-.0009	-.0014	-.0044	-.0020
15.76	3.89	965.3792	.6444	.1863	-.0209	-.0098	.0004	-.0018	-.0096	-.0023
18.08	3.84	957.0997	.7554	.2501	-.0304	-.0171	.0028	-.0023	-.0171	-.0027
20.28	3.78	949.1561	.8593	.3210	-.0408	-.0246	.0079	-.0022	-.0250	-.0034
22.59	3.70	953.3557	.9567	.3998	-.0494	-.0351	.0101	-.0020	-.0365	-.0042
23.38	3.67	960.5857	.9812	.4267	-.0512	-.0396	.0123	-.0021	-.0413	-.0043
.01	4.00	949.2117	-.0032	.0110	.0038	-.0008	-.0014	.0015	-.0008	-.0014

TABLE IV.- Continued

RUN 28

ALPHA	BETA	Q	CL(SA)	CD(SA)	CPM(SA)	CRM(SA)	CYM(SA)	CSF(SA)	CRM(BA)	CYM(BA)
.01	4.00	962.9781	.0007	.0100	.0020	-.0003	-.0010	.0010	-.0003	-.0010
-3.24	4.00	956.2603	-.0814	.0131	.0008	.0002	-.0000	-.0020	.0002	-.0001
-.98	4.00	959.5860	-.0238	.0104	.0013	-.0001	-.0008	.0005	-.0001	-.0008
.03	4.00	963.1111	-.0011	.0102	.0018	-.0001	-.0010	.0009	-.0001	-.0010
1.06	4.00	958.3888	.0245	.0107	.0025	-.0006	-.0008	.0009	-.0005	-.0008
2.12	4.00	961.3818	.0511	.0117	.0031	-.0008	-.0004	.0002	-.0008	-.0005
3.15	4.00	963.1776	.0773	.0138	.0030	-.0007	.0000	-.0011	-.0007	-.0000
4.20	4.00	955.7993	.1123	.0171	.0020	.0002	-.0002	-.0016	.0002	-.0002
5.27	4.00	957.0585	.1484	.0224	.0005	.0010	-.0004	-.0019	.0010	-.0003
6.37	3.99	960.1181	.1920	.0299	-.0025	.0021	-.0006	-.0019	.0022	-.0004
7.48	3.99	960.8496	.2407	.0396	-.0056	.0028	-.0007	-.0028	.0029	-.0003
8.60	3.98	955.6617	.2875	.0510	-.0084	.0029	-.0010	-.0027	.0031	-.0006
9.72	3.97	956.7923	.3388	.0651	-.0113	.0025	-.0011	-.0027	.0026	-.0007
10.90	3.96	949.6752	.3953	.0825	-.0149	.0017	-.0011	-.0035	.0018	-.0007
13.24	3.93	954.3978	.5014	.1234	-.0203	-.0023	-.0004	-.0040	-.0022	-.0010
15.68	3.89	965.1727	.6191	.1783	-.0233	-.0101	.0012	-.0046	-.0100	-.0016
17.99	3.84	965.1062	.7286	.2401	-.0267	-.0177	.0034	-.0056	-.0179	-.0022
20.28	3.78	961.4481	.8276	.3089	-.0257	-.0276	.0068	-.0059	-.0283	-.0032
22.49	3.70	954.3312	.9121	.3805	-.0240	-.0398	.0114	-.0060	-.0411	-.0047
23.54	3.66	959.1266	.9576	.4197	-.0235	-.0460	.0142	-.0062	-.0478	-.0054
.02	4.00	958.6543	.0013	.0096	.0020	-.0003	-.0009	.0009	-.0003	-.0009

RUN 30

ALPHA	BETA	Q	CL(SA)	CD(SA)	CPM(SA)	CRM(SA)	CYM(SA)	CSF(SA)	CRM(BA)	CYM(BA)
.00	4.00	962.9092	.0028	.0100	-.0019	.0003	-.0009	.0001	.0003	-.0009
-3.30	4.00	960.5814	-.0695	.0125	-.0036	.0011	-.0000	-.0025	.0011	-.0001
-.97	4.00	962.5103	-.0178	.0103	-.0023	.0004	-.0007	-.0001	.0004	-.0007
.04	4.00	957.6549	.0036	.0102	-.0020	.0004	-.0008	.0001	.0004	-.0008
1.06	4.00	962.7763	.0285	.0106	-.0012	.0001	-.0006	-.0003	.0001	-.0006
2.09	4.00	963.9735	.0516	.0116	-.0011	.0000	-.0002	-.0015	.0000	-.0002
3.15	4.00	956.1917	.0813	.0134	-.0013	.0002	.0002	-.0023	.0002	.0002
4.21	4.00	954.3958	.1171	.0174	-.0019	.0007	.0000	-.0030	.0007	.0001
5.27	4.00	955.0609	.1562	.0230	-.0040	.0017	-.0003	-.0029	.0017	-.0002
6.38	3.99	957.9876	.1977	.0306	-.0059	.0023	-.0006	-.0030	.0024	-.0004
7.47	3.99	957.3225	.2407	.0393	-.0088	.0032	-.0007	-.0047	.0033	-.0003
8.60	3.99	954.5934	.2907	.0507	-.0120	.0038	-.0009	-.0067	.0039	-.0003
9.72	3.99	961.7123	.3389	.0633	-.0147	.0040	-.0009	-.0094	.0041	-.0003
10.89	3.99	961.2467	.3915	.0796	-.0174	.0037	-.0007	-.0133	.0038	-.0000
13.24	3.98	962.9095	.4963	.1158	-.0209	.0011	.0005	-.0224	.0009	.0006
15.64	3.97	962.4439	.6092	.1649	-.0276	-.0021	.0029	-.0345	-.0028	.0023
17.93	3.94	967.2327	.7168	.2226	-.0366	-.0071	.0064	-.0451	-.0088	.0039
20.17	3.90	962.5769	.8218	.2893	-.0478	-.0124	.0110	-.0556	-.0154	.0061
22.43	3.84	963.5081	.9210	.3652	-.0552	-.0224	.0168	-.0628	-.0271	.0070
23.26	3.81	967.4322	.9508	.3935	-.0548	-.0273	.0191	-.0639	-.0326	.0067
.02	4.00	962.0450	.0060	.0101	-.0019	.0004	-.0007	-.0006	.0004	-.0007

RUN 32

ALPHA	BETA	Q	CL(SA)	CD(SA)	CPM(SA)	CRM(SA)	CYM(SA)	CSF(SA)	CRM(BA)	CYM(BA)
.00	-4.01	956.5317	.0056	.0122	-.0031	.0005	-.0020	.0073	.0005	-.0020
-3.41	-3.99	956.6648	-.1024	.0157	.0037	-.0039	-.0008	.0022	-.0039	-.0006
-.99	-4.01	956.7978	-.0239	.0123	-.0013	-.0007	-.0018	.0061	-.0007	-.0018
.04	-4.01	956.2697	.0055	.0123	-.0031	.0006	-.0020	.0071	.0006	-.0020
1.09	-4.01	952.4607	.0385	.0128	-.0052	.0019	-.0017	.0061	.0019	-.0016
2.10	-4.01	961.6533	.0696	.0142	-.0076	.0033	-.0011	.0049	.0034	-.0010
3.20	-4.00	960.5226	.1064	.0164	-.0096	.0045	-.0006	.0031	.0046	-.0004
4.22	-3.99	960.5891	.1464	.0204	-.0127	.0069	-.0008	.0015	.0070	-.0003
5.38	-3.99	956.3987	.1950	.0274	-.0166	.0091	-.0015	.0014	.0092	-.0007
6.45	-3.97	955.9331	.2408	.0360	-.0219	.0115	-.0025	.0014	.0117	-.0012
7.55	-3.96	958.7267	.2920	.0461	-.0265	.0135	-.0033	-.0010	.0138	-.0015
8.71	-3.94	957.1304	.3482	.0591	-.0323	.0157	-.0040	-.0039	.0161	-.0016
9.83	-3.91	966.7081	.4006	.0732	-.0355	.0162	-.0043	-.0080	.0167	-.0015
11.01	-3.89	956.2657	.46[illegible]	.0914	-.0401	.0167	-.0045	-.0131	.0172	-.0012
13.37	-3.83	960.5226	.5761	.1348	-.0503	.0151	-.0031	-.0251	.0154	.0005
15.74	-3.80	964.9788	.6767	.1861	-.0531	.0043	.0007	-.0355	.0040	.0018
17.96	-3.81	962.6510	.7297	.2342	-.0383	-.0147	.0060	-.0330	-.0159	.0011
20.27	-3.82	953.9377	.8008	.2939	-.0288	-.0293	.0095	-.0280	-.0308	-.0013
22.31	-3.82	956.8643	.8603	.3519	-.0236	-.0408	.0125	-.0221	-.0425	-.0040
23.14	-3.82	952.1418	.8833	.3762	-.0220	-.0454	.0140	-.0196	-.0472	-.0050
.01	-4.01	958.6603	.0057	.0119	-.0032	.0007	-.0019	.0064	.0007	-.0019

TABLE IV.- Continued

RUN 34

ALPHA	BETA	Q	CL(SA)	CD(SA)	CPM(SA)	CRM(SA)	CYM(SA)	CSF(SA)	CRM(BA)	CYM(BA)
.00	-4.01	962.9840	-.0025	.0111	.0022	.0003	-.0025	.0062	.0003	-.0025
-3.58	-3.99	954.8029	-.1154	.0136	.0102	-.0047	-.0009	.0006	-.0047	-.0006
-.98	-4.01	957.3305	-.0304	.0114	.0042	-.0009	-.0023	.0053	-.0010	-.0022
.04	-4.01	964.3809	.0003	.0112	.0021	.0005	-.0024	.0058	.0005	-.0024
1.08	-4.01	957.5300	.0316	.0118	-.0002	.0020	-.0023	.0053	.0021	-.0023
2.14	-4.00	958.5277	.0654	.0130	-.0022	.0033	-.0018	.0038	.0034	-.0016
3.19	-4.00	959.6585	.1005	.0152	-.0042	.0047	-.0014	.0024	.0047	-.0012
4.25	-3.99	957.2641	.1422	.0192	-.0071	.0070	-.0017	.0009	.0071	-.0012
5.33	-3.98	955.5347	.1871	.0256	-.0117	.0095	-.0025	.0008	.0097	-.0016
6.44	-3.97	954.4039	.2352	.0343	-.0167	.0116	-.0032	.0008	.0119	-.0019
7.57	-3.96	954.4039	.2919	.0462	-.0221	.0137	-.0040	.0008	.0141	-.0022
8.70	-3.95	952.2754	.3492	.0605	-.0286	.0146	-.0047	.0007	.0152	-.0024
9.87	-3.93	953.9383	.4129	.0786	-.0363	.0168	-.0058	.0004	.0175	-.0028
11.07	-3.91	963.5828	.4740	.0981	-.0415	.0167	-.0064	.0001	.0176	-.0031
13.39	-3.88	956.3329	.5899	.1459	-.0489	.0128	-.0070	-.0012	.0141	-.0038
15.81	-3.86	950.0139	.7070	.2059	-.0528	.0030	-.0067	-.0015	.0047	-.0057
18.07	-3.85	957.8627	.7939	.2649	-.0503	-.0104	-.0046	-.0011	-.0085	-.0076
20.31	-3.84	960.2572	.8646	.3268	-.0440	-.0256	-.0006	-.0007	-.0238	-.0095
22.34	-3.84	954.3374	.9208	.3857	-.0399	-.0379	.0042	-.0001	-.0366	-.0106
.01	-4.01	961.4544	.0005	.0109	.0018	.0006	-.0025	.0057	.0006	-.0025

RUN 36

ALPHA	BETA	Q	CL(SA)	CD(SA)	CPM(SA)	CRM(SA)	CYM(SA)	CSF(SA)	CRM(BA)	CYM(BA)
.01	-4.01	958.5950	-.0011	.0122	.0039	.0003	-.0024	.0056	.0003	-.0024
-3.45	-3.99	960.4576	-.1171	.0169	.0085	-.0042	-.0013	.0016	-.0043	-.0011
-1.02	-4.00	955.8679	-.0375	.0127	.0049	-.0011	-.0023	.0051	-.0011	-.0022
.02	-4.01	961.0560	-.0039	.0125	.0041	.0002	-.0024	.0054	.0002	-.0024
1.05	-4.01	961.0560	.0288	.0129	.0031	.0015	-.0023	.0050	.0015	-.0023
2.09	-4.00	961.0560	.0598	.0141	.0021	.0026	-.0021	.0041	.0027	-.0020
3.19	-4.00	962.1202	.0983	.0164	.0007	.0042	-.0018	.0028	.0042	-.0016
4.26	-3.99	961.0560	.1390	.0197	-.0014	.0061	-.0017	.0012	.0062	-.0012
5.34	-3.98	961.0560	.1841	.0253	-.0030	.0079	-.0021	.0003	.0080	-.0013
6.47	-3.97	954.8702	.2352	.0338	-.0058	.0098	-.0027	-.0000	.0100	-.0016
7.60	-3.96	954.4046	.2887	.0458	-.0097	.0113	-.0033	.0005	.0116	-.0018
8.73	-3.95	959.6592	.3414	.0595	-.0144	.0123	-.0039	.0003	.0127	-.0019
9.87	-3.94	954.4046	.4030	.0768	-.0196	.0131	-.0047	.0005	.0137	-.0024
11.06	-3.92	951.0788	.4634	.0970	-.0239	.0124	-.0052	.0003	.0131	-.0028
13.40	-3.89	954.4046	.5785	.1436	-.0338	.0094	-.0060	.0004	.0105	-.0036
15.80	-3.87	956.6661	.6884	.2002	-.0409	.0002	-.0048	.0002	.0015	-.0046
18.03	-3.86	953.4062	.7809	.2597	-.0482	-.0107	-.0024	.0006	-.0094	-.0056
20.19	-3.85	954.4046	.8530	.3197	-.0553	-.0226	.0017	.0009	-.0218	-.0063
22.30	-3.85	959.5927	.9050	.3786	-.0634	-.0343	.0069	.0030	-.0343	-.0066
23.09	-3.85	958.8611	.9100	.3964	-.0674	-.0384	.0094	.0041	-.0390	-.0064
-.01	-4.01	953.0743	-.0025	.0123	.0039	.0004	-.0023	.0051	.0004	-.0023

RUN 38

ALPHA	BETA	Q	CL(SA)	CD(SA)	CPM(SA)	CRM(SA)	CYM(SA)	CSF(SA)	CRM(BA)	CYM(BA)
.01	-4.01	958.2622	.0045	.0128	-.0005	-.0001	-.0021	.0067	-.0001	-.0021
-3.14	-4.00	957.7301	-.0998	.0160	.0029	-.0037	-.0014	.0036	-.0037	-.0012
-.98	-4.01	958.3288	-.0257	.0129	-.0002	-.0009	-.0021	.0062	-.0009	-.0020
.03	-4.01	964.3816	.0017	.0128	-.0006	-.0001	-.0022	.0069	-.0001	-.0022
1.09	-4.01	958.7288	.0359	.0134	-.0017	.0013	-.0021	.0064	.0013	-.0020
2.12	-4.01	960.0229	.0707	.0147	-.0032	.0027	-.0017	.0054	.0028	-.0016
3.20	-4.00	961.5215	.1060	.0171	-.0049	.0041	-.0015	.0040	.0042	-.0012
4.26	-3.99	959.3931	.1472	.0205	-.0063	.0054	-.0012	.0019	.0055	-.0008
5.35	-3.98	959.8587	.1912	.0261	-.0087	.0078	-.0015	.0010	.0079	-.0008
6.48	-3.98	957.5308	.2390	.0348	-.0112	.0095	-.0023	.0012	.0097	-.0012
7.61	-3.96	962.9856	.2932	.0465	-.0140	.0106	-.0032	.0010	.0110	-.0017
8.74	-3.94	956.2668	.3507	.0593	-.0191	.0132	-.0039	-.0017	.0137	-.0018
9.86	-3.93	954.6039	.4041	.0740	-.0237	.0144	-.0044	-.0039	.0149	-.0018
11.06	-3.90	962.8517	.4598	.0918	-.0283	.0148	-.0046	-.0068	.0154	-.0017
13.37	-3.87	954.4044	.5700	.1342	-.0387	.0116	-.0034	-.0133	.0121	-.0006
15.69	-3.85	954.4044	.6551	.1878	-.0460	-.0007	.0001	-.0156	-.0007	-.0001
17.93	-3.86	954.8700	.7456	.2433	-.0545	-.0115	.0018	-.0076	-.0115	-.0019
20.08	-3.85	958.1957	.8100	.2789	-.0570	-.0214	.0042	-.0031	-.0216	-.0034
22.18	-3.84	955.6016	.8608	.3352	-.0634	-.0304	.0076	.0003	-.0311	-.0045
.01	-4.01	951.8102	.0054	.0127	-.0012	.0004	-.0022	.0069	.0004	-.0022

TABLE IV.- Continued

RUN 40

ALPHA	BETA	Q	CL(SA)	CD(SA)	CPM(SA)	CRM(SA)	CYM(SA)	CSF(SA)	CRM(BA)	CYM(BA)
.01	-4.01	961.0526	-.0027	.0128	.0027	.0006	-.0019	.0044	.0006	-.0019
-3.46	-3.99	959.1238	-.1148	.0173	.0035	-.0035	-.0015	.0015	-.0036	-.0013
-.98	-4.00	961.0526	-.0338	.0132	.0027	-.0007	-.0018	.0038	-.0008	-.0018
.05	-4.01	961.0526	-.0023	.0129	.0027	.0008	-.0018	.0042	.0008	-.0018
1.08	-4.00	952.6718	.0275	.0133	.0032	.0014	-.0017	.0039	.0015	-.0017
2.13	-4.00	957.5939	.0611	.0144	.0030	.0028	-.0017	.0036	.0028	-.0016
3.22	-4.00	959.3231	.1005	.0165	.0024	.0044	-.0016	.0027	.0044	-.0013
4.28	-3.99	956.8621	.1401	.0195	.0018	.0057	-.0016	.0020	.0058	-.0011
5.38	-3.98	957.7268	.1825	.0240	.0010	.0071	-.0015	.0007	.0072	-.0009
6.50	-3.98	964.2450	.2289	.0319	.0001	.0085	-.0019	.0008	.0087	-.0009
7.62	-3.97	966.3069	.2762	.0423	-.0013	.0092	-.0021	.0007	.0094	-.0008
8.77	-3.96	960.6535	.3326	.0561	-.0049	.0103	-.0024	.0010	.0105	-.0008
9.88	-3.95	953.9355	.3870	.0715	-.0091	.0107	-.0026	.0011	.0110	-.0008
11.08	-3.94	960.0549	.4499	.0918	-.0154	.0099	-.0029	.0016	.0103	-.0009
13.44	-3.91	969.4993	.5657	.1382	-.0300	.0065	-.0029	.0026	.0070	-.0014
15.75	-3.90	961.0525	.6679	.1918	-.0465	-.0004	-.0015	.0045	.0000	-.0016
17.93	-3.89	956.3965	.7571	.2497	-.0663	-.0077	.0011	.0065	-.0076	-.0014
20.06	-3.88	967.1050	.8236	.3072	-.0916	-.0142	.0044	.0097	-.0149	-.0007
.02	-4.01	946.6853	-.0012	.0125	.0026	.0009	-.0019	.0043	.0009	-.0019

RUN 42

ALPHA	BETA	Q	CL(SA)	CD(SA)	CPM(SA)	CRM(SA)	CYM(SA)	CSF(SA)	CRM(BA)	CYM(BA)
.01	-4.01	961.0510	.0054	.0136	-.0019	.0000	-.0019	.0062	.0000	-.0019
-3.38	-4.00	954.3996	-.1055	.0175	-.0016	-.0036	-.0016	.0036	-.0037	-.0014
-.99	-4.01	961.0510	-.0247	.0140	-.0023	-.0010	-.0019	.0060	-.0010	-.0018
.05	-4.01	962.8468	.0052	.0138	-.0020	.0000	-.0018	.0060	.0000	-.0018
1.09	-4.01	964.2433	.0379	.0144	-.0022	.0016	-.0017	.0055	.0017	-.0017
2.13	-4.01	957.6586	.0722	.0157	-.0021	.0024	-.0016	.0052	.0025	-.0015
3.24	-4.00	961.8489	.1103	.0180	-.0027	.0038	-.0014	.0042	.0039	-.0012
4.28	-4.00	960.8512	.1472	.0211	-.0037	.0053	-.0014	.0032	.0053	-.0010
5.38	-3.99	960.5852	.1905	.0256	-.0049	.0069	-.0014	.0022	.0070	-.0008
6.49	-3.98	958.0577	.2361	.0337	-.0054	.0078	-.0017	.0020	.0080	-.0008
7.63	-3.97	959.3880	.2876	.0452	-.0071	.0093	-.0022	.0018	.0095	-.0009
8.75	-3.96	958.1907	.3379	.0576	-.0096	.0103	-.0025	.0007	.0106	-.0009
9.89	-3.94	953.9338	.3924	.0720	-.0135	.0118	-.0027	-.0009	.0120	-.0006
11.06	-3.92	966.2386	.4515	.0898	-.0187	.0127	-.0026	-.0037	.0130	-.0001
13.41	-3.89	966.1056	.5642	.1334	-.0324	.0113	-.0016	-.0063	.0113	.0010
15.73	-3.88	961.6493	.6723	.1894	-.0533	.0038	.0004	-.0027	.0036	.0014
17.92	-3.87	959.1219	.7533	.2462	-.0709	-.0036	.0023	.0015	-.0041	.0011
20.06	-3.87	954.3993	.8233	.3062	-.0957	-.0104	.0049	.0064	-.0114	.0011
22.04	-3.84	965.3738	.8911	.3667	-.1218	-.0112	.0061	.0089	-.0127	.0014
.02	-4.01	951.2066	.0065	.0135	-.0020	.0001	-.0017	.0058	.0001	-.0017

RUN 44

ALPHA	BETA	Q	CL(SA)	CD(SA)	CPM(SA)	CRM(SA)	CYM(SA)	CSF(SA)	CRM(BA)	CYM(BA)
6.65	.00	958.1850	.2270	.0367	.0046	.0014	-.0012	.0006	.0015	-.0010
6.66	-3.85	957.7194	.2359	.0378	-.0002	.0078	-.0019	.0012	.0079	-.0009
6.68	-7.79	957.7194	.2494	.0394	-.0062	.0139	-.0028	.0023	.0141	-.0011
6.69	-9.01	948.4073	.2580	.0406	-.0099	.0172	-.0033	.0029	.0174	-.0013
6.69	-10.60	951.6001	.2591	.0408	-.0111	.0183	-.0036	.0032	.0186	-.0014
6.69	-9.77	951.5336	.2566	.0404	-.0095	.0168	-.0032	.0025	.0171	-.0012
6.69	-8.74	960.3134	.2530	.0398	-.0081	.0156	-.0030	.0023	.0158	-.0011
6.68	-7.79	958.5175	.2517	.0396	-.0065	.0143	-.0027	.0020	.0145	-.0012
6.68	-6.79	962.9073	.2472	.0389	-.0049	.0126	-.0026	.0022	.0128	-.0011
6.67	-5.82	955.7240	.2430	.0385	-.0031	.0108	-.0024	.0022	.0110	-.0011
6.67	-4.80	958.5175	.2410	.0383	-.0016	.0092	-.0021	.0018	.0094	-.0010
6.66	-3.85	957.4533	.2365	.0378	-.0001	.0076	-.0019	.0016	.0078	-.0010
6.65	-2.88	957.7194	.2339	.0378	.0011	.0063	-.0018	.0016	.0064	-.0011
6.65	-1.92	952.9304	.2303	.0376	.0025	.0044	-.0015	.0013	.0046	-.0010
6.65	-.96	957.7194	.2275	.0373	.0037	.0029	-.0013	.0009	.0030	-.0010
6.65	-.00	957.7194	.2261	.0371	.0048	.0012	-.0011	.0007	.0013	-.0010
6.64	.96	953.3295	.2237	.0369	.0058	-.0003	-.0009	.0001	-.0002	-.0009
6.64	1.91	957.7194	.2215	.0368	.0066	-.0019	-.0008	.0003	-.0018	-.0010
6.64	2.87	957.2538	.2186	.0365	.0076	-.0036	-.0005	-.0003	-.0036	-.0009
6.64	3.81	957.2538	.2167	.0364	.0082	-.0049	-.0004	-.0003	-.0048	-.0010
6.64	4.76	951.7371	.2164	.0365	.0088	-.0065	-.0002	-.0004	-.0064	-.0010
6.64	5.71	964.9025	.2137	.0361	.0093	-.0079	.0000	-.0012	-.0079	-.0009
6.64	6.63	961.1115	.2125	.0362	.0098	-.0094	.0002	-.0012	-.0093	-.0009
6.64	7.57	956.9877	.2117	.0360	.0100	-.0107	.0003	-.0019	-.0107	-.0008
6.64	8.15	957.7194	.2097	.0359	.0102	-.0114	.0006	-.0020	-.0114	-.0008
6.64	.01	956.9212	.2298	.0367	.0047	.0013	-.0012	.0010	.0014	-.0010

TABLE IV.- Continued

RUN 46

ALPHA	BETA	Q	CL(SA)	CD(SA)	CPM(SA)	CRM(SA)	CYM(SA)	CSF(SA)	CRM(BA)	CYM(BA)
6.65	.01	957.7194	.2348	.0378	-.0010	.0019	-.0013	.0013	.0020	-.0010
6.67	-3.84	961.5770	.2461	.0388	-.0061	.0075	-.0019	.0031	.0077	-.0010
6.69	-7.80	954.0610	.2616	.0406	-.0125	.0134	-.0028	.0048	.0137	-.0012
6.70	-9.80	948.8063	.2680	.0414	-.0153	.0158	-.0033	.0060	.0161	-.0014
6.71	-10.97	955.3248	.2714	.0419	-.0172	.0175	-.0037	.0069	.0178	-.0017
6.70	-9.78	956.3225	.2674	.0412	-.0155	.0160	-.0033	.0062	.0163	-.0015
6.69	-8.76	954.8592	.2637	.0407	-.0138	.0146	-.0031	.0057	.0149	-.0014
6.70	-7.79	962.9071	.2621	.0405	-.0121	.0131	-.0028	.0049	.0133	-.0012
6.69	-6.78	964.9359	.2567	.0397	-.0107	.0118	-.0026	.0045	.0121	-.0012
6.67	-5.82	954.1941	.2527	.0393	-.0091	.0104	-.0023	.0039	.0106	-.0011
6.66	-4.81	954.3936	.2475	.0387	-.0075	.0089	-.0021	.0035	.0091	-.0011
6.66	-3.84	956.4555	.2466	.0388	-.0062	.0075	-.0020	.0032	.0077	-.0011
6.66	-2.89	952.9302	.2433	.0386	-.0048	.0061	-.0017	.0025	.0063	-.0010
6.66	-1.92	957.5862	.2414	.0386	-.0037	.0050	-.0017	.0025	.0051	-.0011
6.65	-.94	958.5173	.2377	.0383	-.0021	.0032	-.0014	.0018	.0033	-.0010
6.65	-.00	958.7169	.2347	.0380	-.0010	.0018	-.0012	.0012	.0020	-.0010
6.66	.98	957.7192	.2344	.0383	.0005	-.0001	-.0011	.0009	.0000	-.0011
6.65	1.92	957.7192	.2311	.0380	.0012	-.0011	-.0010	.0006	-.0009	-.0011
6.65	2.90	958.7169	.2284	.0378	.0024	-.0028	-.0009	.0001	-.0027	-.0012
6.65	3.81	957.71[illegible]	.2259	.0376	.0035	-.0045	-.0007	-.0004	-.0044	-.0012
6.65	4.79	957.719[illegible]	.2245	.0376	.0042	-.0057	-.0005	-.0009	-.0056	-.0012
6.64	5.73	956.4554	.2208	.0372	.0050	-.0070	-.0003	-.0017	-.0070	-.0012
6.65	6.67	955.3912	.2208	.0374	.0055	-.0082	-.0001	-.0026	-.0081	-.0011
6.65	7.59	956.7880	.2181	.0371	.0060	-.0097	.0001	-.0032	-.0096	-.0010
6.64	8.20	957.7192	.2158	.0369	.0063	-.0104	.0002	-.0035	-.0103	-.0010
6.66	.01	962.5080	.2362	.0381	-.0010	.0018	-.0012	.0010	.0019	-.0010

RUN 48

ALPHA	BETA	Q	CL(SA)	CD(SA)	CPM(SA)	CRM(SA)	CYM(SA)	CSF(SA)	CRM(BA)	CYM(BA)
-.01	-.00	957.9778	-.0178	.0130	.0006	-.0006	.0001	.0001	-.0006	.0001
-2.93	.01	957.7118	-.1064	.0159	-.0018	-.0023	.0007	-.0031	-.0023	.0008
-.99	.00	954.6522	-.0469	.0131	-.0010	-.0008	.0003	-.0007	-.0008	.0003
.04	-.00	959.5761	-.0162	.0129	.0006	-.0005	.0002	.0001	-.0005	.0002
1.06	-.00	961.6358	.0096	.0131	.0024	-.0003	.0001	.0005	-.0003	.0001
2.12	-.00	960.1061	.0387	.0140	.0038	.0002	.0002	.0001	.0002	.0002
3.19	.00	959.1749	.0734	.0163	.0050	.0007	.0004	-.0011	.0007	.0004
4.23	.00	962.8994	.1060	.0189	.0059	.0010	.0003	-.0020	.0010	.0004
5.31	.01	960.7046	.1451	.0233	.0062	.0019	.0002	-.0036	.0018	.0004
6.44	.02	960.9706	.1892	.0300	.0063	.0027	-.0001	-.0061	.0027	.0002
7.53	.03	958.2437	.2334	.0384	.0044	.0038	-.0003	-.0089	.0038	.0003
8.65	.04	951.6590	.2844	.0502	.0020	.0049	-.0011	-.0112	.0050	-.0003
9.79	.05	957.7116	.3380	.0645	-.0008	.0061	-.0019	-.0144	.0063	-.0008
10.94	.06	957.3125	.3870	.0799	-.0035	.0066	-.0026	-.0176	.0070	-.0013
13.30	.09	962.1012	.4995	.1209	-.0119	.0081	-.0044	-.0258	.0089	-.0025
15.67	.13	956.9134	.6151	.1729	-.0242	.0102	-.0074	-.0359	.0118	-.0044
17.92	.18	955.8402	.7224	.2325	-.0375	.0113	-.0102	-.0482	.0139	-.0062
20.15	.22	952.7896	.8219	.2994	-.0546	.0124	-.0126	-.0633	.0160	-.0075
-.00	-.00	956.7139	-.0167	.0123	.0007	-.0005	.0002	-.0001	-.0005	.0002

RUN 50

ALPHA	BETA	Q	CL(SA)	CD(SA)	CPM(SA)	CRM(SA)	CYM(SA)	CSF(SA)	CRM(BA)	CYM(BA)
-.01	-.00	957.2477	-.0155	.0156	.0088	-.0006	-.0016	.0046	-.0006	-.0016
-3.25	.00	956.1834	-.1417	.0195	.0092	-.0025	-.0007	.0009	-.0026	-.0006
-.98	-.00	956.7820	-.0506	.0159	.0085	-.0011	-.0015	.0039	-.0011	-.0015
.02	-.00	958.1788	-.0142	.0153	.0089	-.0007	-.0016	.0042	-.0007	-.0016
1.04	-.00	963.4331	.0228	.0155	.0094	-.0002	-.0016	.0042	-.0002	-.0016
2.06	-.00	964.3642	.0612	.0164	.0093	.0004	-.0014	.0035	.0005	-.0013
3.11	-.00	964.3642	.1052	.0182	.0095	.0006	-.0011	.0030	.0007	-.0010
4.13	-.00	963.1005	.1506	.0213	.0087	.0017	-.0008	.0019	.0018	-.0006
5.18	.00	965.4283	.1972	.0260	.0090	.0014	-.0007	.0009	.0015	-.0005
6.26	.00	964.3641	.2488	.0342	.0081	.0023	-.0008	.0008	.0024	-.0006
7.34	.00	961.9697	.3073	.0463	.0051	.0029	-.0010	.0004	.0030	-.0006
8.43	.00	960.3734	.3664	.0609	.0005	.0025	-.0011	.0008	.0026	-.0007
9.50	.00	965.0720	.4275	.0778	-.0052	.0015	-.0012	.0013	.0017	-.0009
10.61	-.00	955.5866	.4831	.0964	-.0102	-.0014	-.0009	.0018	-.0012	-.0012
12.83	-.01	956.3827	.5982	.1422	-.0255	-.0083	-.0003	.0035	-.0080	-.0021
15.03	-.03	953.8552	.6833	.1906	-.0388	-.0196	.0023	.0057	-.0196	-.0028
17.11	-.05	952.9906	.7452	.2389	-.0504	-.0311	.0066	.0088	-.0317	-.0029
19.12	-.08	955.8506	.7748	.2817	-.0654	-.0385	.0109	.0133	-.0390	-.0023
21.09	-.09	958.3781	.8020	.3257	-.0898	-.0398	.0136	.0175	-.0423	-.0016
-.00	-.00	955.4567	-.0122	.0146	.0090	-.0008	-.0017	.0042	-.0008	-.0017

TABLE IV.- Concluded

RUN 52

ALPHA	BETA	Q	CL(SA)	CD(SA)	CPM(SA)	CRM(SA)	CYM(SA)	CSF(SA)	CRM(BA)	CYM(BA)
.00	-.00	960.0994	-.0002	.0159	-.0001	.0000	-.0012	.0040	.0000	-.0012
-3.09	-.00	959.7692	-.1100	.0192	-.0007	-.0013	-.0006	.0010	-.0013	-.0005
-.95	-.00	957.7090	-.0341	.0159	-.0008	-.0003	-.0012	.0033	-.0004	-.0012
.05	-.00	961.4961	.0025	.0155	-.0001	.0001	-.0012	.0039	.0001	-.0012
1.04	-.00	956.5743	.0383	.0158	.0006	.0003	-.0011	.0035	.0004	-.0011
2.07	-.00	960.9640	.0753	.0173	.0008	.0007	-.0011	.0033	.0008	-.0010
3.11	-.00	966.6171	.1172	.0193	.0009	.0013	-.0008	.0024	.0014	-.0008
4.13	-.00	960.0993	.1571	.0223	.0007	.0019	-.0006	.0014	.0019	-.0004
5.19	.00	955.3771	.2054	.0258	.0003	.0025	-.0004	-.0004	.0026	-.0002
6.26	.00	958.1705	.2544	.0340	-.0005	.0031	-.0004	-.0013	.0031	-.0001
7.36	.01	954.4458	.3123	.0447	-.0017	.0034	-.0008	-.0017	.0035	-.0003
8.44	.01	958.1039	.3714	.0579	-.0051	.0044	-.0009	-.0027	.0045	-.0003
9.51	.01	954.7118	.4247	.0728	-.0082	.0042	-.0012	-.0020	.0044	-.0004
10.60	.01	952.5169	.4832	.0906	-.0118	.0037	-.0013	-.0029	.0039	-.0006
12.85	.01	963.6243	.5997	.1337	-.0225	.0022	-.0010	-.0046	.0024	-.0005
15.10	.01	961.9614	.7127	.1890	-.0435	-.0024	.0013	-.0098	-.0027	.0006
17.14	-.03	960.8974	.7623	.2363	-.0575	-.0200	.0053	.0020	-.0206	-.0009
19.14	-.07	957.5053	.7876	.2805	-.0683	-.0338	.0103	.0102	-.0353	-.0013
.01	-.00	959.8996	.0015	.0153	-.0002	.0000	-.0012	.0038	.0000	-.0012

RUN 54

ALPHA	BETA	Q	CL(SA)	CD(SA)	CPM(SA)	CRM(SA)	CYM(SA)	CSF(SA)	CRM(BA)	CYM(BA)
.02	-.01	957.1773	.0142	.0225	-.0007	.0007	-.0021	.0077	.0007	-.0021
-3.13	-.00	957.9756	-.1339	.0245	.0028	-.0019	-.0010	.0038	-.0019	-.0009
-.93	-.01	954.1177	-.0284	.0227	-.0002	.0001	-.0019	.0068	.0001	-.0019
.05	-.01	959.2391	.0138	.0228	.0000	.0002	-.0021	.0079	.0002	-.0021
1.05	-.01	960.5693	.0548	.0236	-.0012	.0012	-.0021	.0081	.0012	-.0021
2.07	-.01	963.1632	.1010	.0247	-.0021	.0019	-.0016	.0070	.0020	-.0016
3.12	-.00	965.9613	.1539	.0268	-.0037	.0033	-.0012	.0051	.0033	-.0010
4.13	-.00	961.0340	.2064	.0298	-.0043	.0040	-.0008	.0041	.0040	-.0005
5.17	-.00	959.1726	.2604	.0352	-.0046	.0043	-.0006	.0028	.0043	-.0002
6.24	-.00	957.1772	.3194	.0450	-.0069	.0054	-.0009	.0022	.0055	-.0003
7.31	.00	956.7782	.3857	.0593	-.0123	.0055	-.0011	.0009	.0056	-.0004
8.38	.00	956.7782	.4509	.0761	-.0204	.0054	-.0017	.0025	.0056	-.0008
9.44	-.00	950.5924	.5122	.0950	-.0262	.0024	-.0017	.0035	.0026	-.0013
10.56	-.00	961.5003	.5705	.1165	-.0302	-.0023	-.0015	.0043	-.0022	-.0020
12.69	-.01	955.1156	.6533	.1586	-.0348	-.0147	.0002	.0063	-.0144	-.0030
14.88	-.03	954.6497	.7315	.2082	-.0432	-.0284	.0033	.0092	-.0283	-.0041
16.90	-.05	954.7163	.7731	.2520	-.0467	-.0420	.0078	.0149	-.0425	-.0047
18.93	-.08	956.7117	.7959	.2937	-.0536	-.0501	.0121	.0217	-.0513	-.0048
.02	-.01	948.9296	.0142	.0217	-.0009	.0009	-.0019	.0071	.0009	-.0019

RUN 56

ALPHA	BETA	Q	CL(SA)	CD(SA)	CPM(SA)	CRM(SA)	CYM(SA)	CSF(SA)	CRM(BA)	CYM(BA)
.00	-.01	956.9106	.0021	.0212	-.0020	.0006	-.0009	.0050	.0006	-.0009
-3.67	-.00	954.6496	-.1720	.0260	.0036	-.0024	.0000	.0007	-.0024	.0002
-.96	-.00	960.0365	-.0394	.0211	-.0007	-.0004	-.0009	.0048	-.0004	-.0009
.05	-.01	960.7016	.0041	.0211	-.0018	.0005	-.0010	.0058	.0005	-.0010
1.04	-.01	960.3025	.0496	.0218	-.0029	.0012	-.0010	.0057	.0012	-.0010
2.05	-.00	959.5067	.0913	.0227	-.0046	.0024	-.0006	.0046	.0024	-.0006
3.10	-.00	962.1648	.1428	.0249	-.0055	.0031	-.0003	.0036	.0031	-.0002
4.13	-.00	962.0318	.1924	.0279	-.0065	.0037	.0001	.0019	.0037	.0003
5.15	.00	955.7843	.2455	.0327	-.0083	.0050	.0002	-.0003	.0050	.0007
6.22	.00	956.5114	.3010	.0404	-.0087	.0052	.0002	-.0017	.0051	.0008
7.27	.01	955.6513	.3655	.0519	-.0125	.0064	-.0001	-.0037	.0064	.0007
8.36	.01	955.5848	.4313	.0670	-.0176	.0069	-.0004	-.0041	.0069	.0006
9.42	.01	959.1717	.4912	.0838	-.0234	.0068	-.0008	-.0043	.0068	.0003
10.54	.01	951.6559	.5639	.1050	-.0308	.0059	-.0010	-.0047	.0060	.0001
12.72	.01	959.9713	.6822	.1505	-.0452	.0021	-.0003	-.0070	.0021	.0001
14.99	.01	954.3829	.7965	.2112	-.0767	-.0058	.0030	-.0122	-.0063	.0014
17.01	-.03	954.3829	.8047	.2491	-.0652	-.0292	.0083	.0019	-.0304	-.0006
18.90	-.06	959.7703	.8167	.2880	-.0620	-.0433	.0138	.0093	-.0454	-.0009
-.00	-.00	954.8485	-.0015	.0204	-.0017	.0005	-.0008	.0047	.0005	-.0008

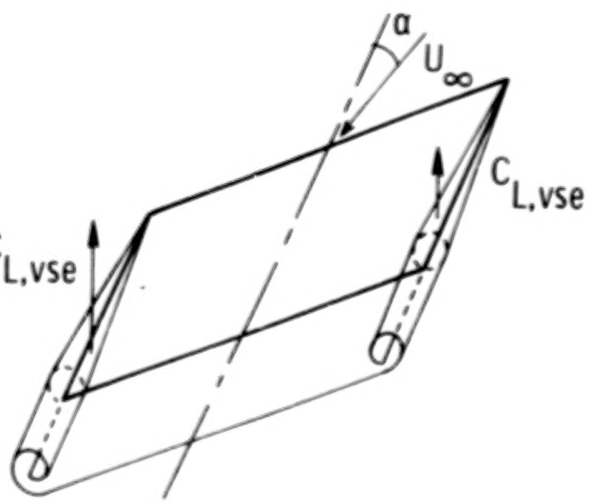

(a) Side-edge effect. (b) Leading-edge and augmented effect.

Figure 1.- Concept of augmented-vortex lift applied to skewed wing.

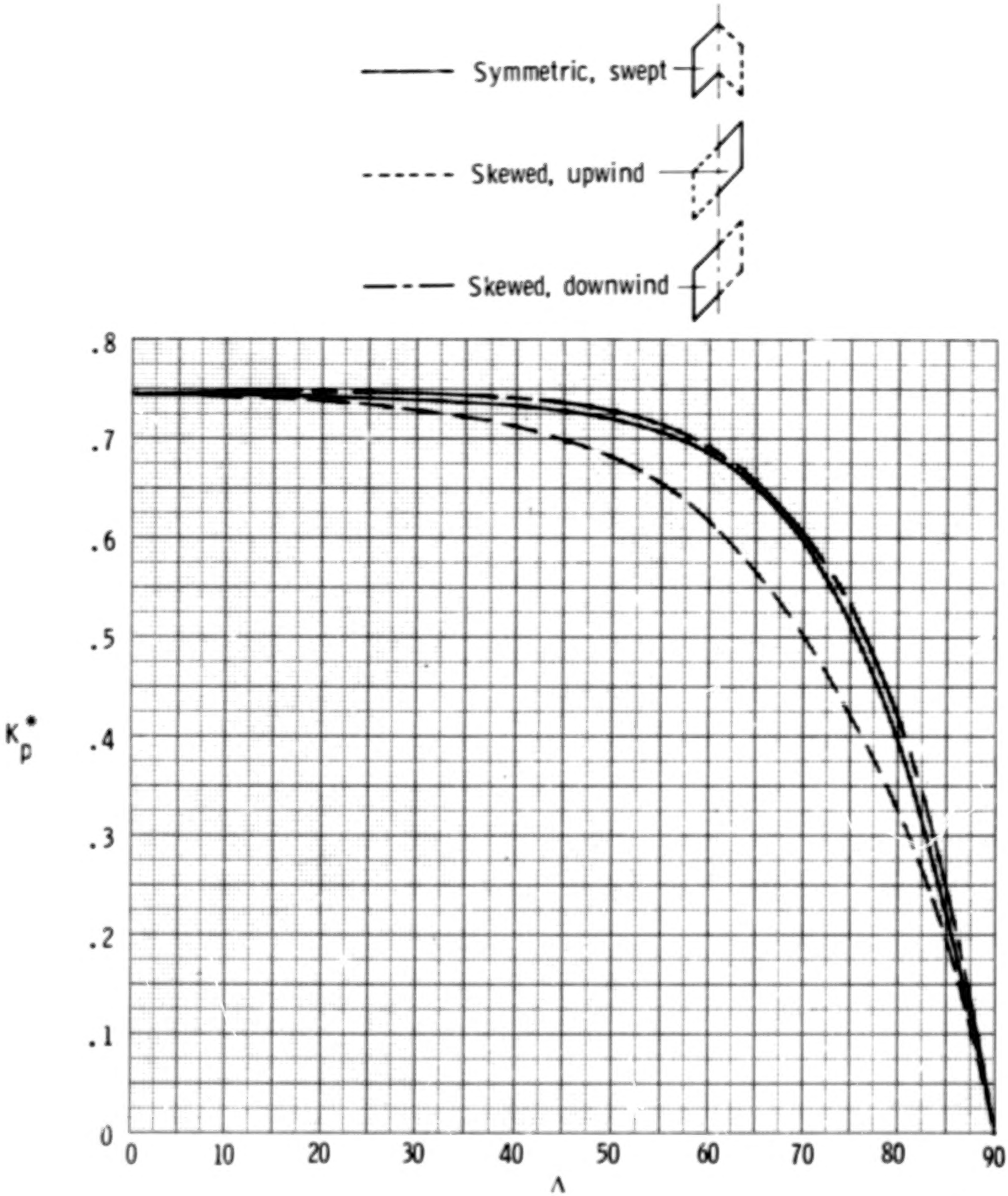

(a) K_p^*.

Figure 2.- Effect of sweep on theoretical lift factors for wing semispan. $A = 1.0$; $M_\infty = 0$.

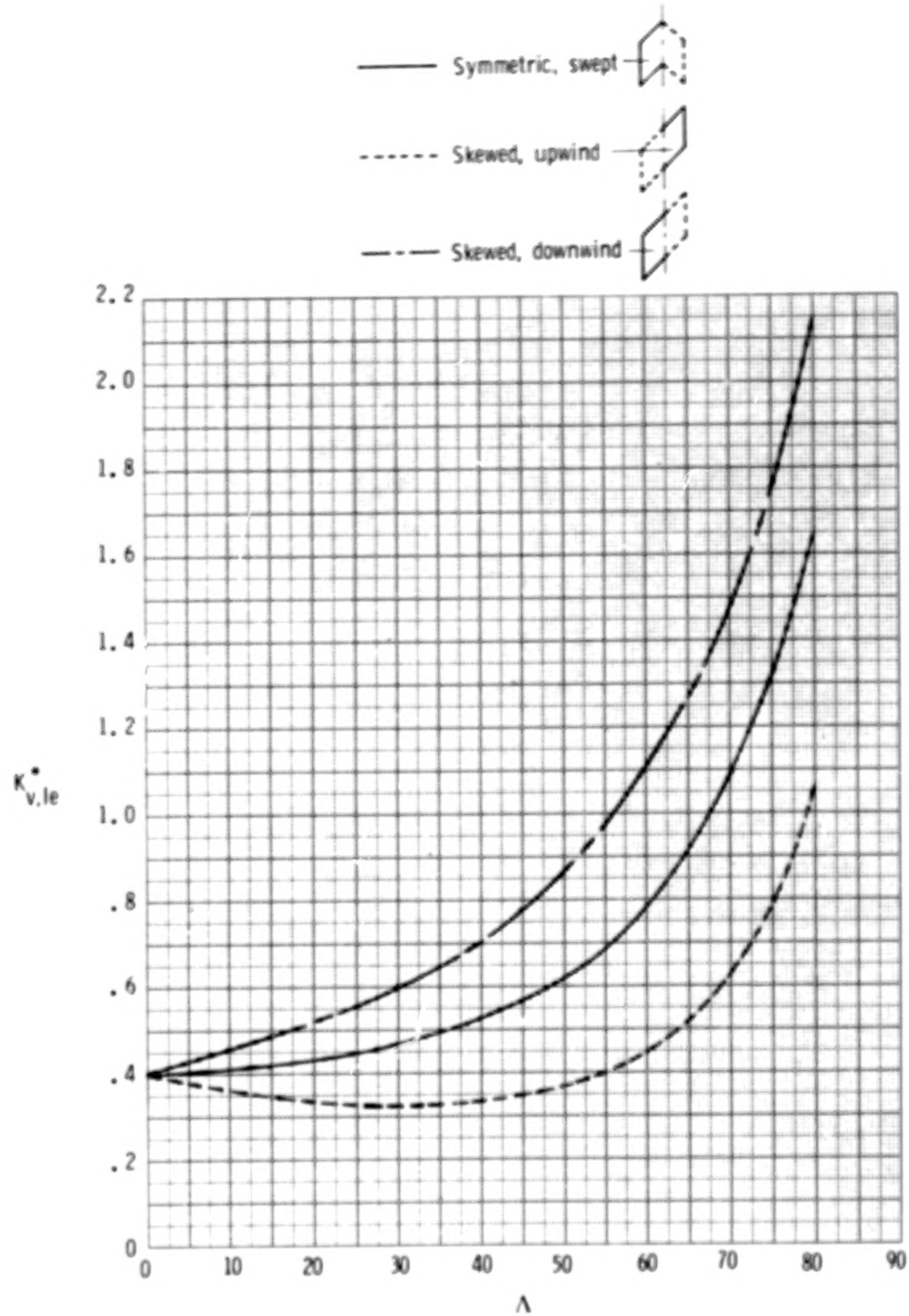

(b) $K^*_{v,le}$.

Figure 2.- Continued.

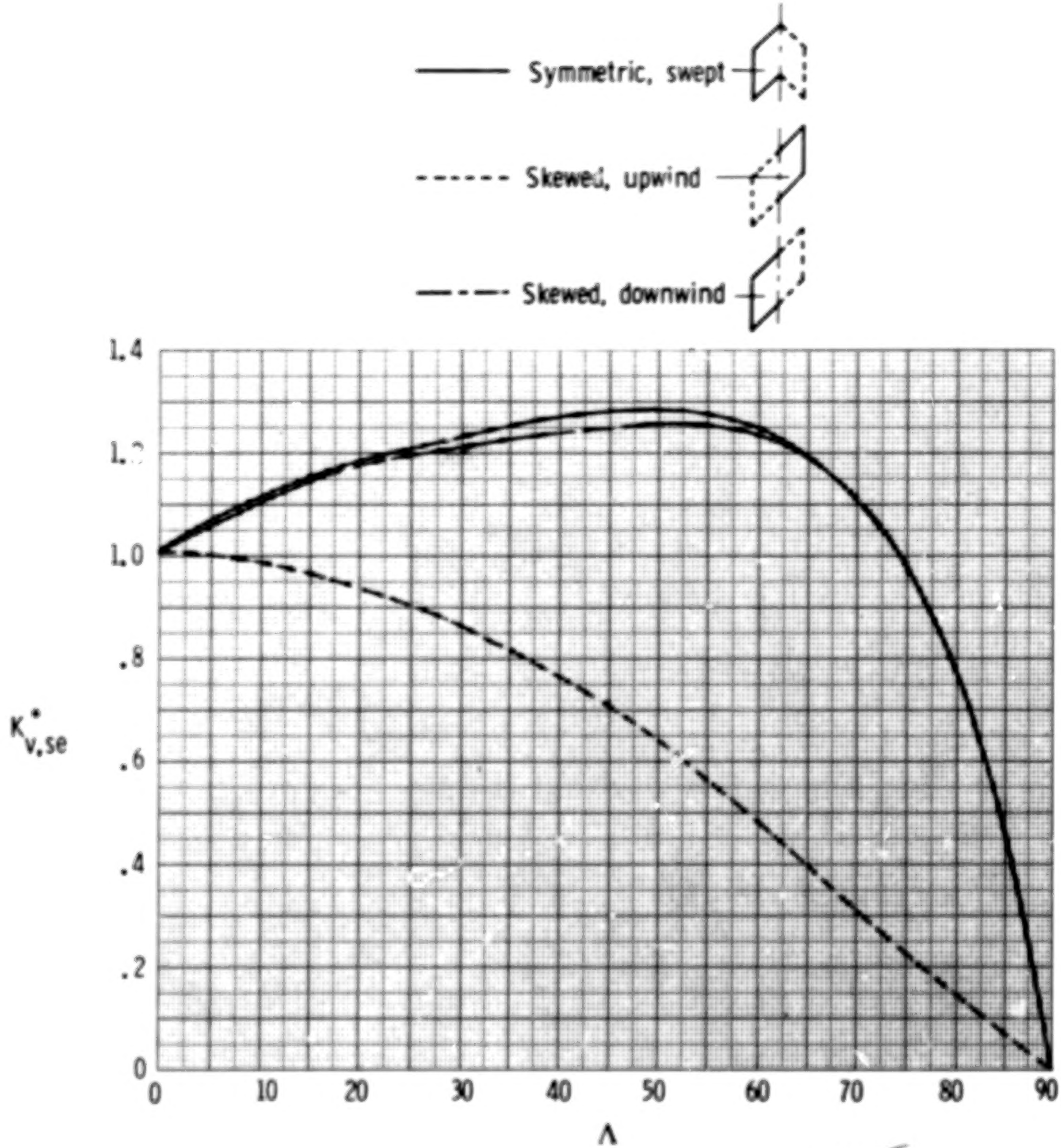

35.

(c) $K^*_{v,se}$.

Figure 2.- Concluded.

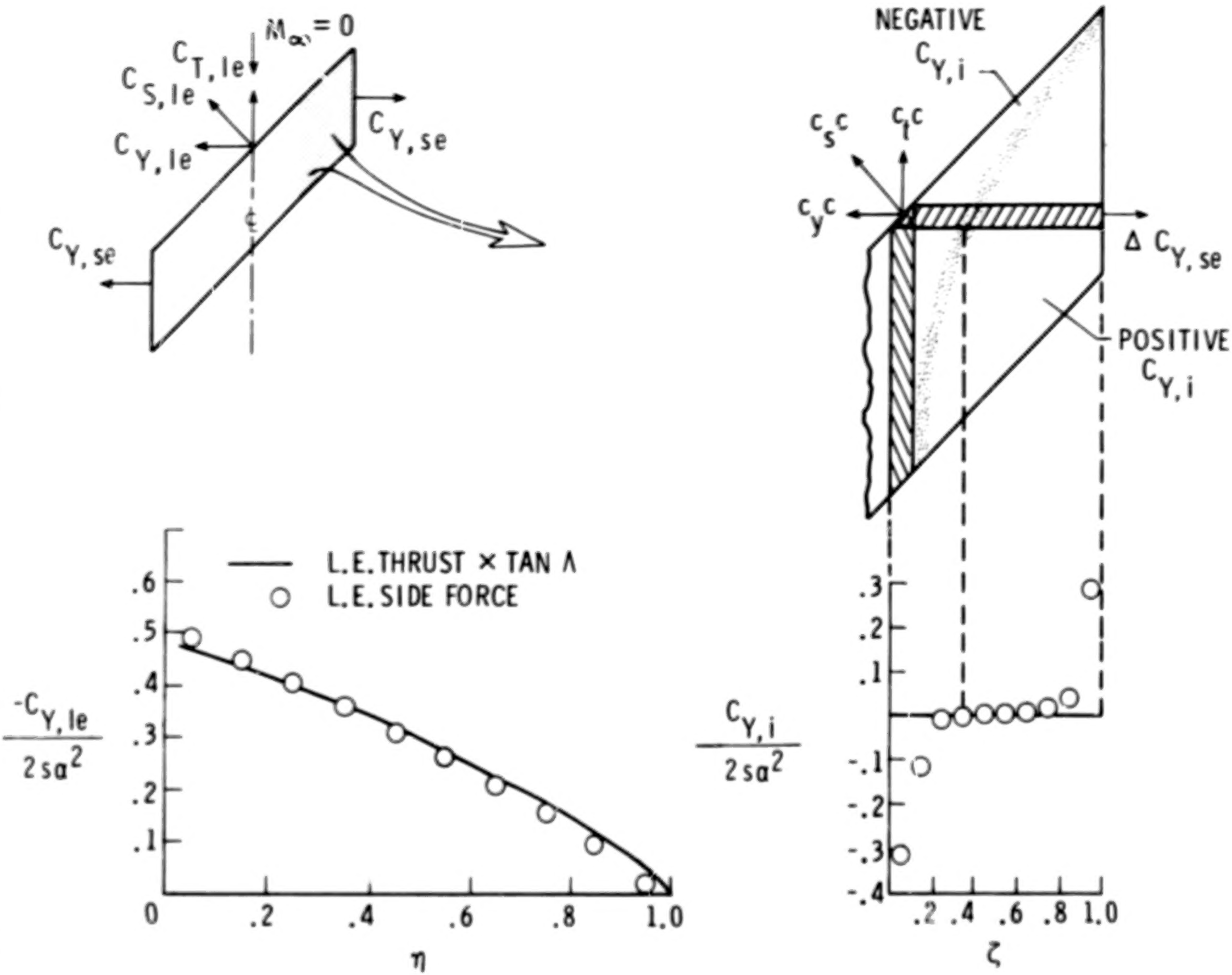

Figure 3.- Effect of forward sweep on side-edge suction. (α in radians.)

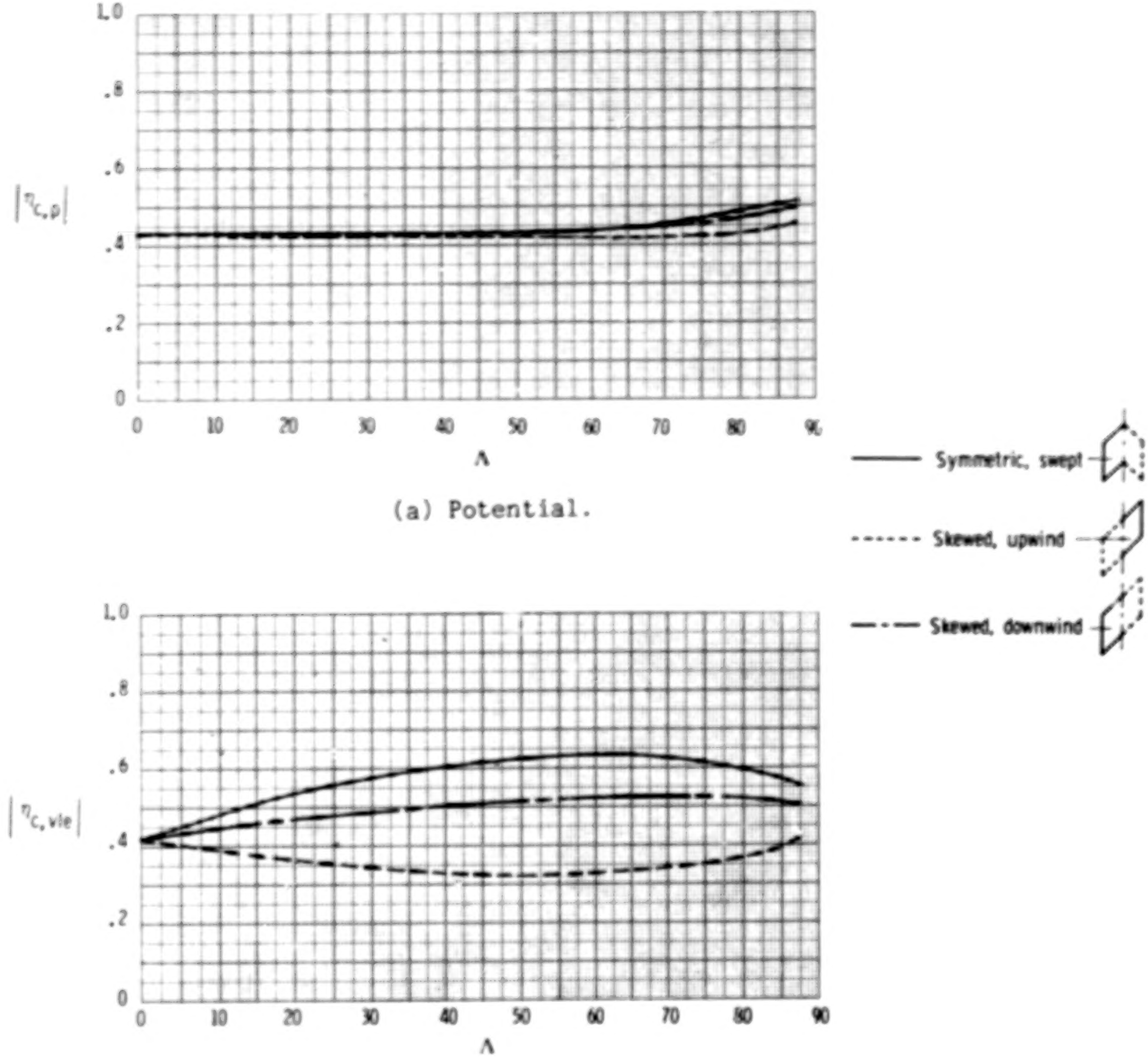

(a) Potential.

(b) Leading-edge vortex.

Figure 4.- Effect of sweep on centroids of theoretical lift factors for wing semispan. A = 1.0; M_∞ = 0.

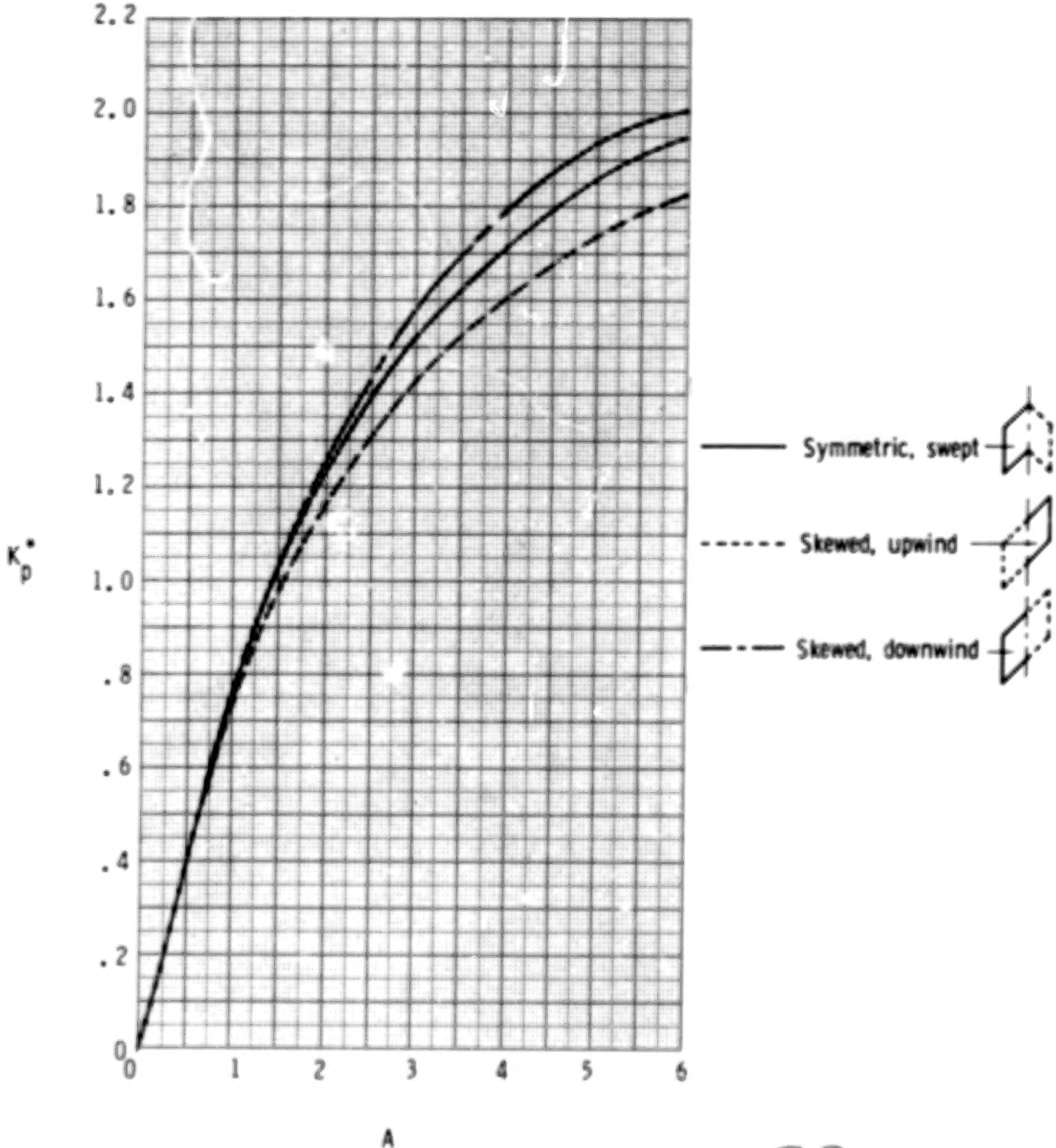

38

(a) K_p^*.

Figure 5.- Effect of aspect ratio on theoretical lift factors for wing semispan. $\Lambda = 30^{\circ}$; $M_{\infty} = 0$.

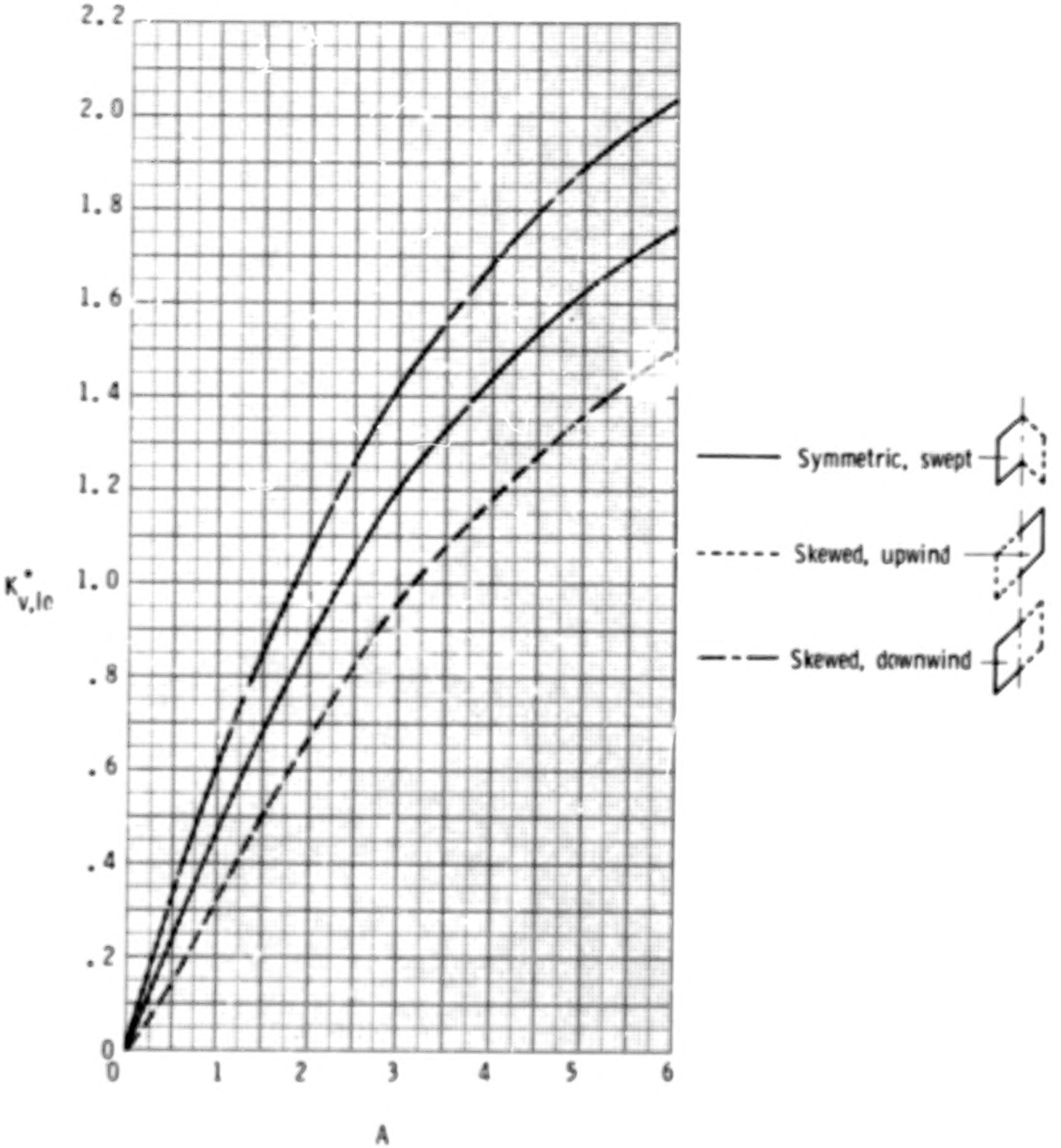

(b) $K^*_{v,le}$.

Figure 5.- Continued.

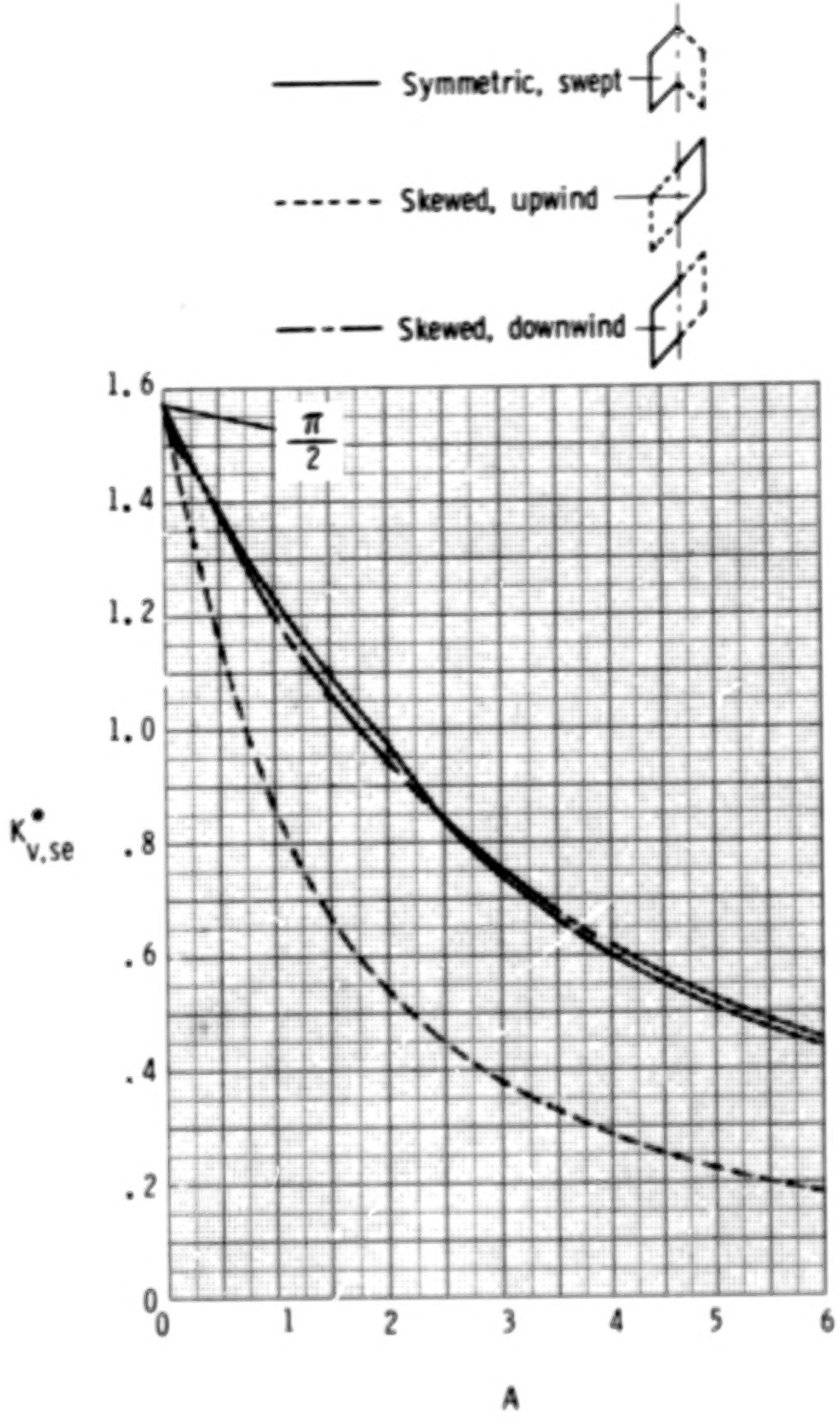

(c) $K^{\bullet}_{v,se}$.

Figure 5.- Concluded.

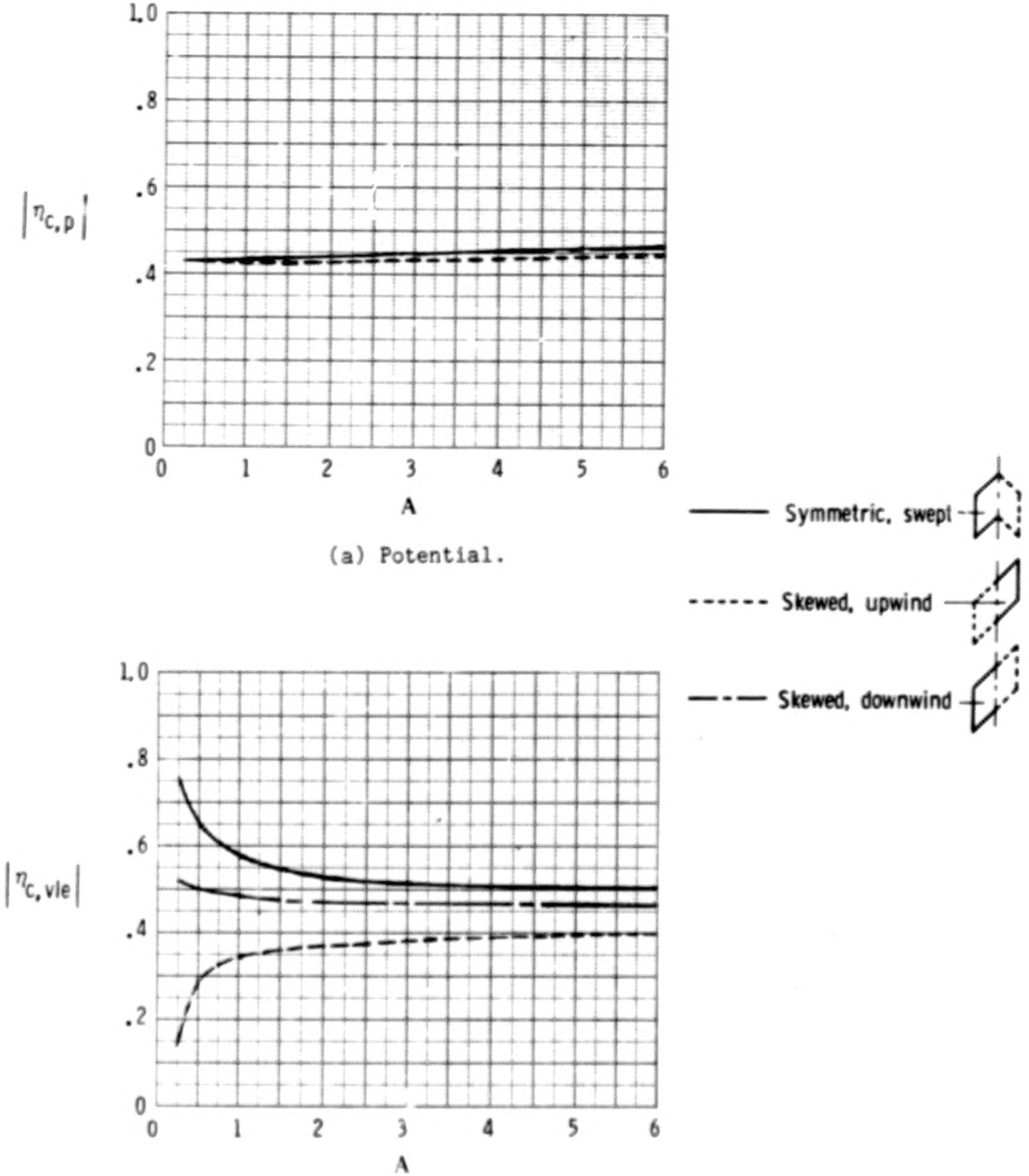

(a) Potential.

(b) Leading-edge vortex.

Figure 6.- Effect of aspect ratio on centroids of theoretical lift factors for wing semispan. $\Lambda = 30^{\circ}$; $M_{\infty} = 0$.

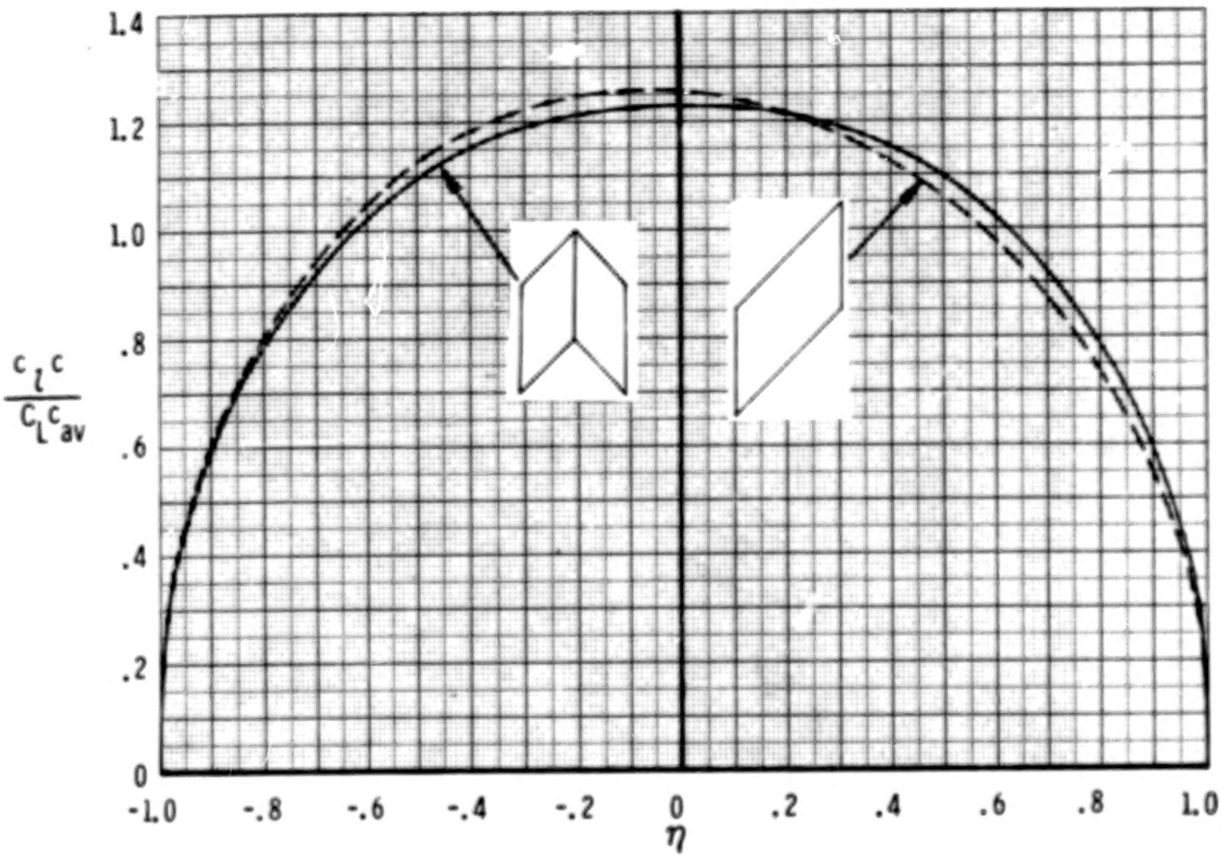

(a) Potential-span-load coefficient.

Figure 7.- Potential-span-load coefficient and section suction coefficient distributions on a swept wing and on a skewed wing. $\Lambda = 45^{\circ}$; $A = 1.0$; $M_{\infty} = 0$.

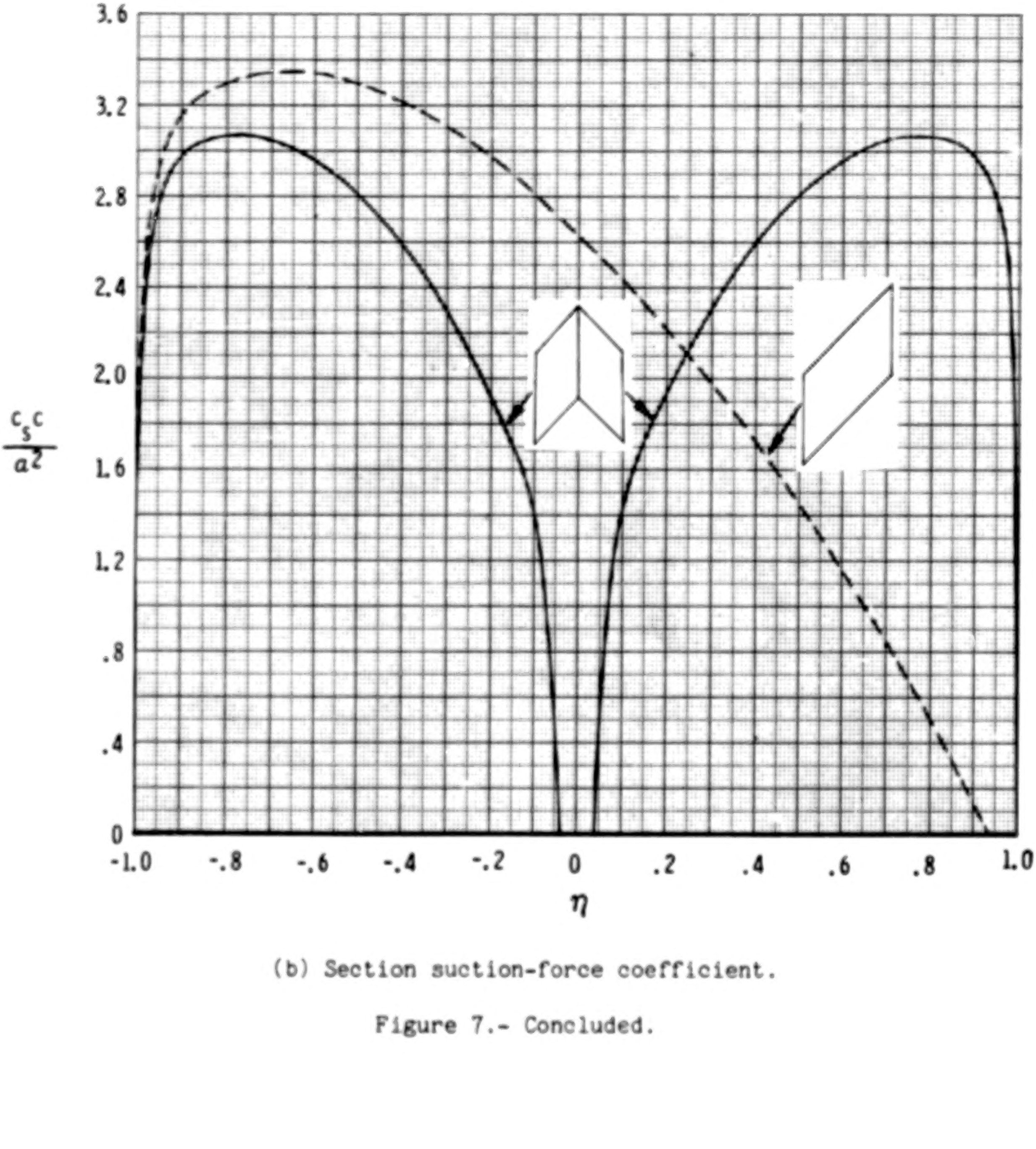

(b) Section suction-force coefficient.

Figure 7.- Concluded.

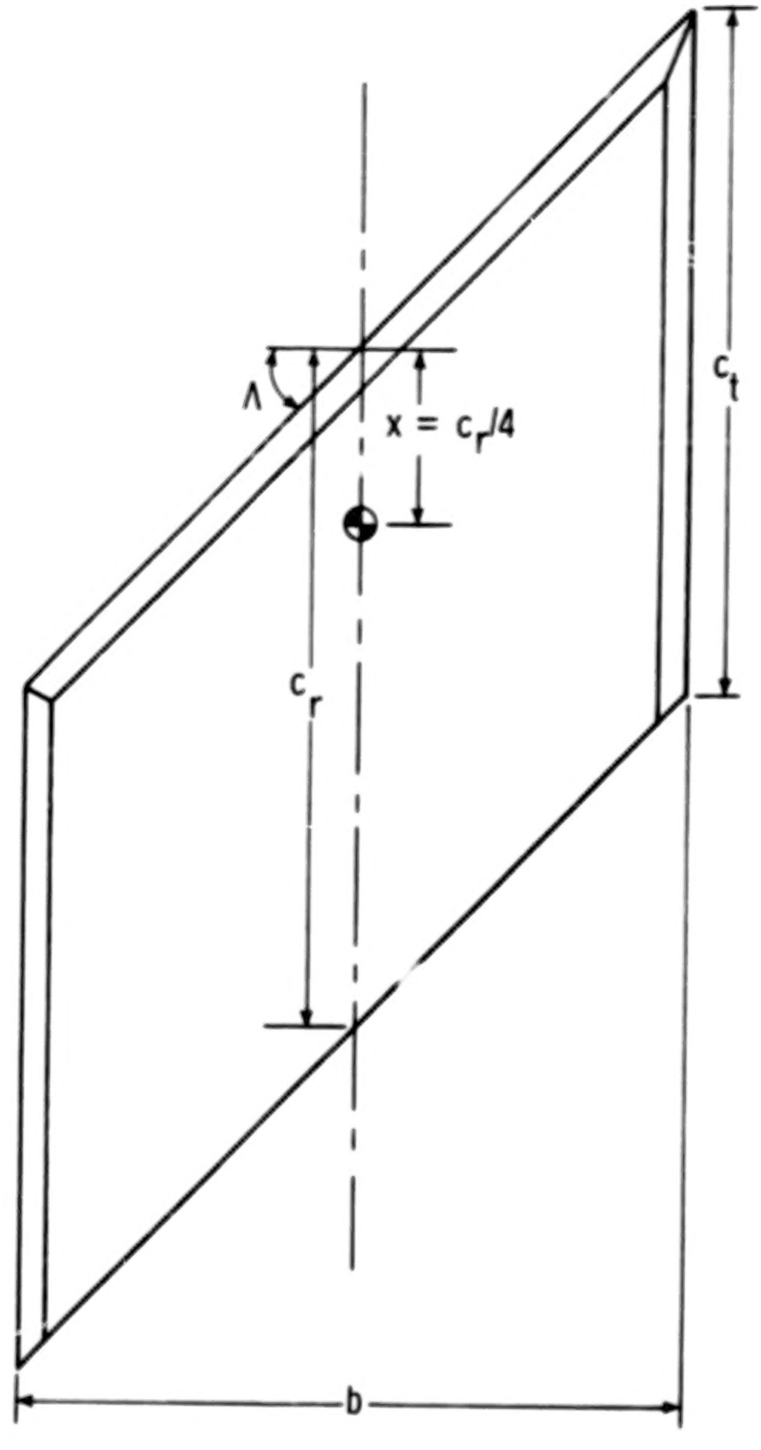

(a) Models I, II, III. IV, and V.

Figure 8.- General layout of model planforms. (See table I.)

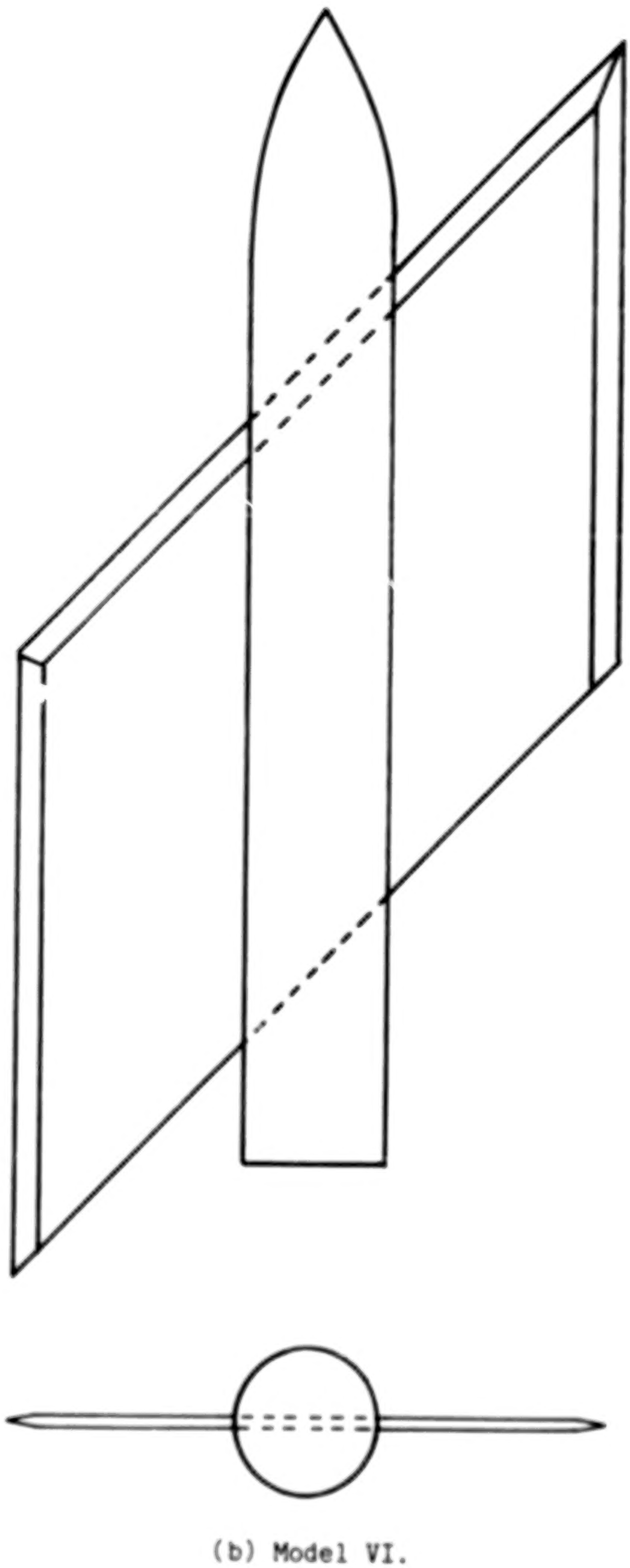

(b) Model VI.

Figure 8.- Concluded.

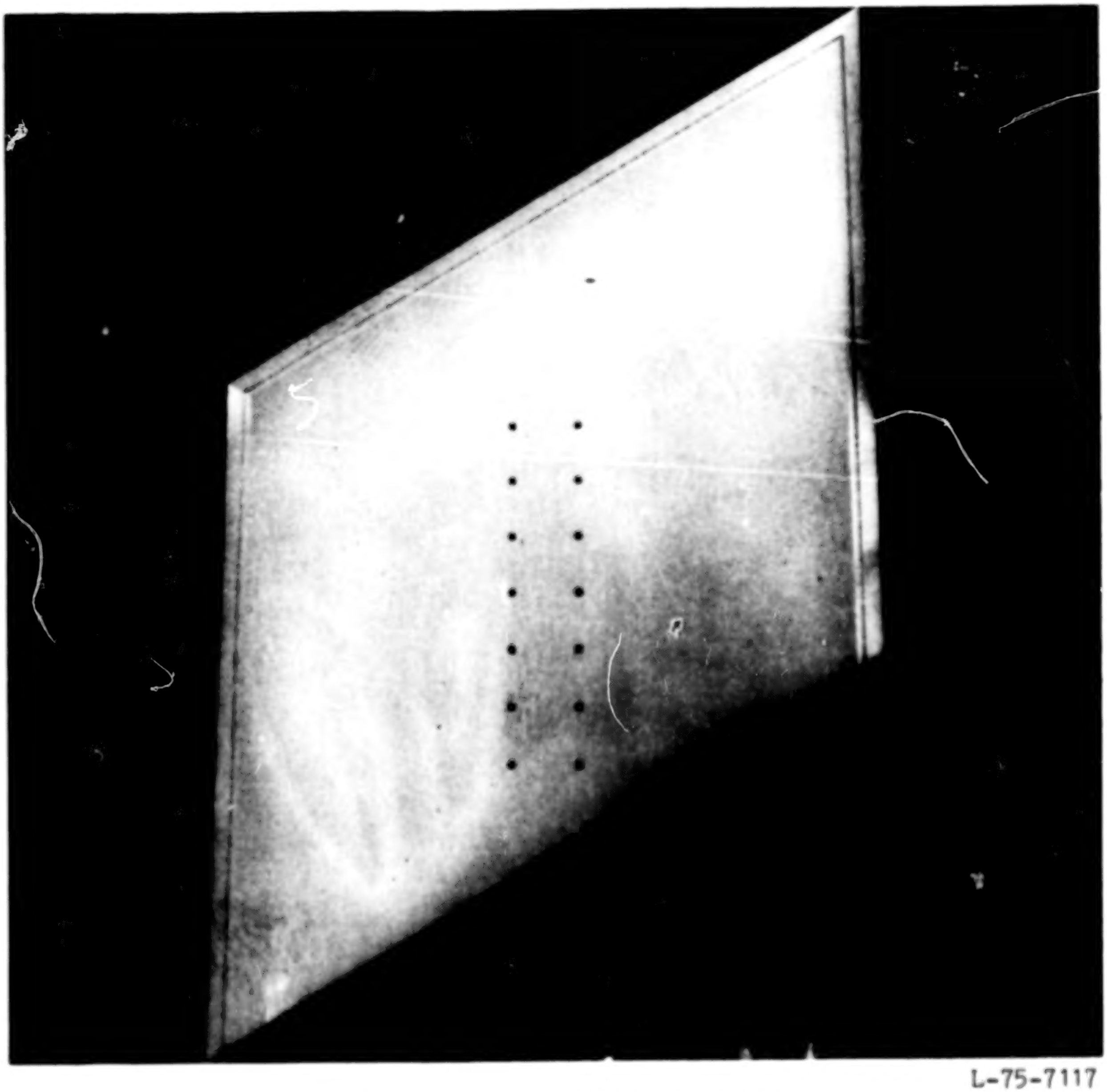

L-75-7117

(a) Model I, $\Lambda = 30^{\circ}$, $A = 1.0$.

Figure 9.- Model planforms.

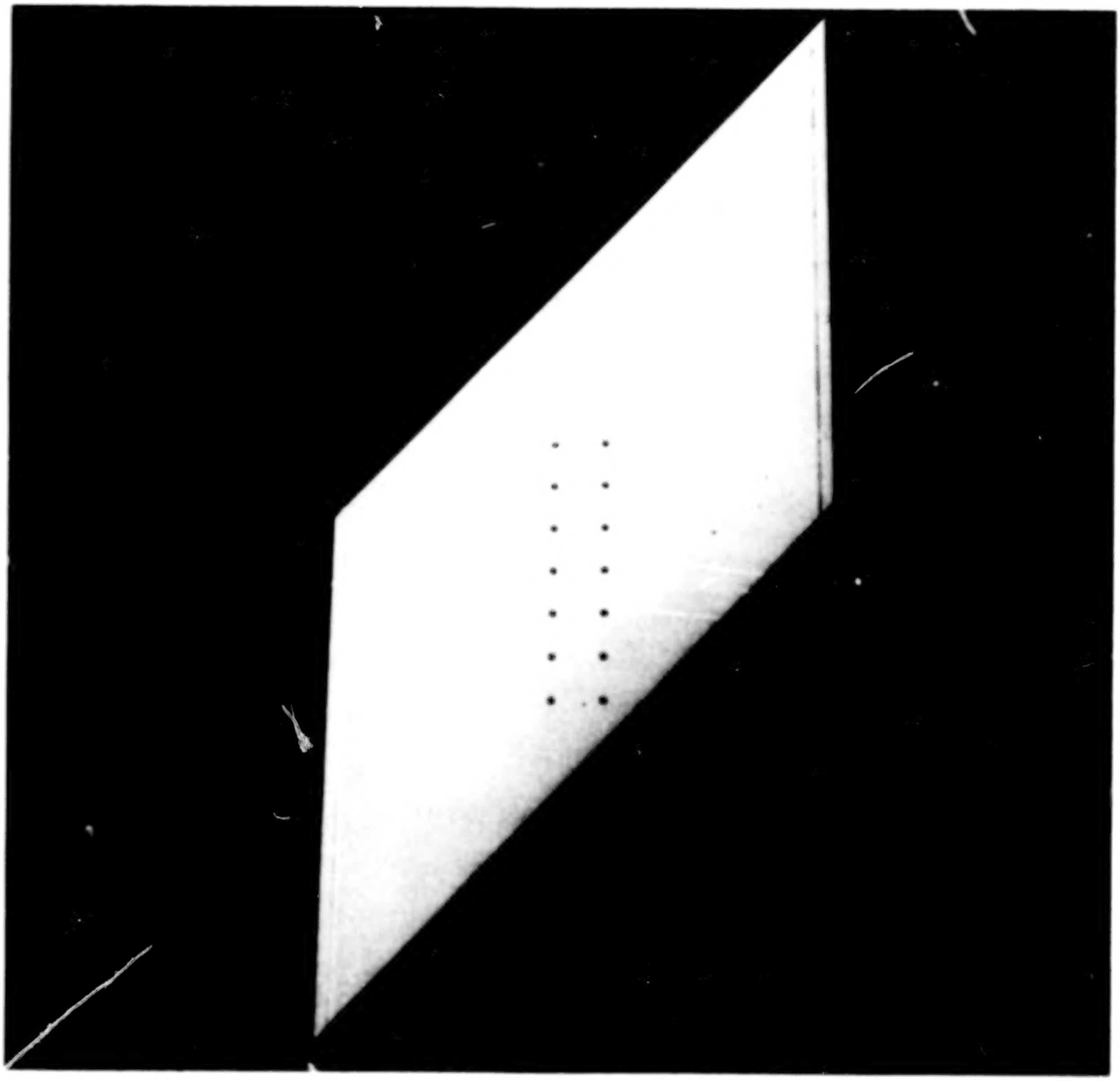

L-75-7119

(b) Model II, $\Lambda = 45^{\circ}$, $A = 1.0$.

Figure 9.- Continued.

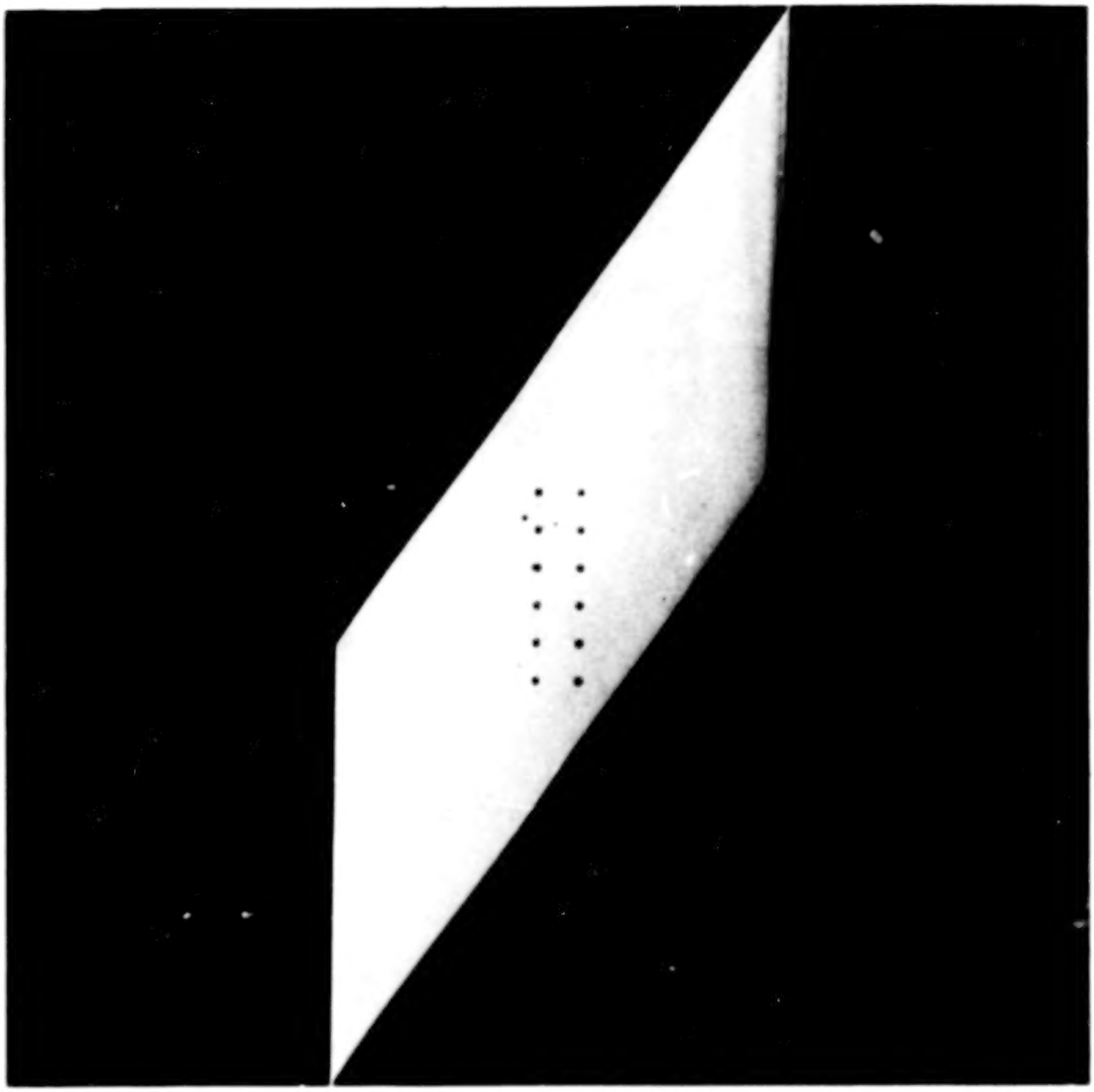

L-75-7120

(c) Model III, $\Lambda = 55^{\circ}$, $A = 1.0$.

Figure 9.- Continued.

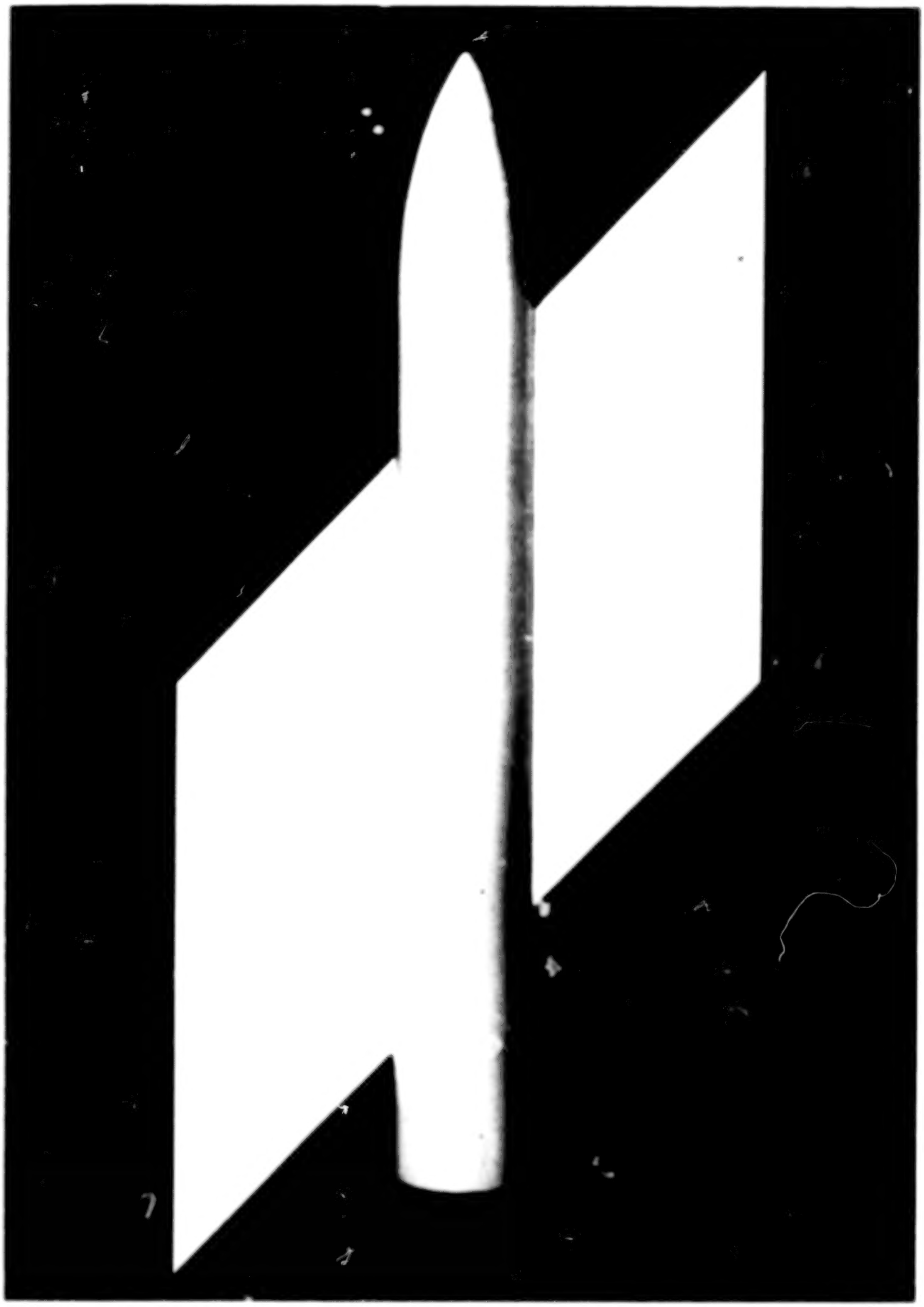

L-75-8372

(d) Model VI, $\Lambda = 45^{\circ}$, $A = 1.0$.

Figure 9.- Concluded.

119

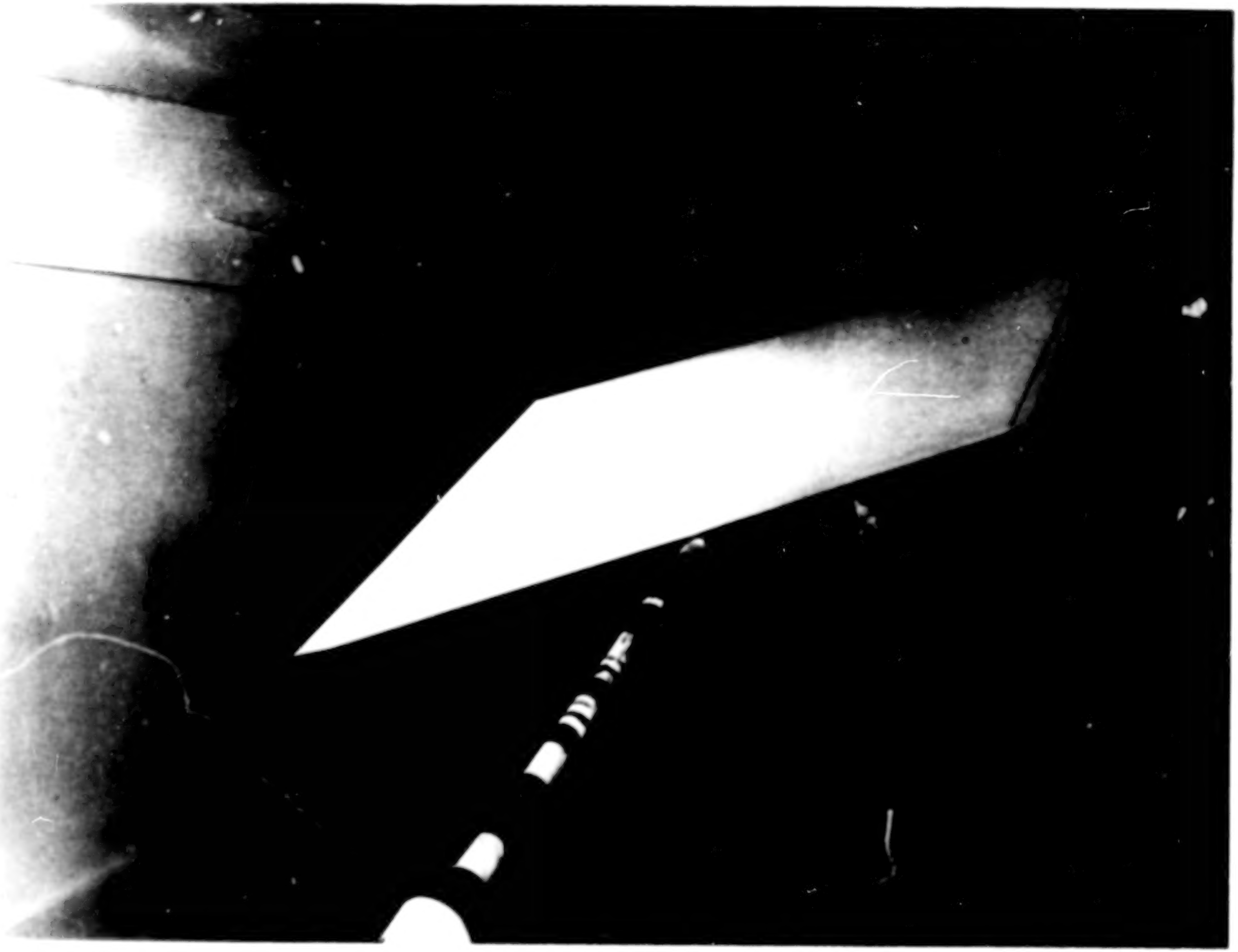

L-75-7134

(a) One-quarter rear view of model II.

Figure 10.- Installation of model.

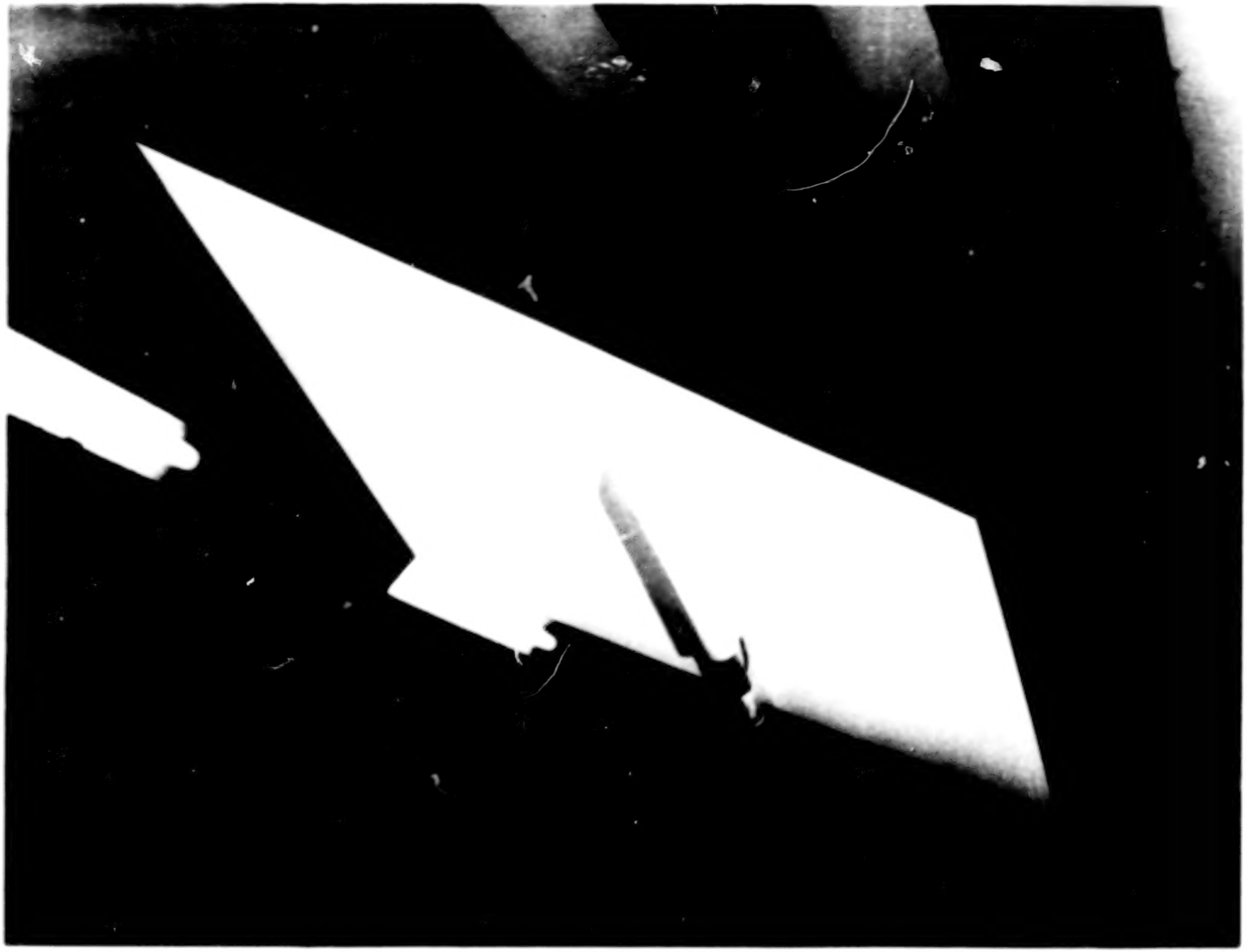

L-75-7133

(b) One-quarter front view of model II.

Figure 10.- Concluded.

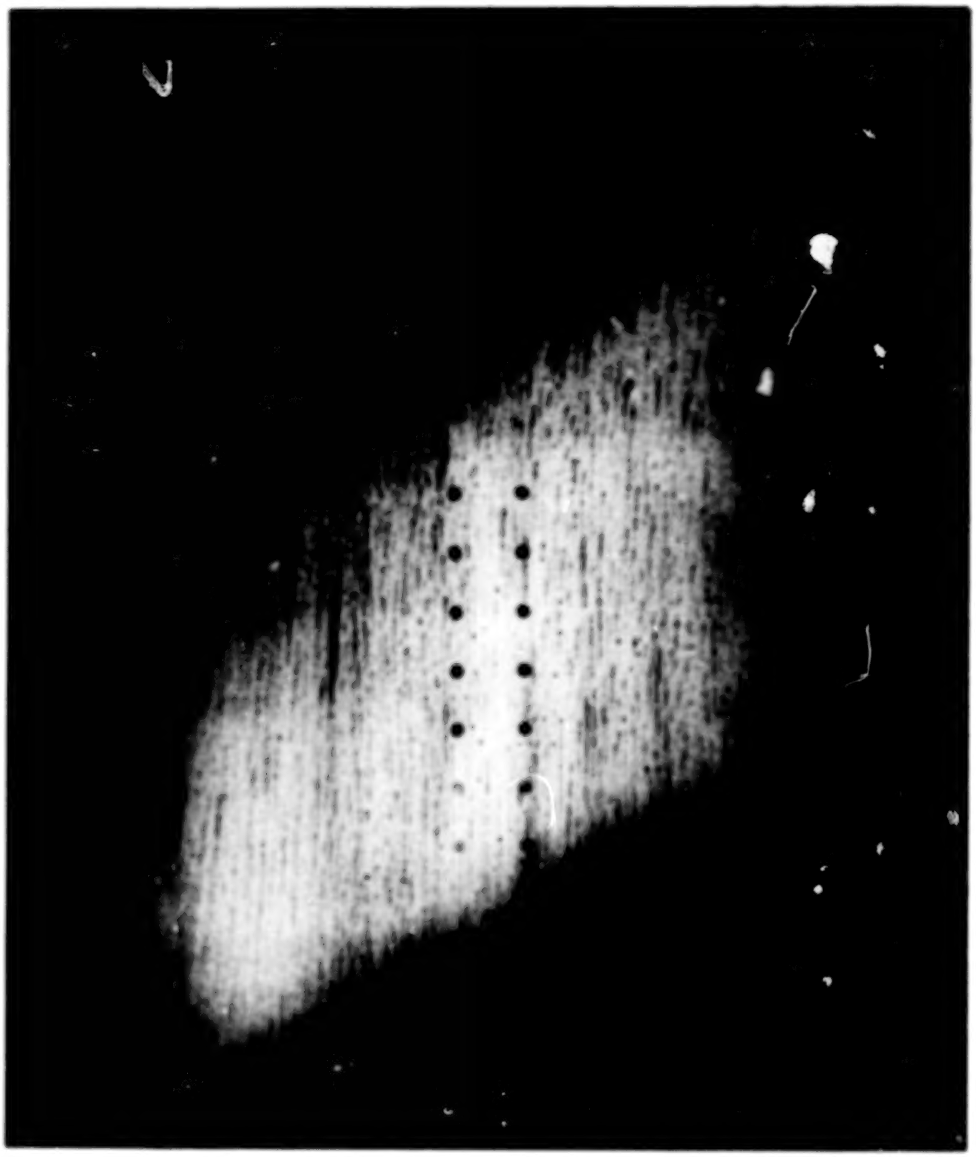

L-77-315

(a) $\alpha = 5^{\circ}$.

Figure 11.- Oil-flow patterns on model I. $\Lambda = 30^{\circ}$; $A = 1.0$; $M_{\infty} = 0.12$.

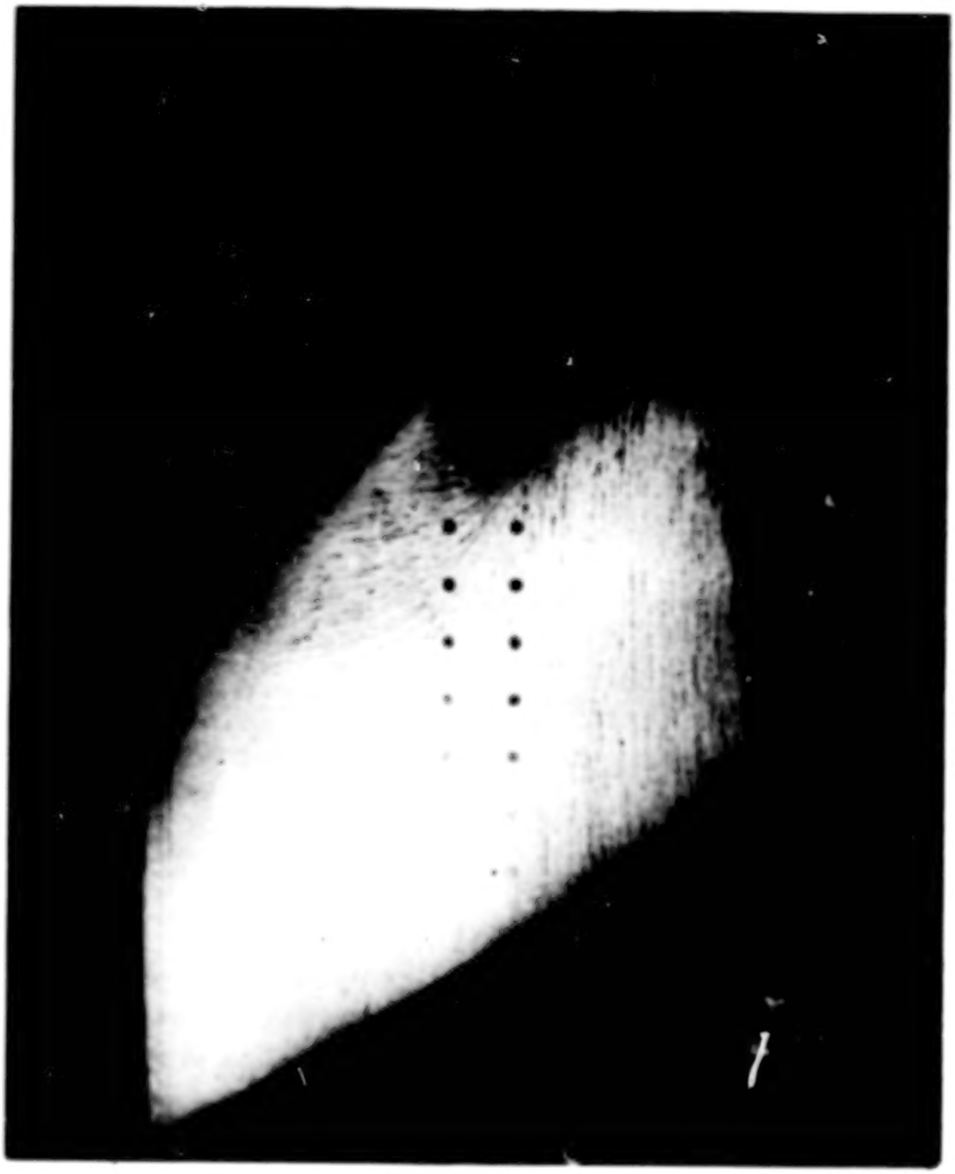

L-77-316

(b) $\alpha = 10^{\circ}$.

Figure 11.- Continued.

L-77-317

(c) $\alpha = 15^{\circ}$.

Figure 11.- Concluded.

L-77-318

(a) $\alpha \approx 5^{\circ}$.

Figure 12.- Oil-flow patterns on model II. $\Lambda = 45^{\circ}$; $A = 1.0$; $M_{\infty} \approx 0.12$.

L-77-319

(b) $\alpha \approx 10^{\circ}$.

Figure 12.- Continued.

L-77-320

(c) $\alpha \approx 15^{\circ}$.

Figure 12.- Concluded.

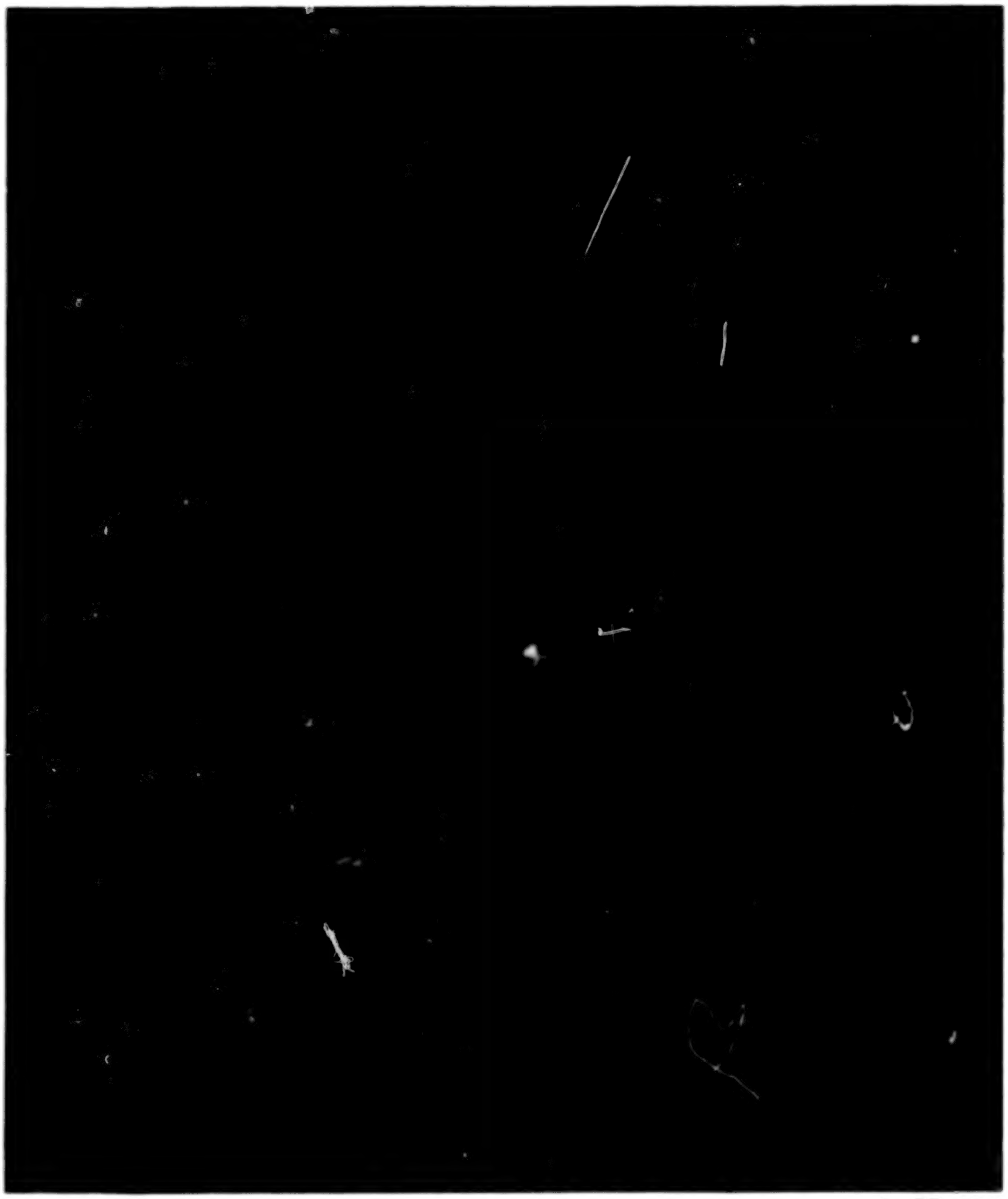

L-77-321

(a) $\alpha \approx 5^{\circ}$.

Figure 13.- Oil-flow patterns on model III. $\Lambda = 55^{\circ}$; $A = 1.0$; $M_{\infty} \approx 0.12$.

L-77-322

(b) $\alpha \approx 10^{\circ}$.

Figure 13.- Continued.

L-77-323

(c) $\alpha = 15^{\circ}$.

Figure 13.- Concluded.

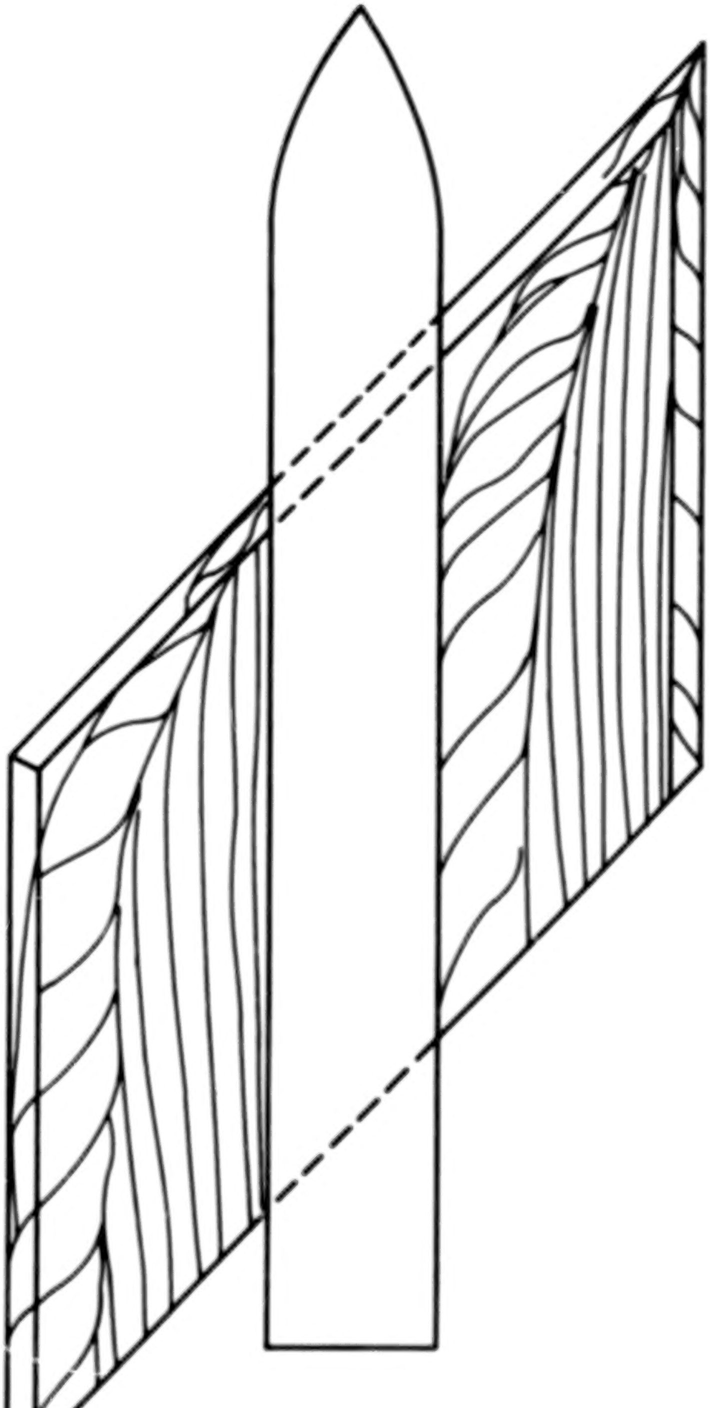

(a) Low angle of attack.

Figure 14.- Sketch of flow pattern on wing-fuselage model.

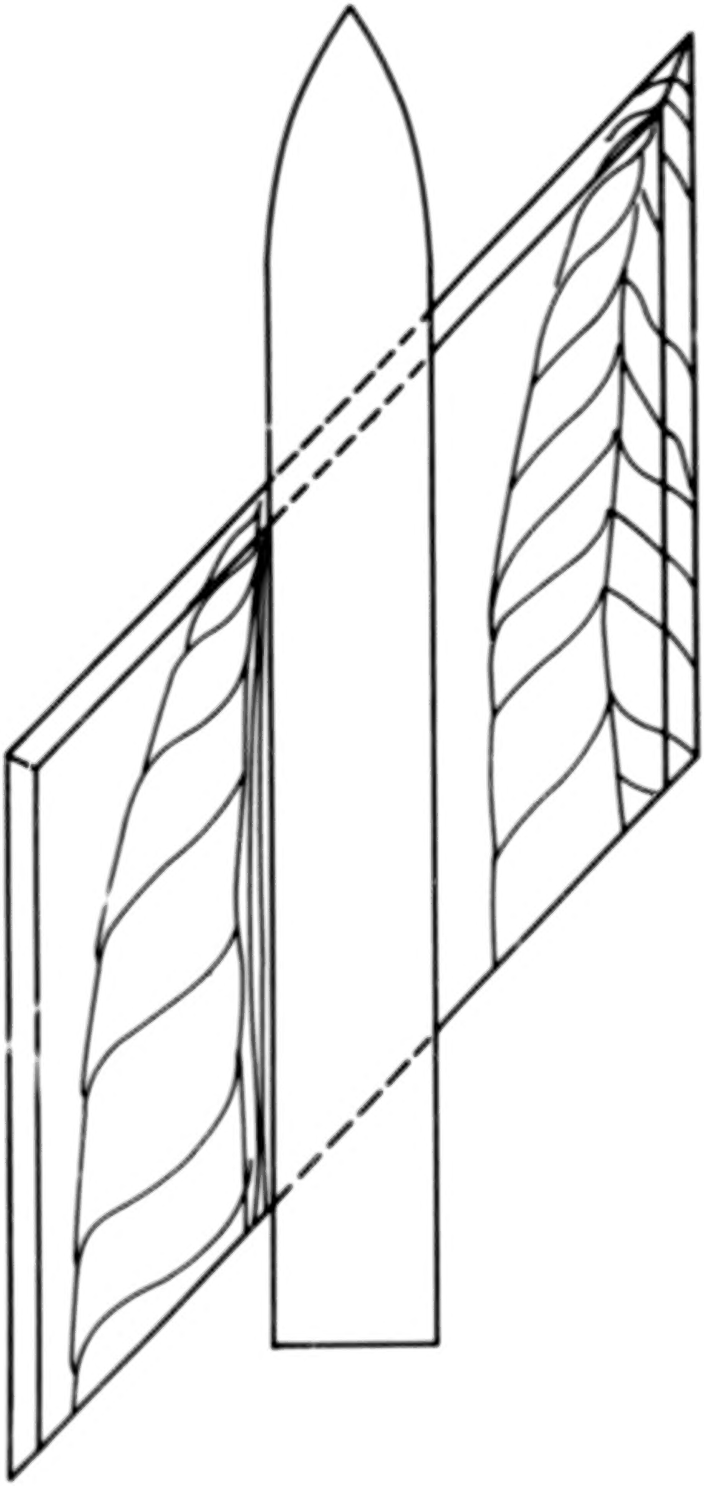

(b) High angle of attack.

Figure 14.- Concluded.

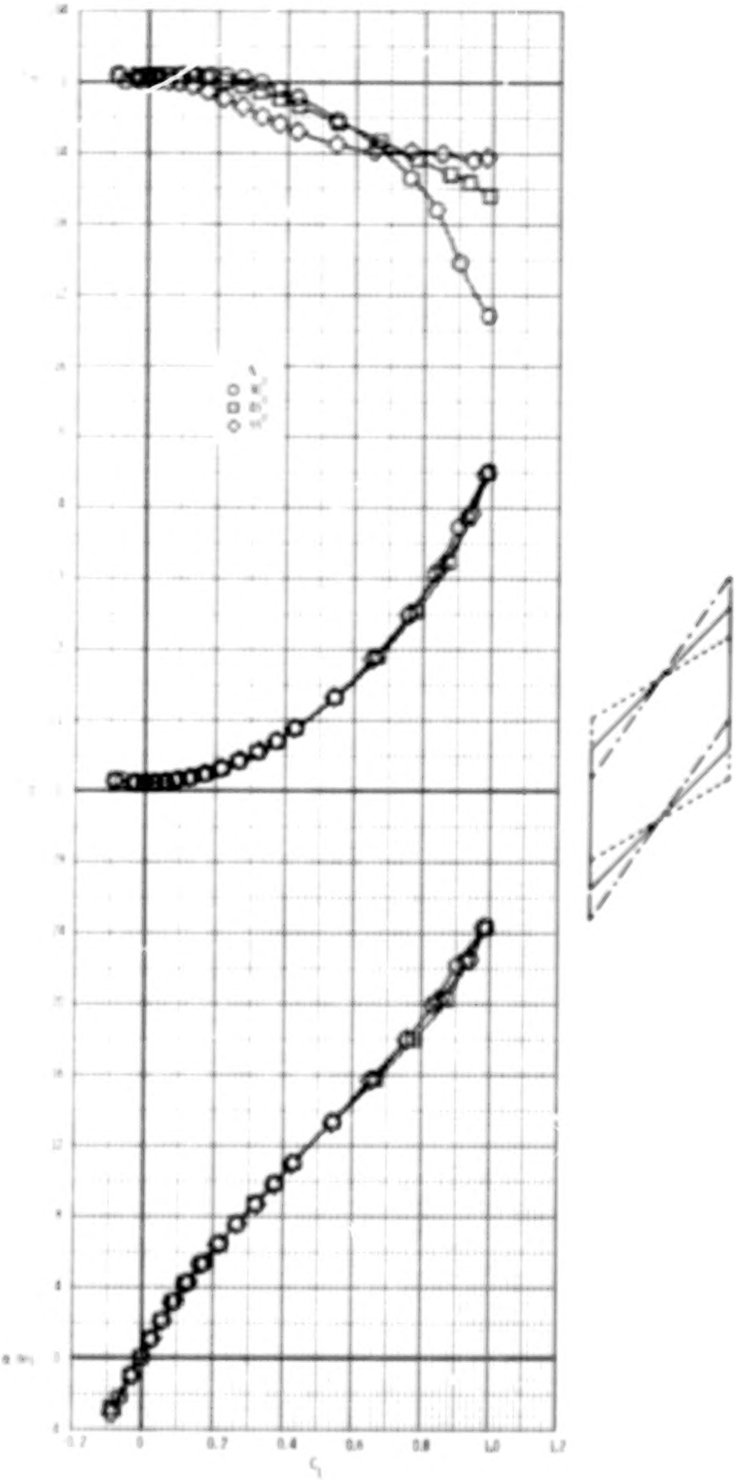

Figure 15.- Effect of leading-edge sweep on longitudinal aerodynamic characteristics of skewed wing. $A = 1.0$; $M_\infty = 0.12$.

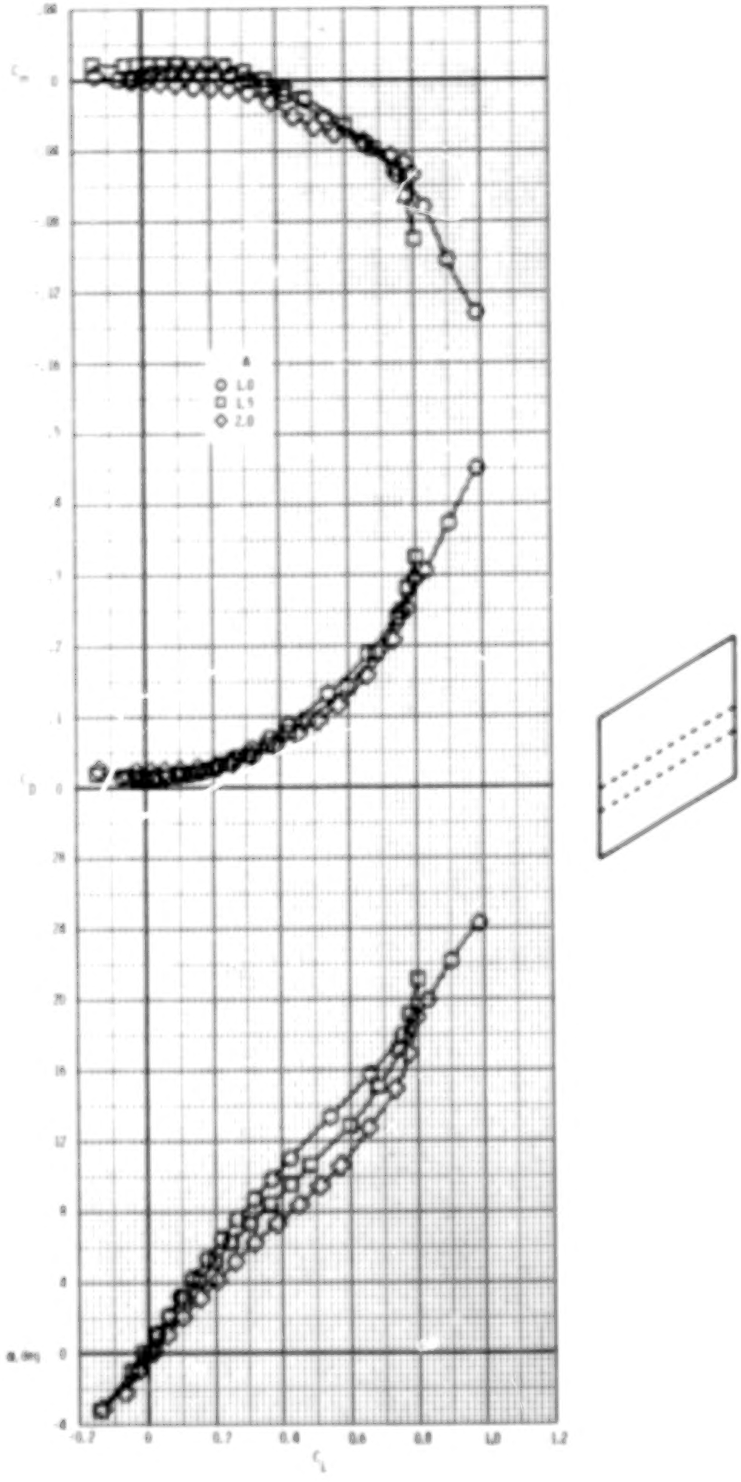

Figure 16.- Effect of aspect ratio on longitudinal aerodynamic characteristics of skewed wing. $\Lambda = 30^{\circ}$; $M_{\infty} = 0.12$.

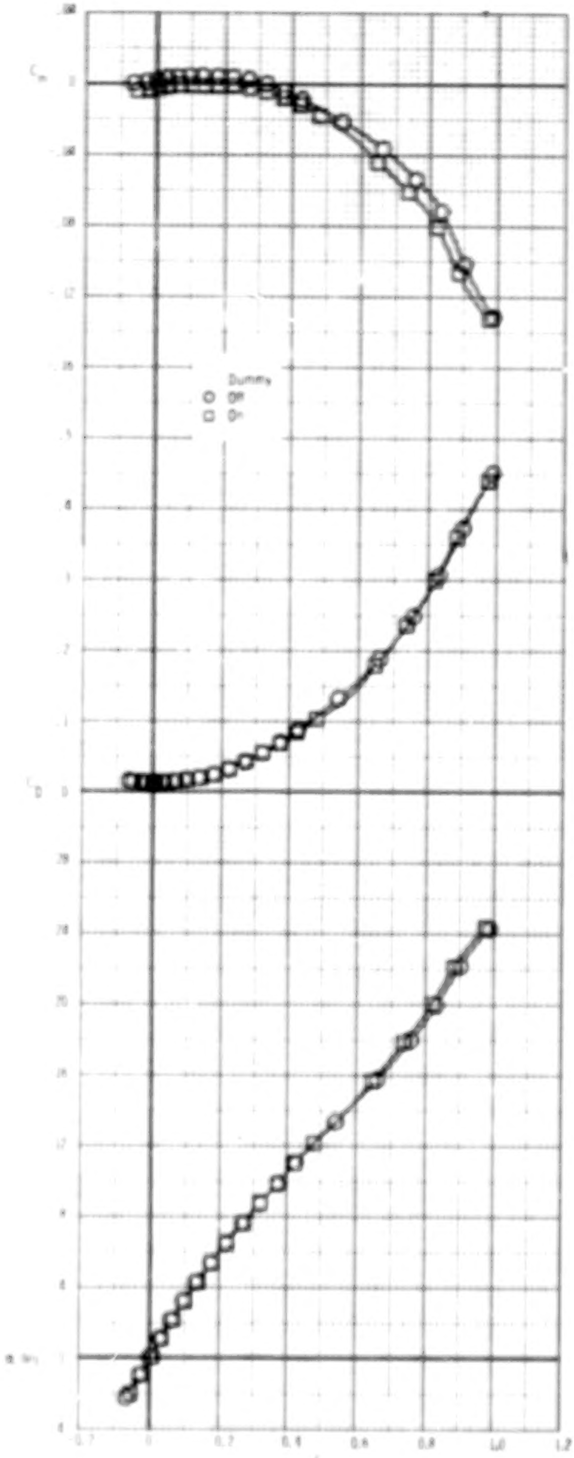

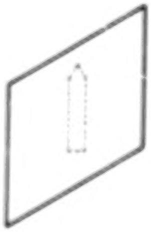

(a) $\Lambda = 30^{\circ}$, $A = 1.0$.

Figure 17.- Effect of dummy balance housing on longitudinal aerodynamic characteristics of skewed wing for models I to V, $M_{\infty} = 0.12$.

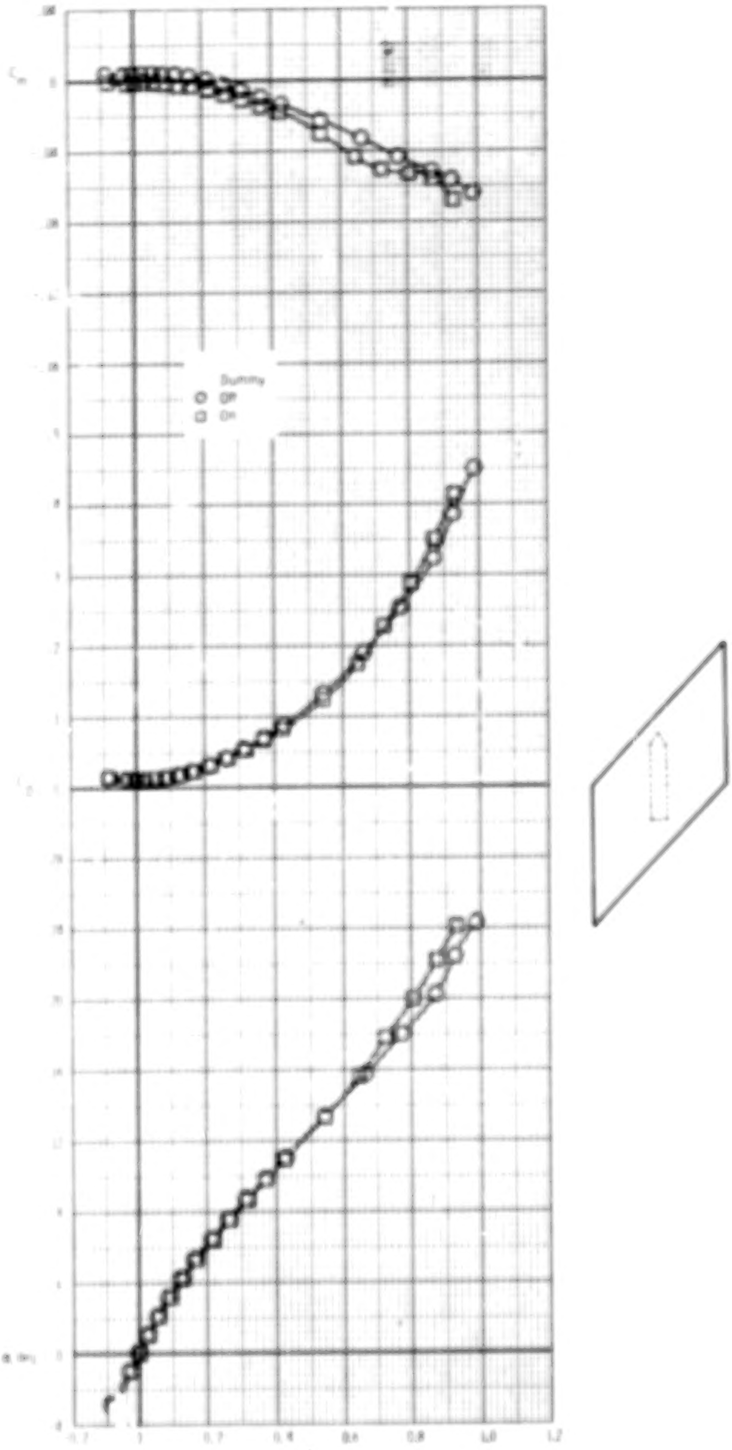

(b) $\Lambda = 45^{\circ}$, $A = 1.0$.

Figure 17.- Continued.

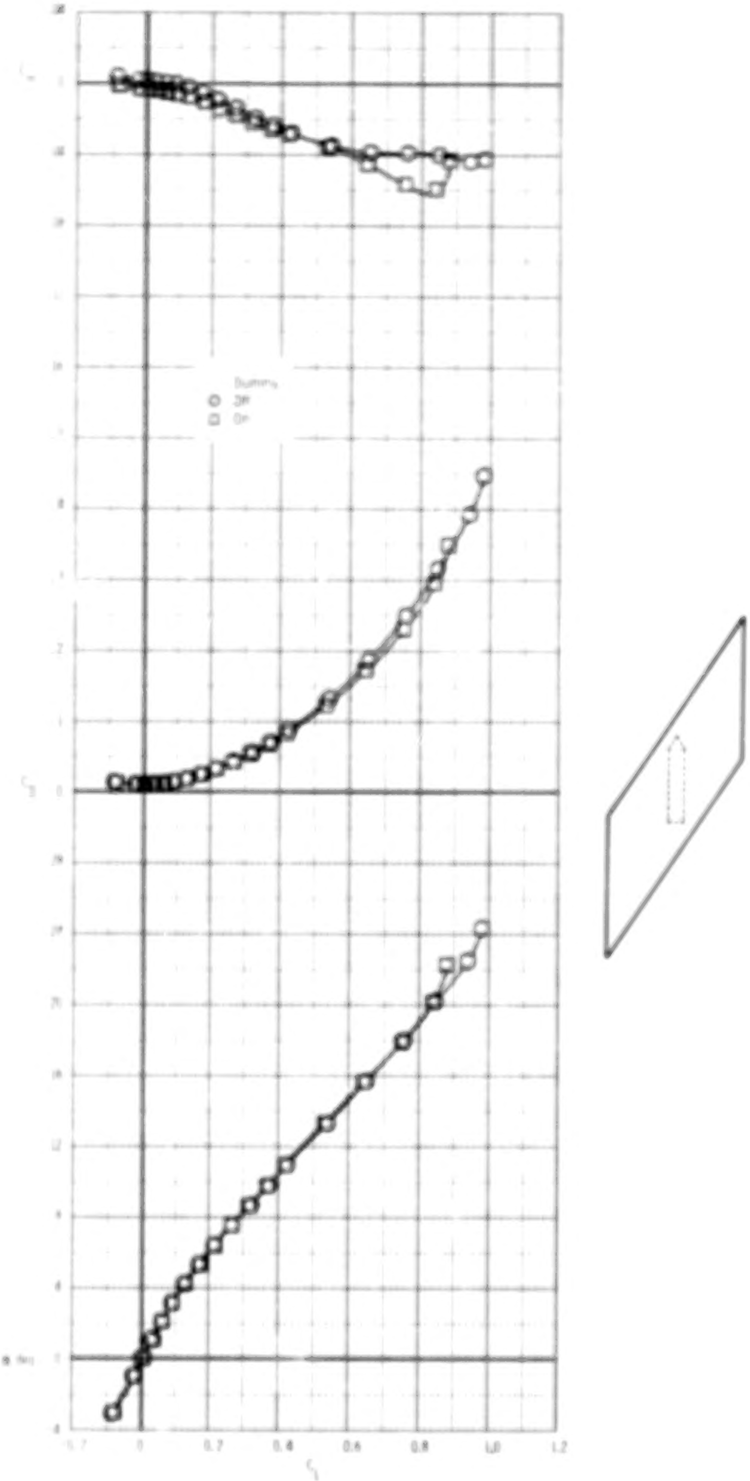

(c) $\Lambda = 55^{\circ}$, $A = 1.0$.

Figure 17.- Continued.

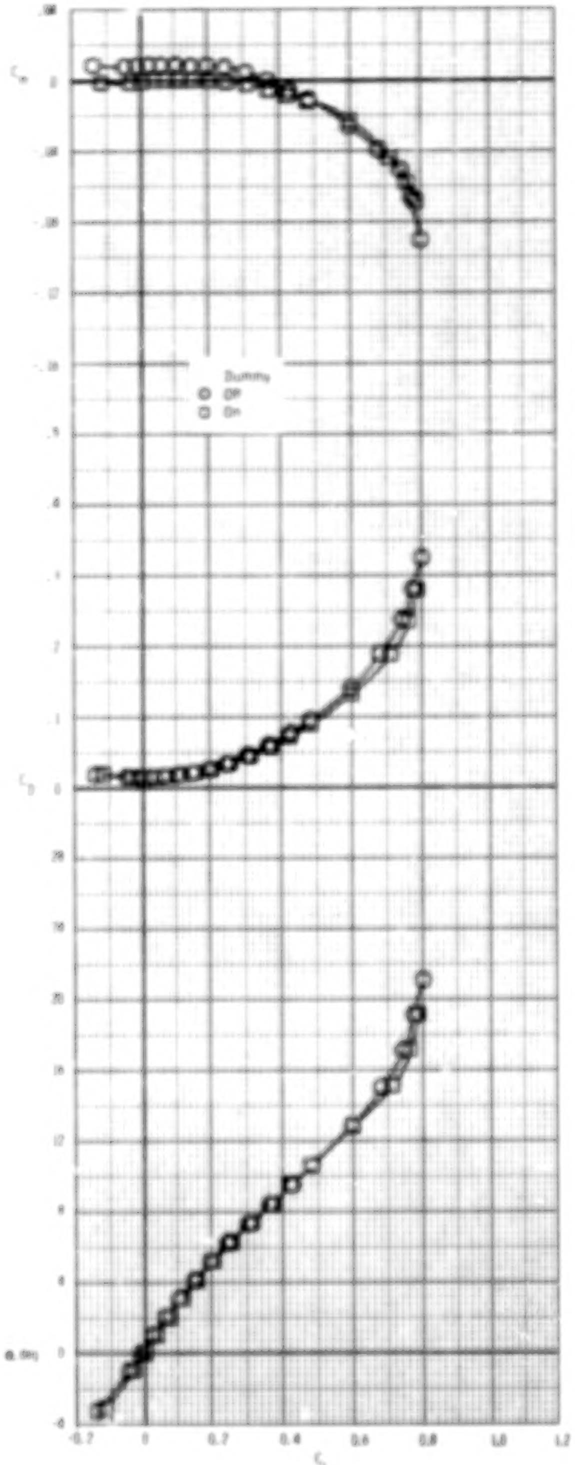

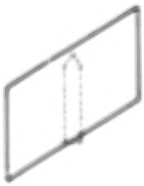

(d) $\Lambda = 30^{o}$, $A = 1.5$.

Figure 17.- Continued.

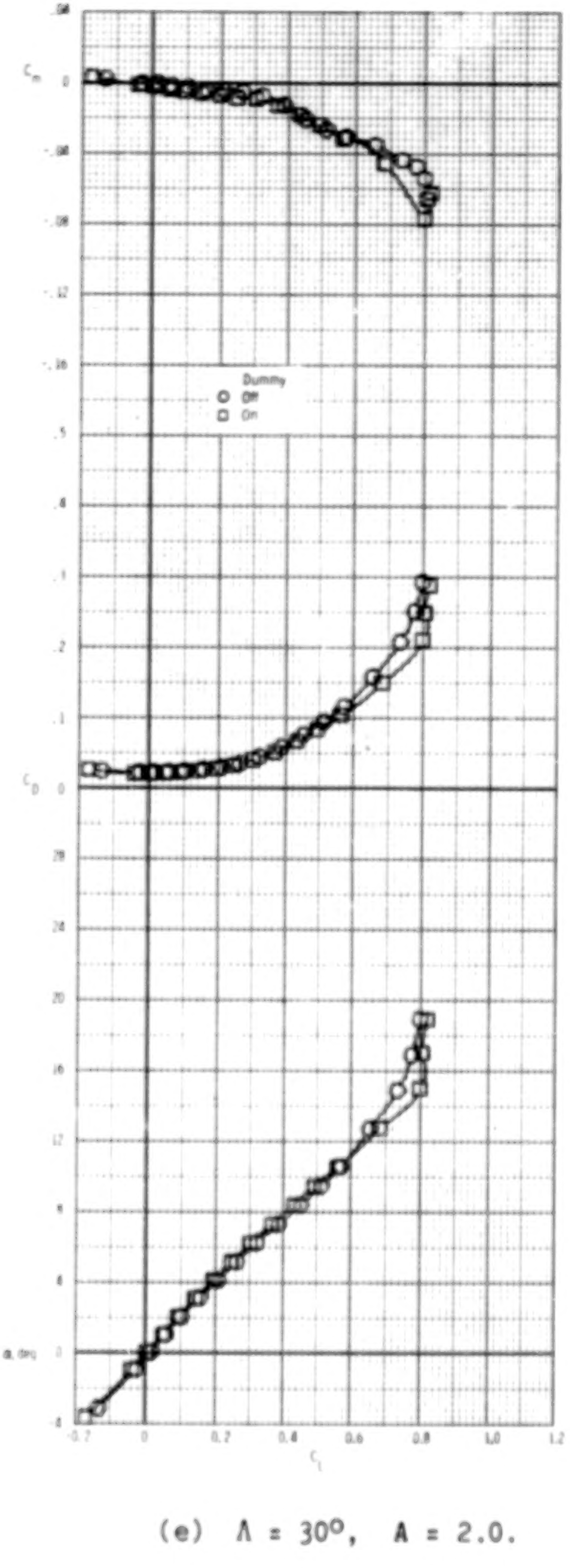

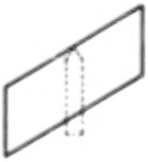

(e) $\Lambda = 30^{\circ}$, $A = 2.0$.

Figure 17.- Concluded.

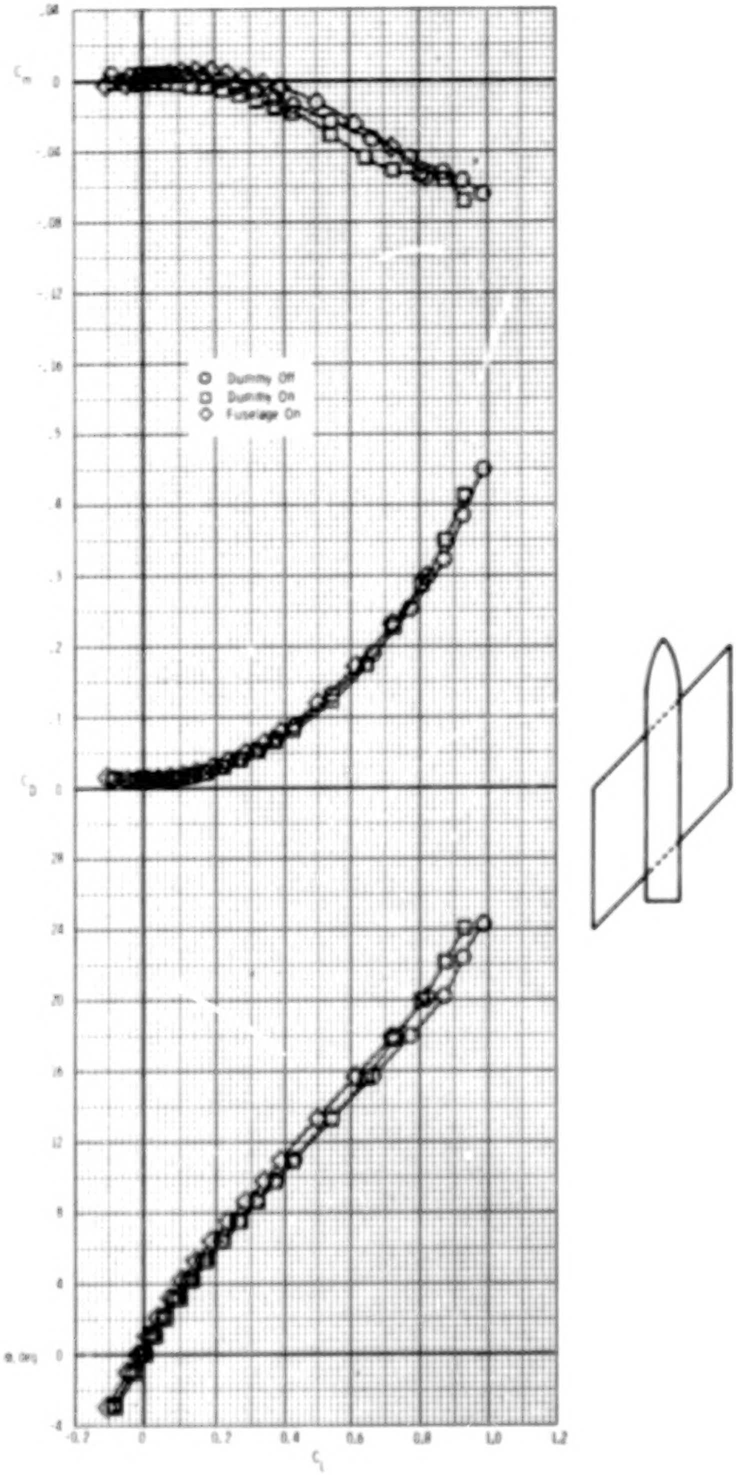

Figure 18.- Effect of cylindrical fuselage and dummy balance housing on longitudinal aerodynamic characteristics of skewed wings. $\Lambda = 45^{\circ}$; $A = 1.0$; $M_{\infty} = 0.12$.

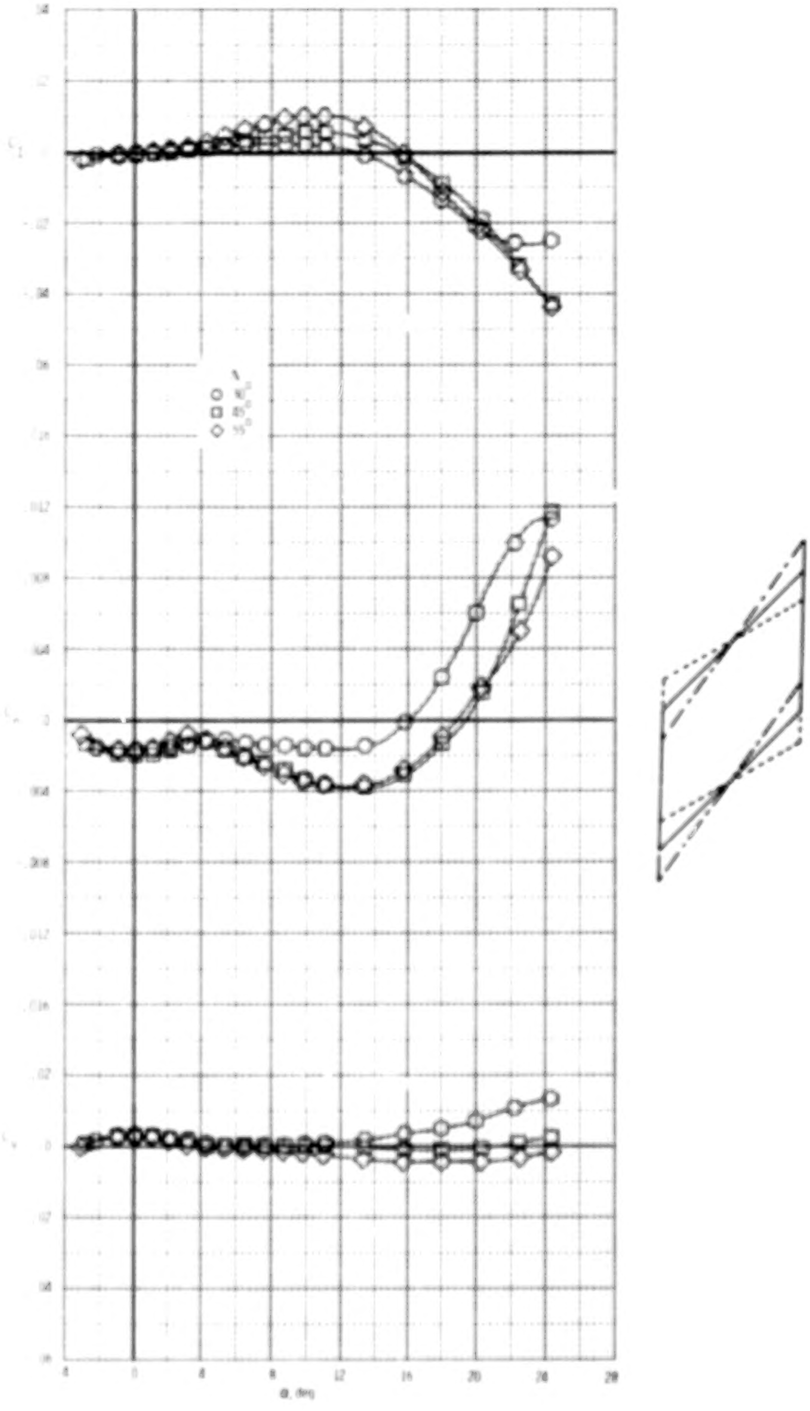

Figure 19.- Effect of leading-edge sweep on lateral-directional aerodynamic characteristics of skewed wings. $\beta = 0^{o}$; $A = 1.0$; $M_{\infty} = 0.12$.

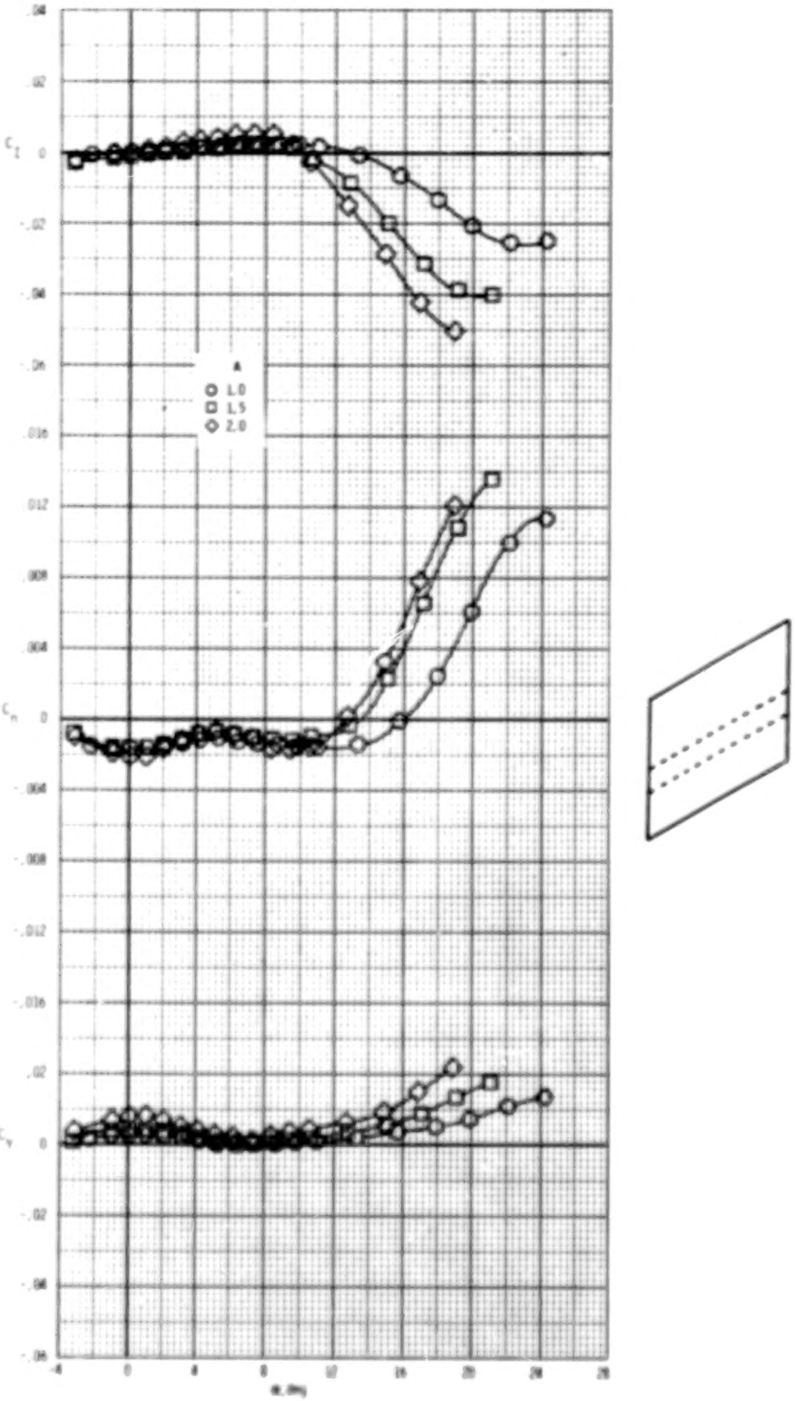

Figure 20.- Effect of aspect ratio on lateral-directional aerodynamic characteristics of skewed wings. $\beta = 0^{\circ}$; $\Lambda = 30^{\circ}$; $M_{\infty} = 0.12$.

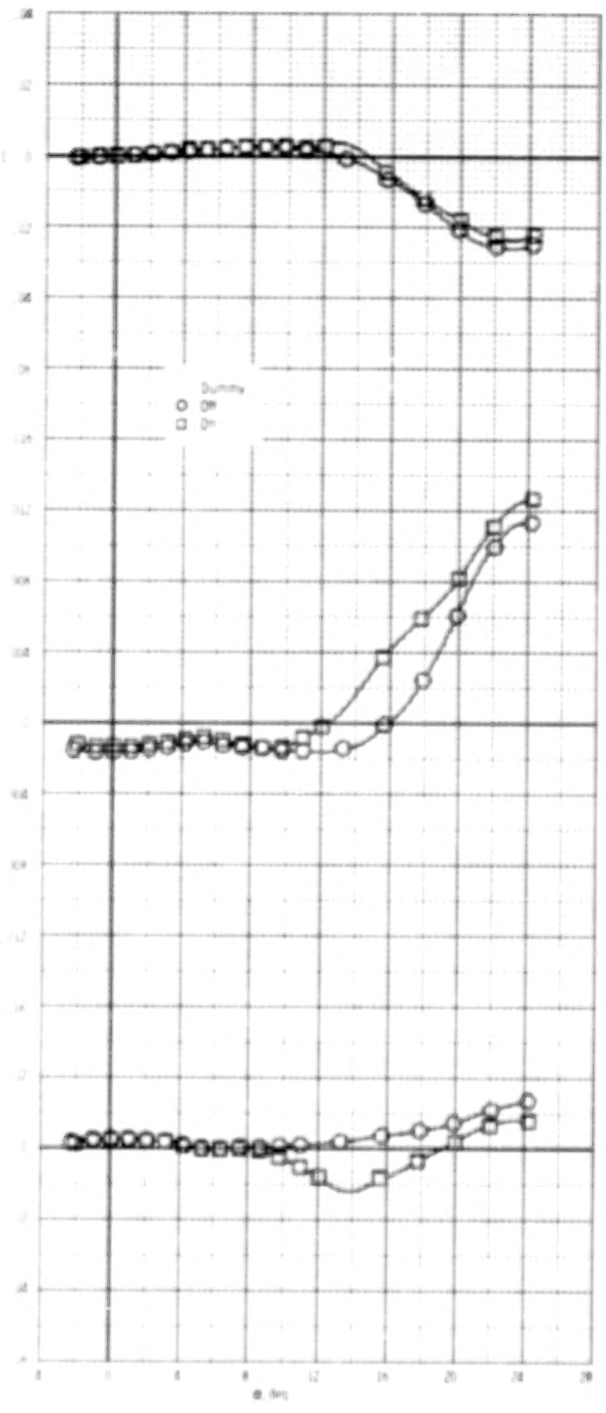

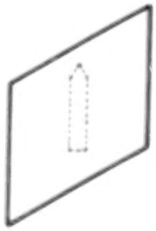

(a) $\Lambda = 30^{\circ}$, $A = 1.0$.

Figure 21.- Effect of dummy balance housing on lateral-directional aerodynamic characteristics of skewed wings. $\beta = 0^{\circ}$; $M_{\infty} = 0.12$.

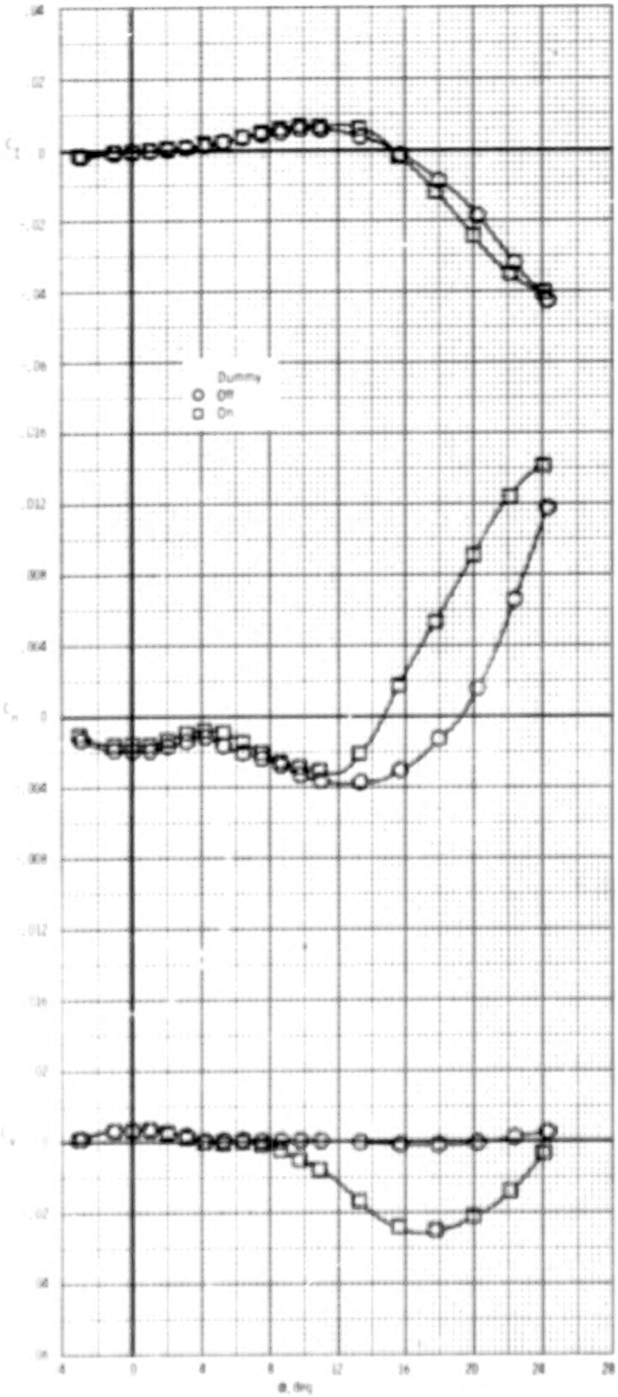

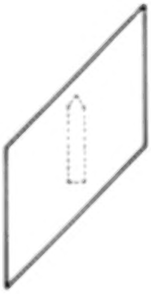

(b) $\Lambda = 45^{o}$, $A = 1.0$.

Figure 21.- Continued.

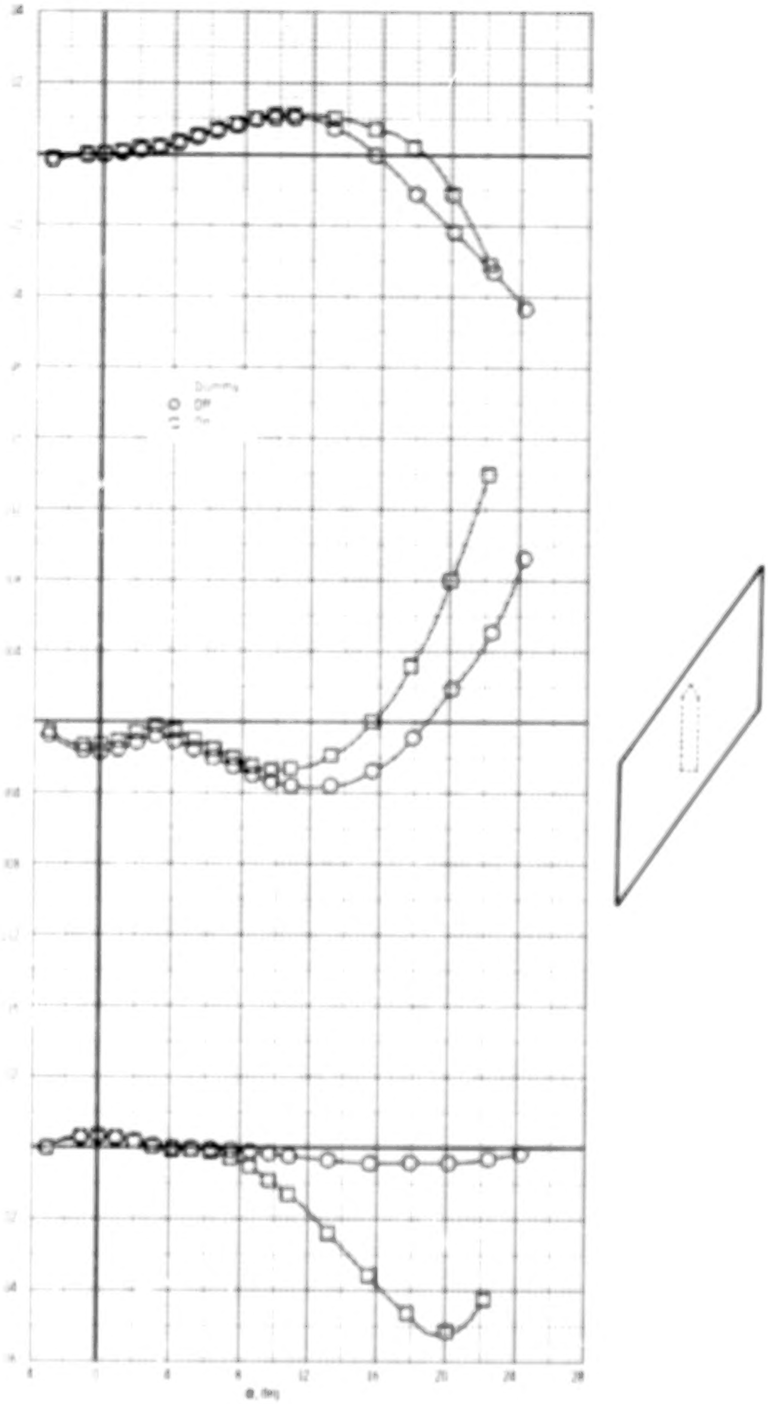

(c) $\Lambda = 55^{\circ}$, $A = 1.0$.

Figure 21.- Continued.

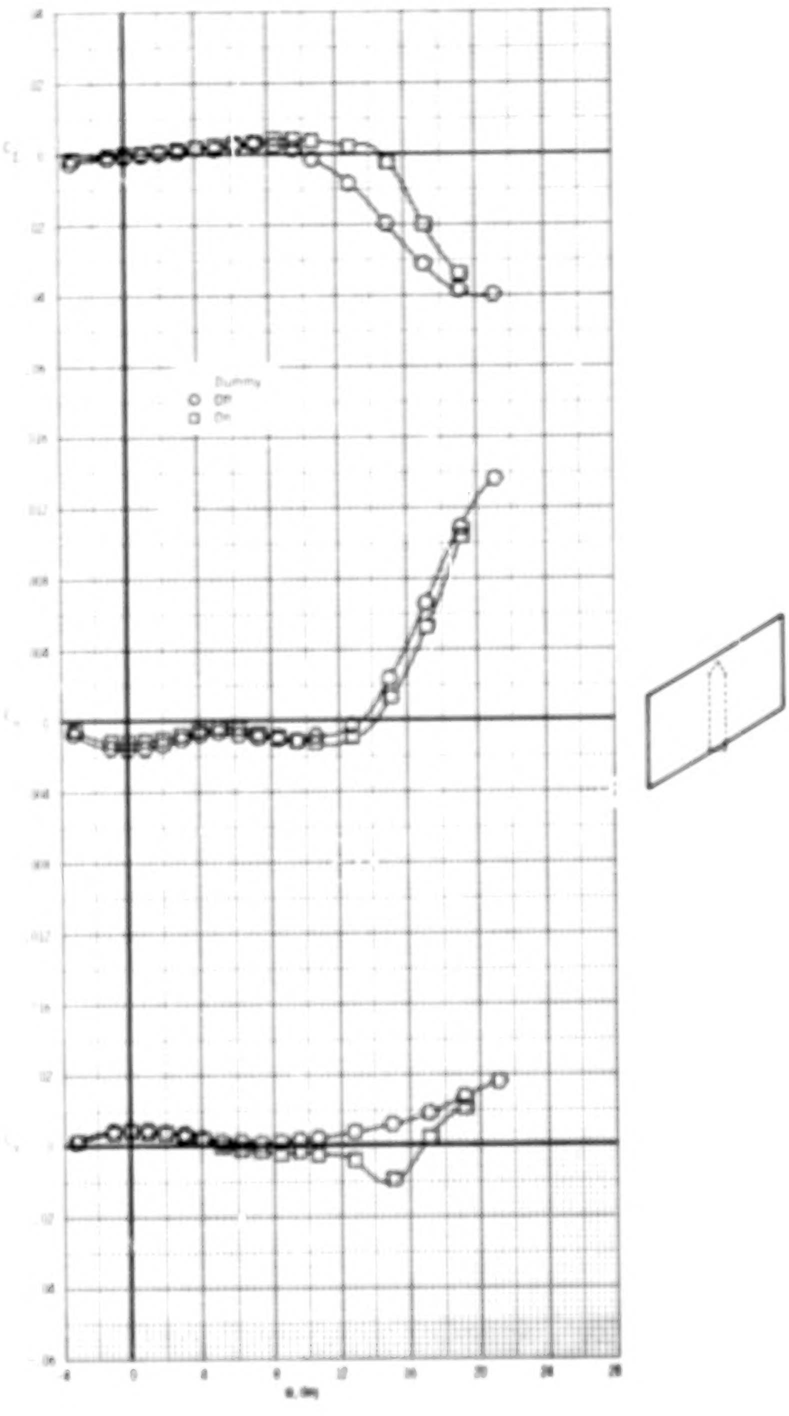

(d) $\Lambda = 30^{\circ}$, $A = 1.5$.

Figure 21.- Continued.

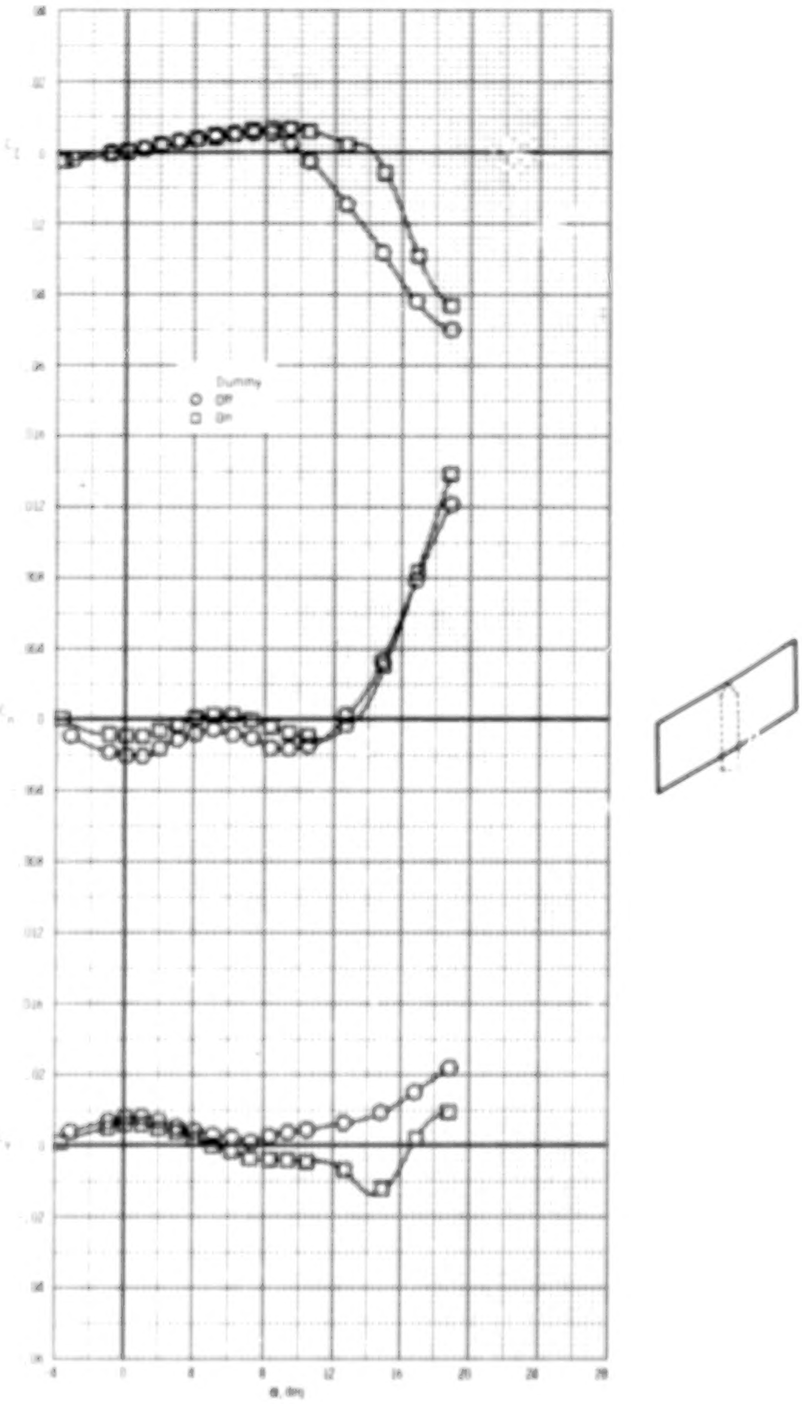

(e) Λ = 30°, A = 2.0.

Figure 21.- Concluded.

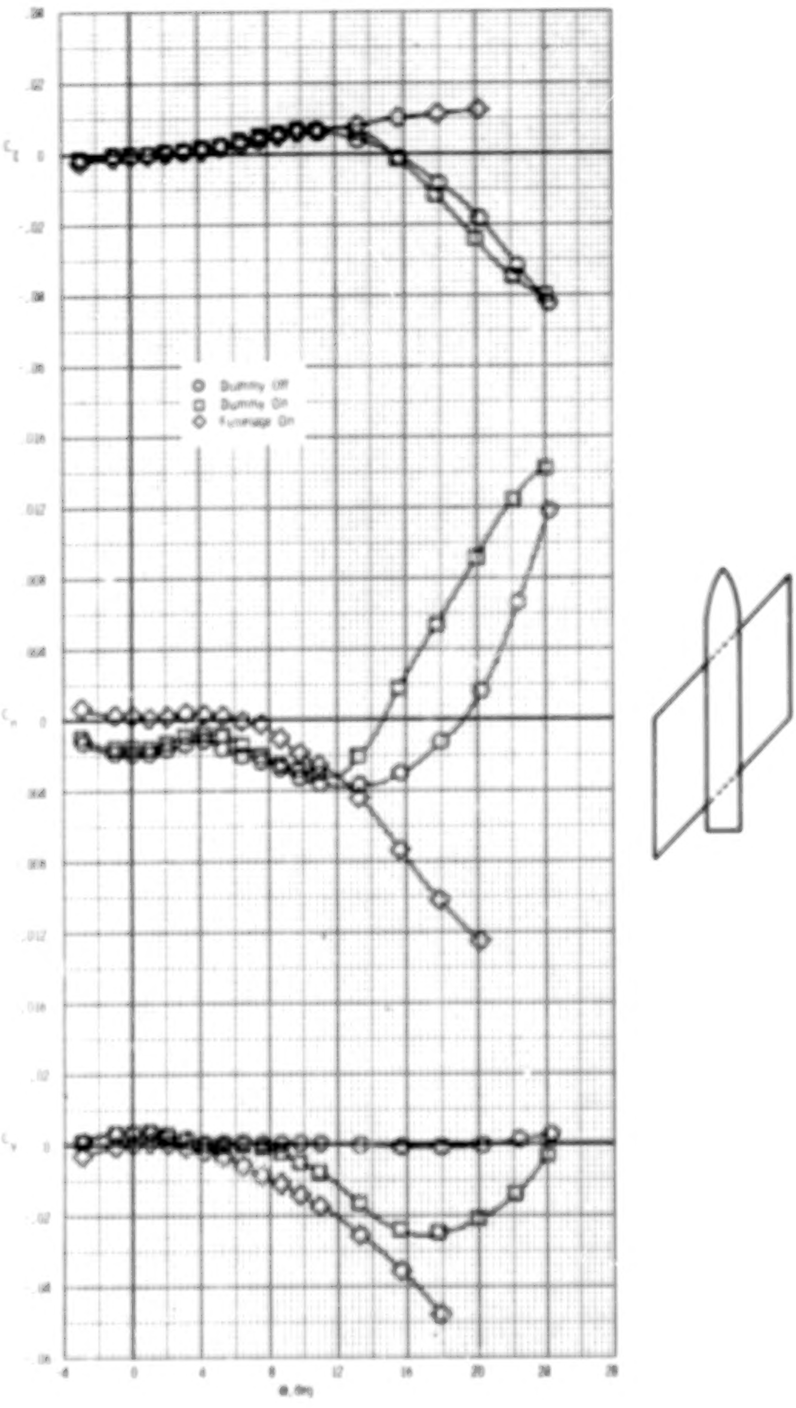

Figure 22.- Effect of cylindrical fuselage and dummy balance housing on lateral-directional aerodynamic characteristics of skewed wings. $\beta = 0^\circ$; $\Lambda = 45^\circ$; $A = 1.0$; $M_\infty = 0.12$.

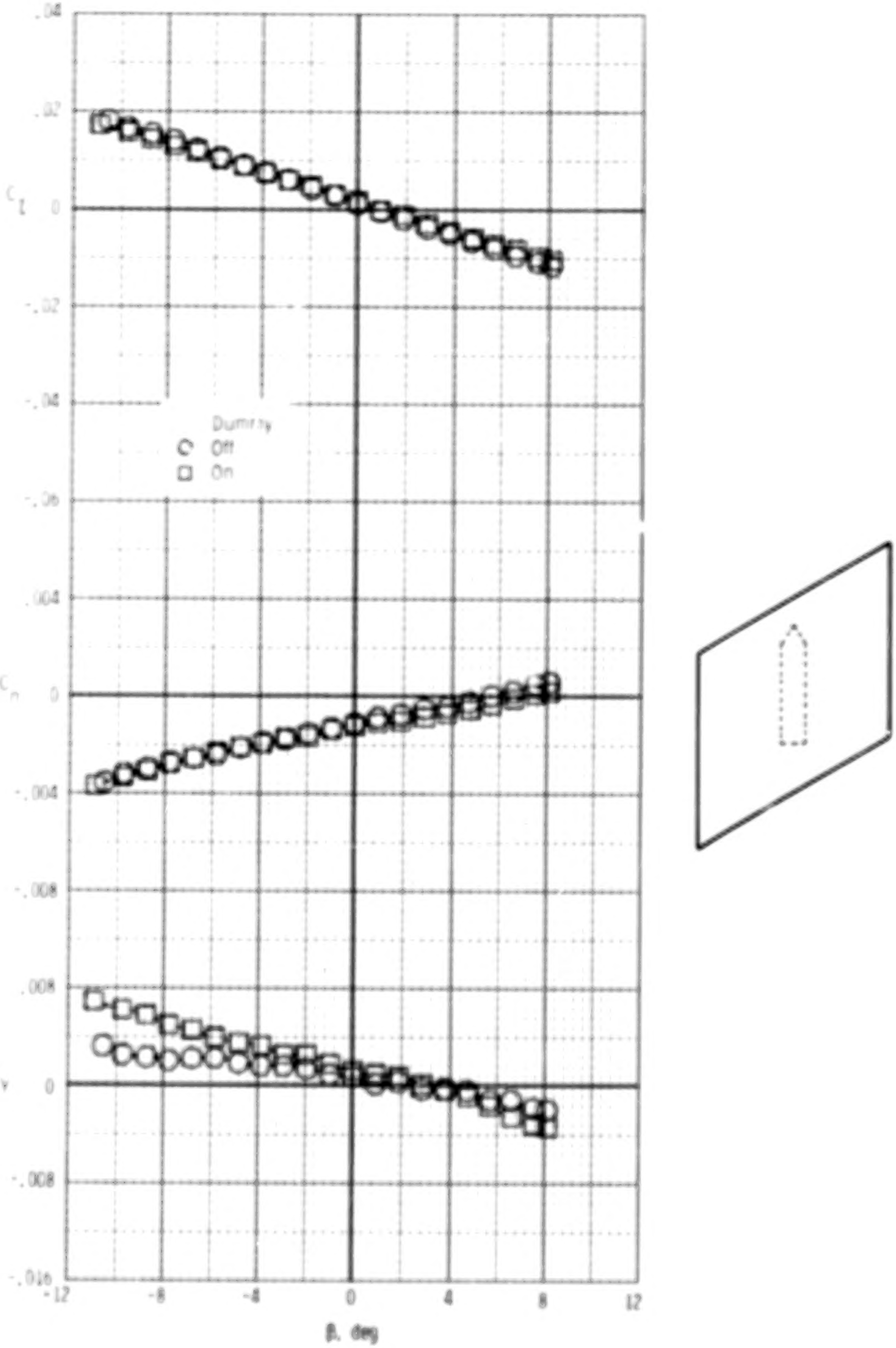

(a) $\alpha = 6^{\circ}$.

Figure 23.- Effect of sideslip angle and dummy balance housing on lateral-directional aerodynamic characteristics of skewed wings. $\Lambda = 30^{\circ}$; $A = 1.0$; $M_{\infty} = 0.12$.

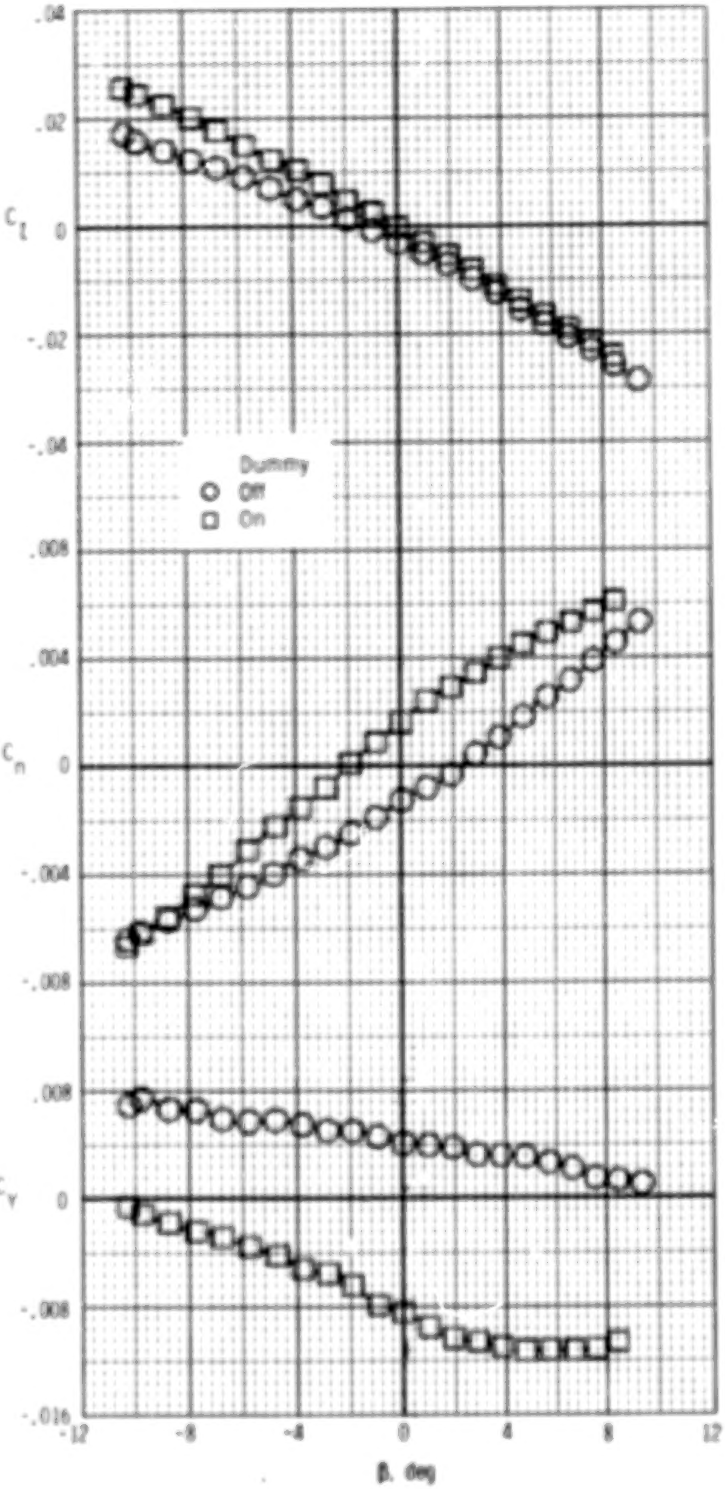

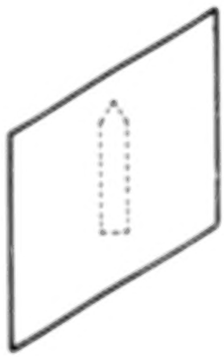

(b) α = 12°.

Figure 23.- Concluded.

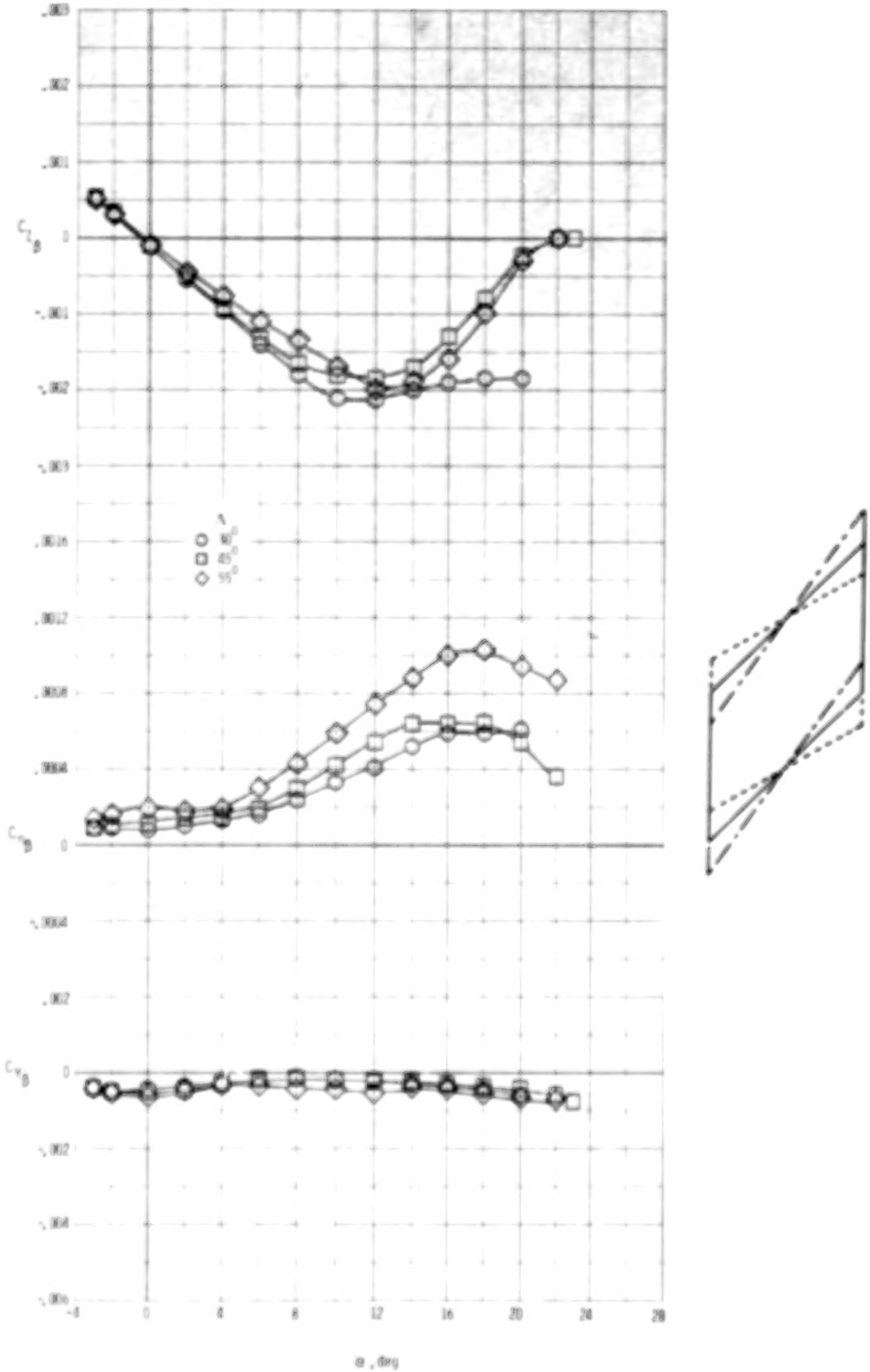

Figure 24.- Effect of leading-edge sweep on lateral-directional stability derivatives (calculated for 4° and -4° sideslip) of skewed wings. $A = 1.0$; $M_\infty = 0.12$.

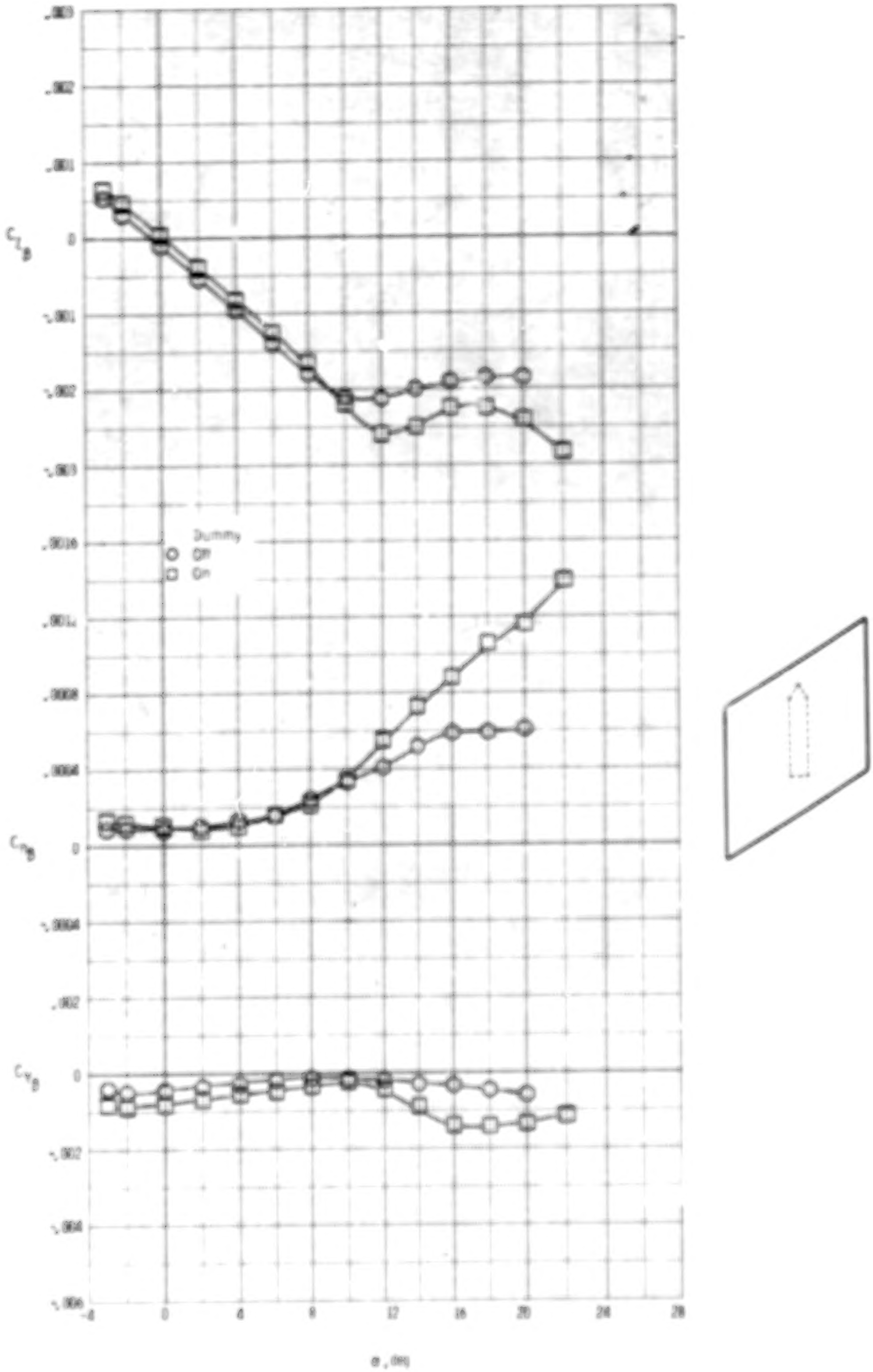

(a) $\Lambda = 30^{\circ}$.

Figure 25.- Effect of dummy balance housing on lateral-directional aerodynamic stability derivatives (calculated for 4° and -4° sideslip) of skewed wings. $A = 1.0$; $M_{\infty} = 0.12$.

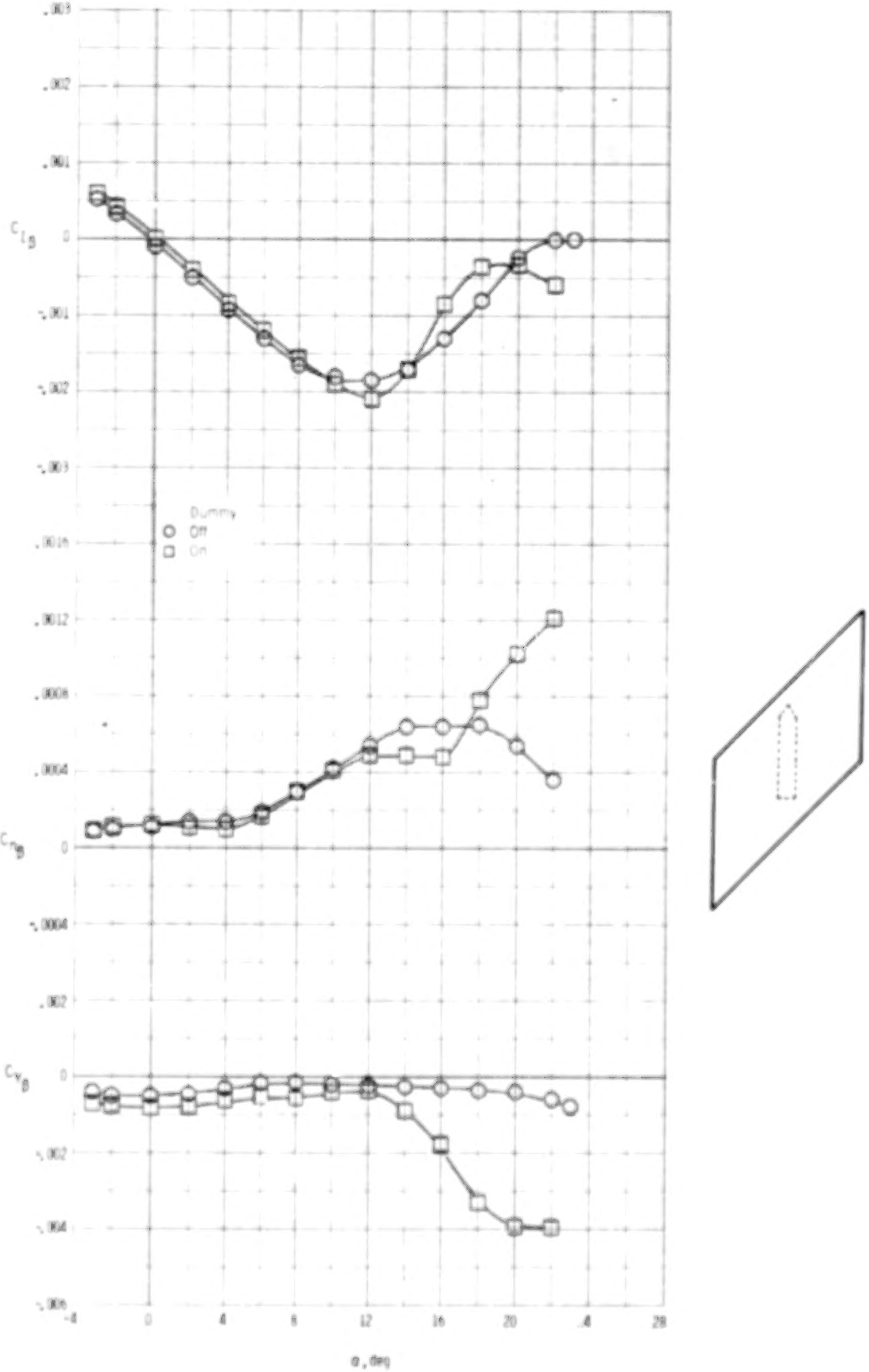

(b) Λ = 45°.

Figure 25.- Continued.

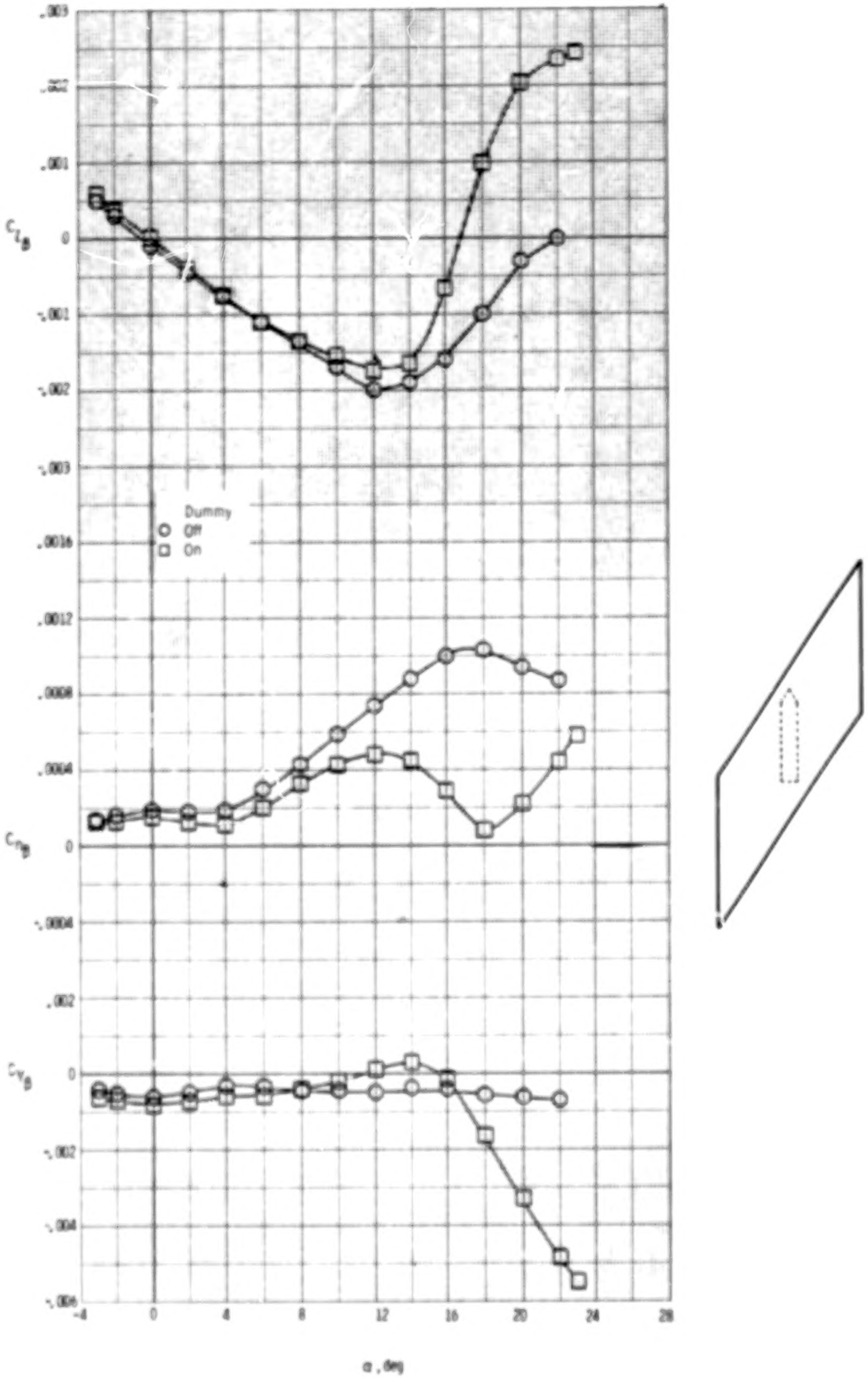

(c) Λ = 55°.

Figure 25.- Concluded.

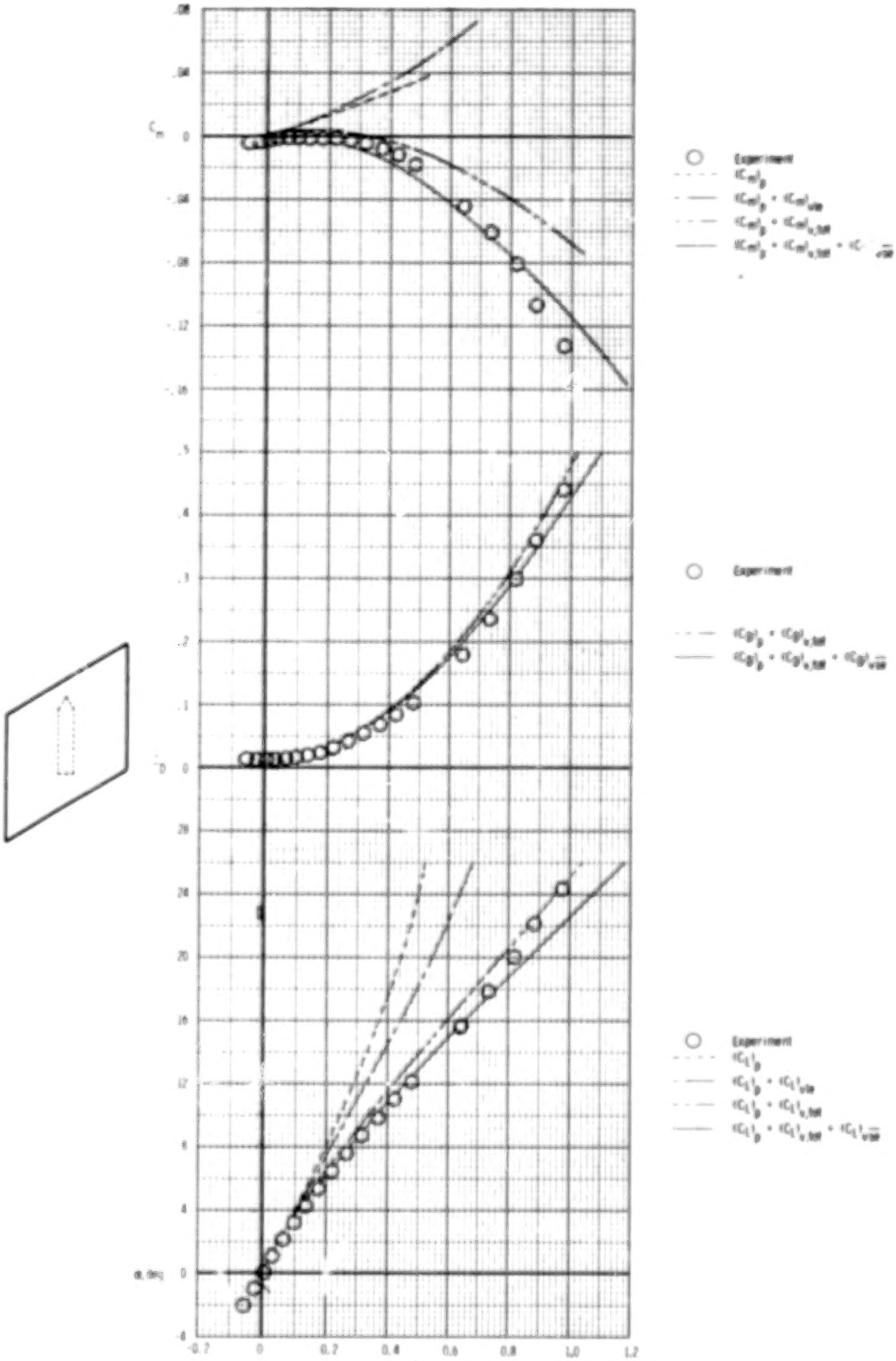

(a) $\Lambda = 30^{\circ}$, $A = 1.0$.

Figure 26.- Comparison of theoretical and experimental longitudinal aerodynamic characteristics of skewed wing. Dummy balance housing on; $M_{\infty} = 0.12$.

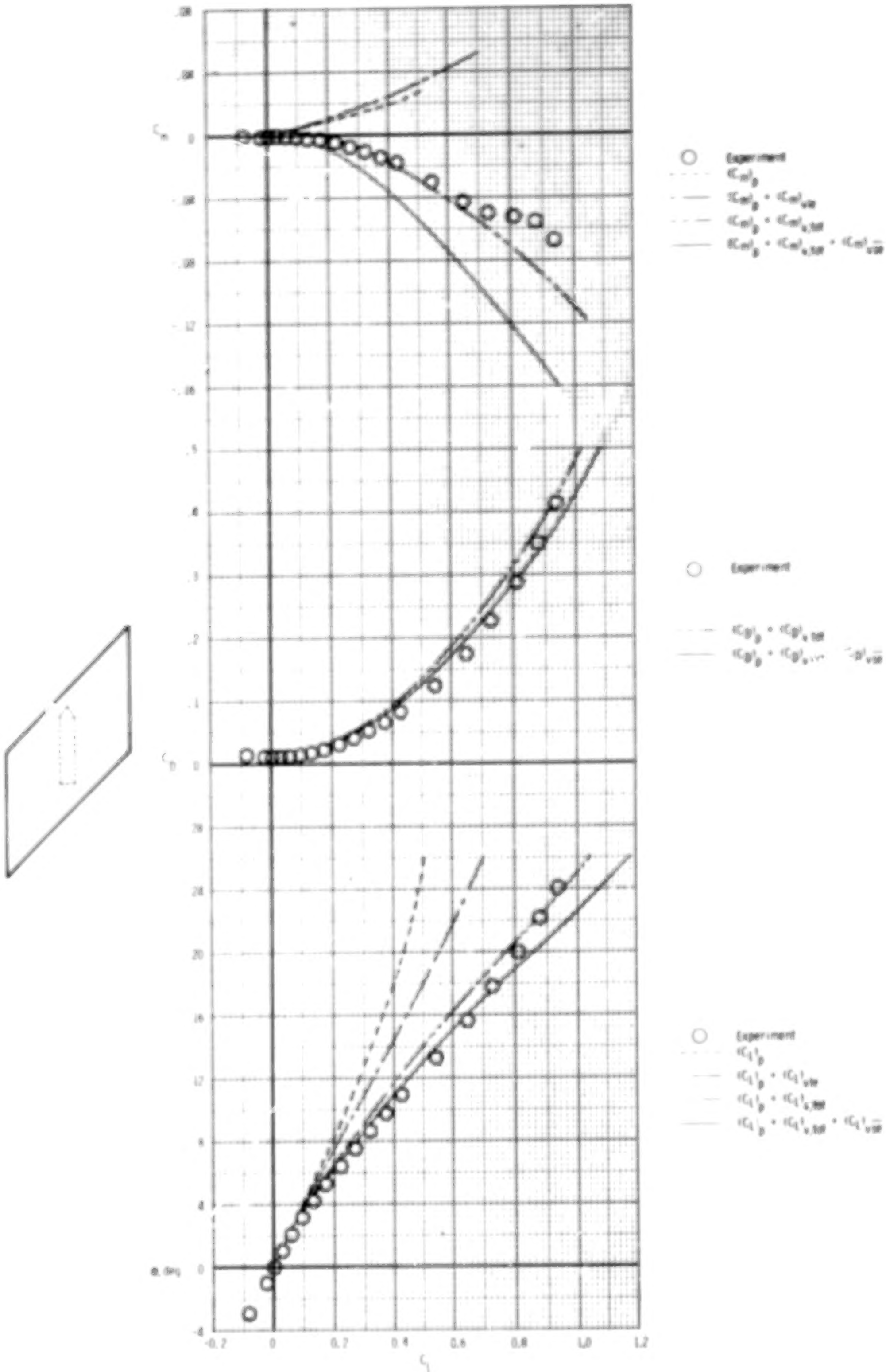

(b) $\Lambda = 45^{\circ}$, $A = 1.0$.

Figure 26.- Continued.

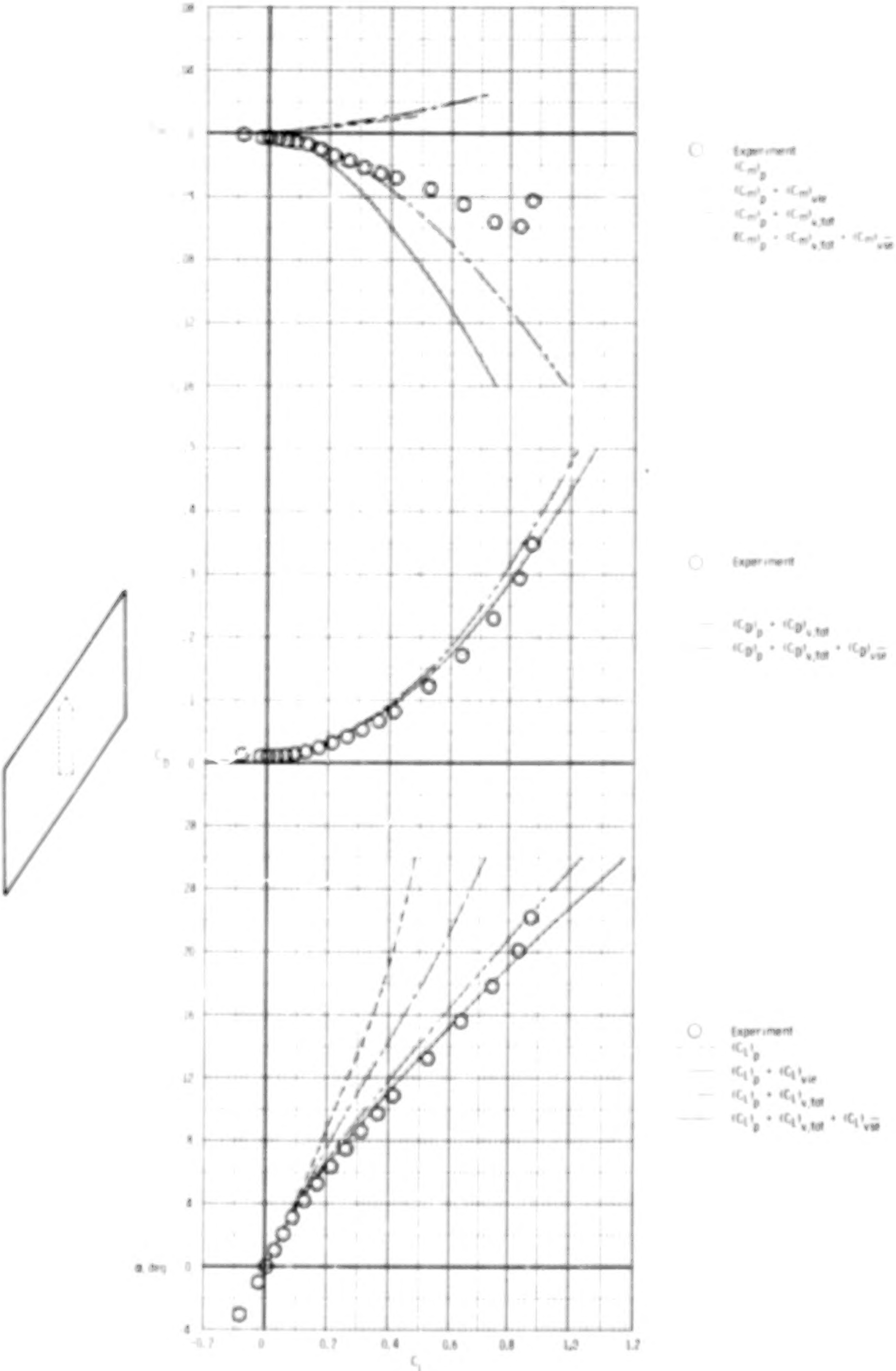

(c) Λ = 55°, A = 1.0.

Figure 26.- Continued.

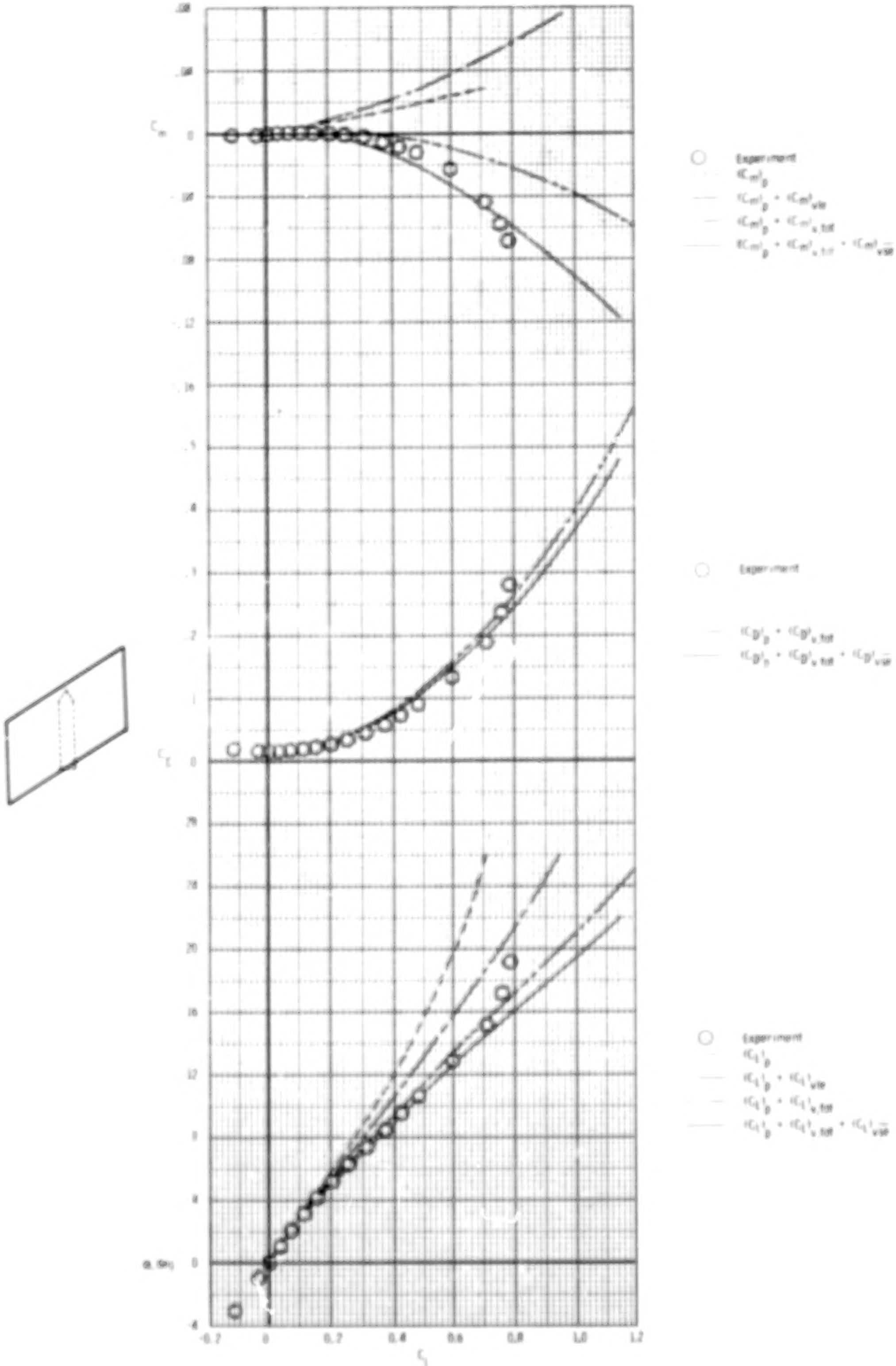

(d) $\Lambda = 30^{\circ}$, $A = 1.5$.

Figure 26.- Continued.

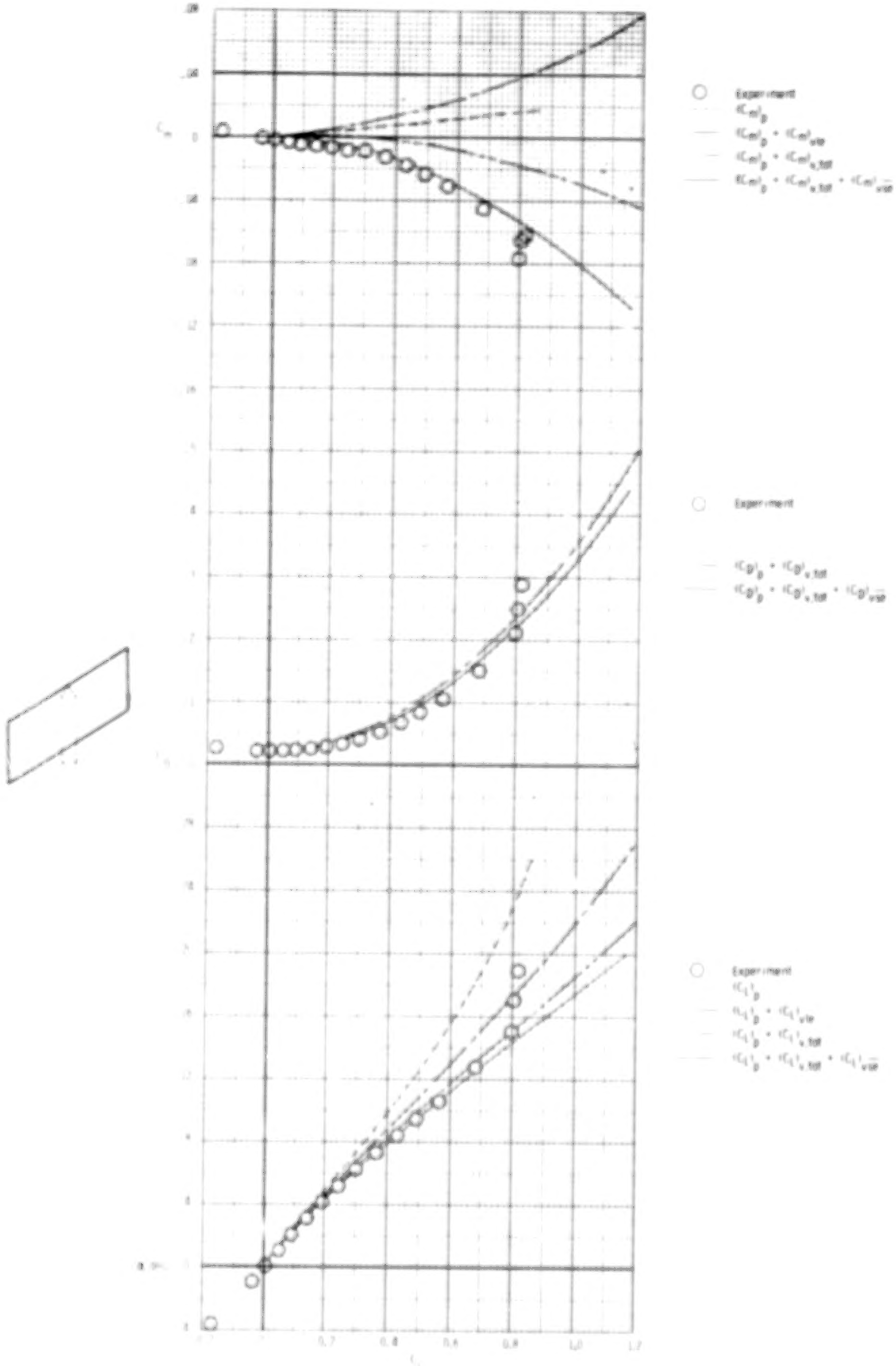

(e) $\Lambda = 30^{\circ}$, $A = 2.0$.

Figure 26.- Concluded.

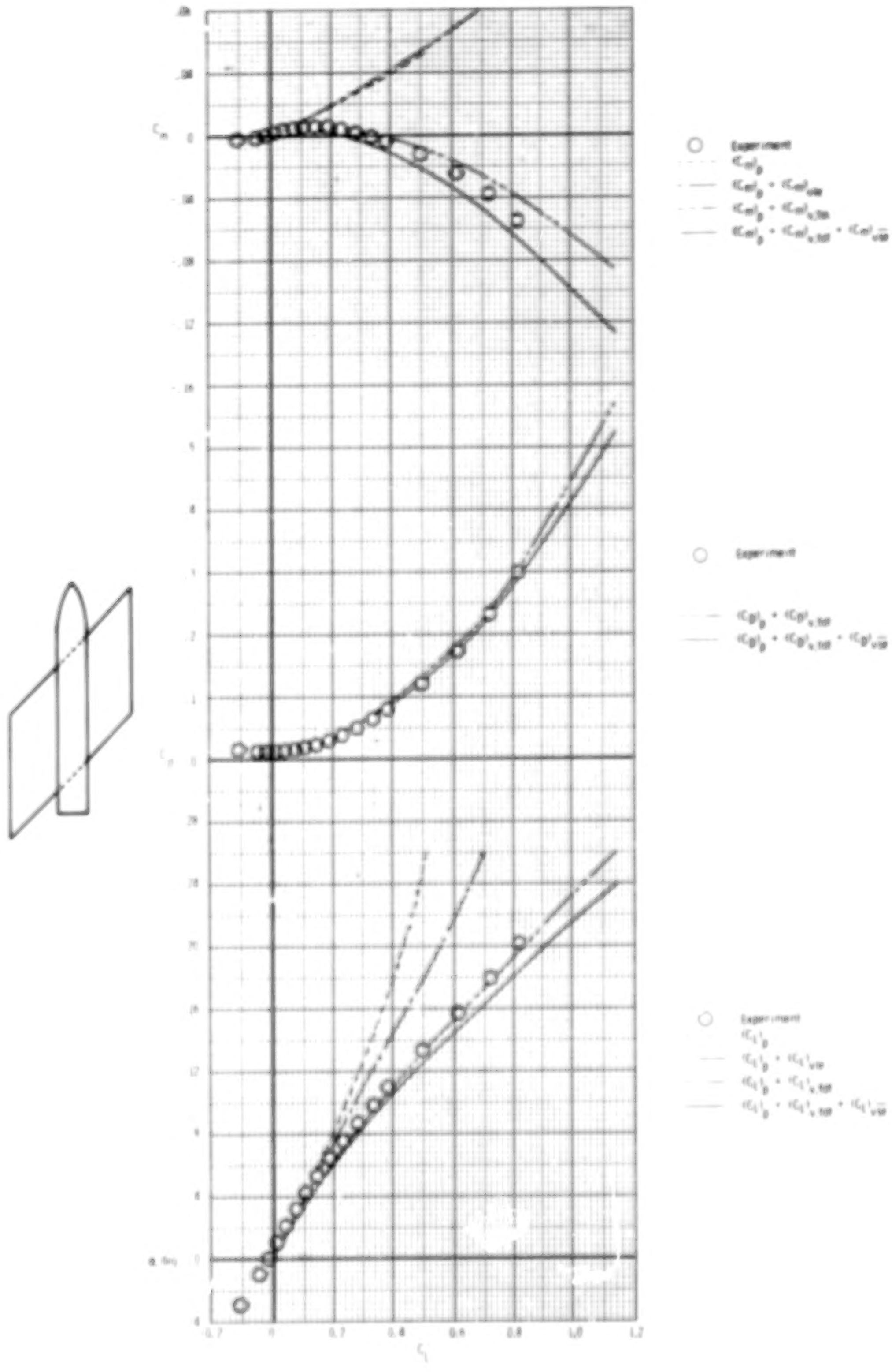

Figure 27.- Comparison of theoretical and experimental longitudinal aerodynamic characteristics for model VI. $\Lambda = 45^{o}$; $A = 1.0$; $M_{\infty} = 0.12$.

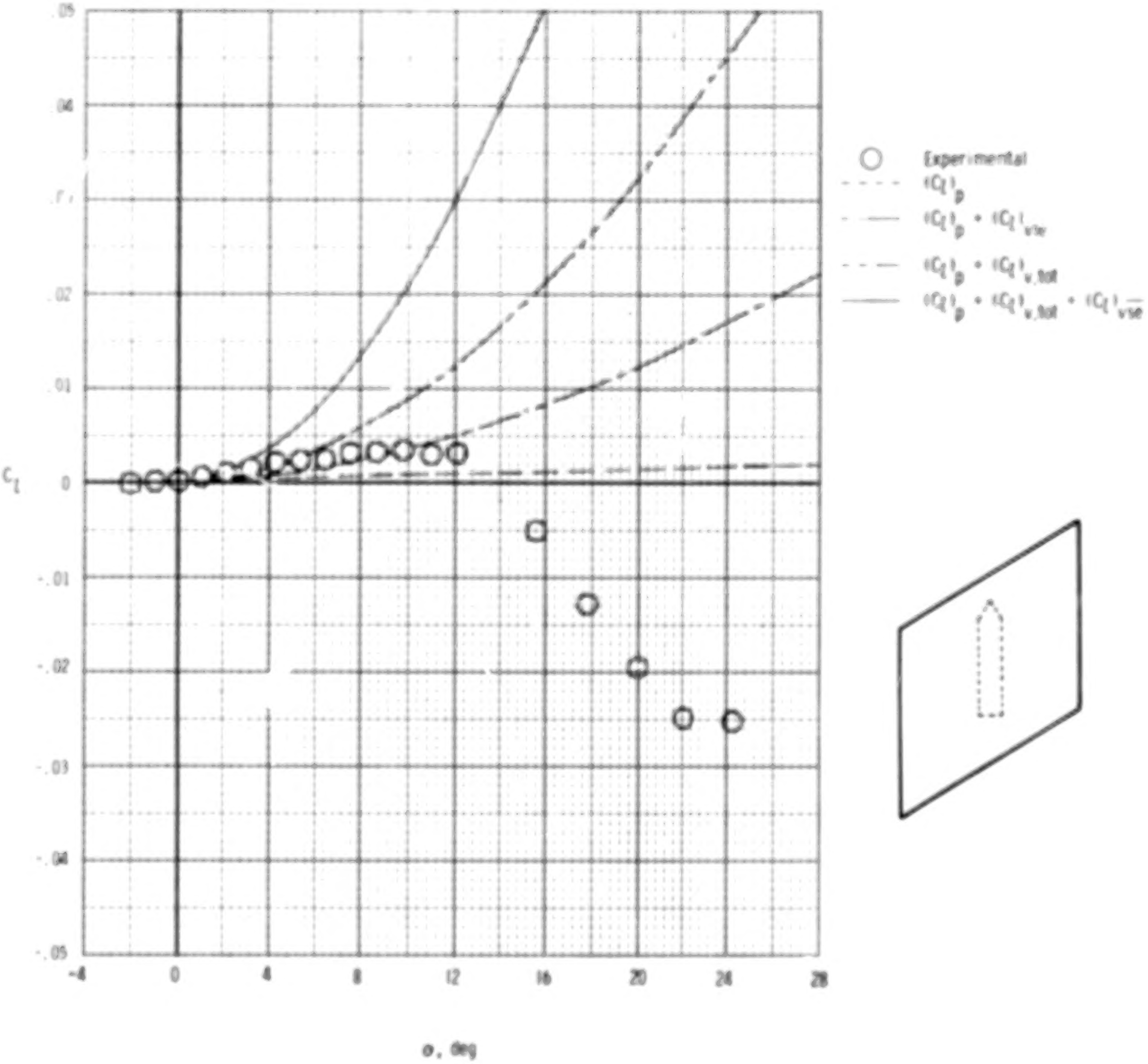

(a) $\Lambda = 30^{\circ}$, $A = 1.0$.

Figure 28.- Comparison of theoretical and experimental rolling-moment characteristics. Dummy balance housing on; $M_\infty = 0.12$.

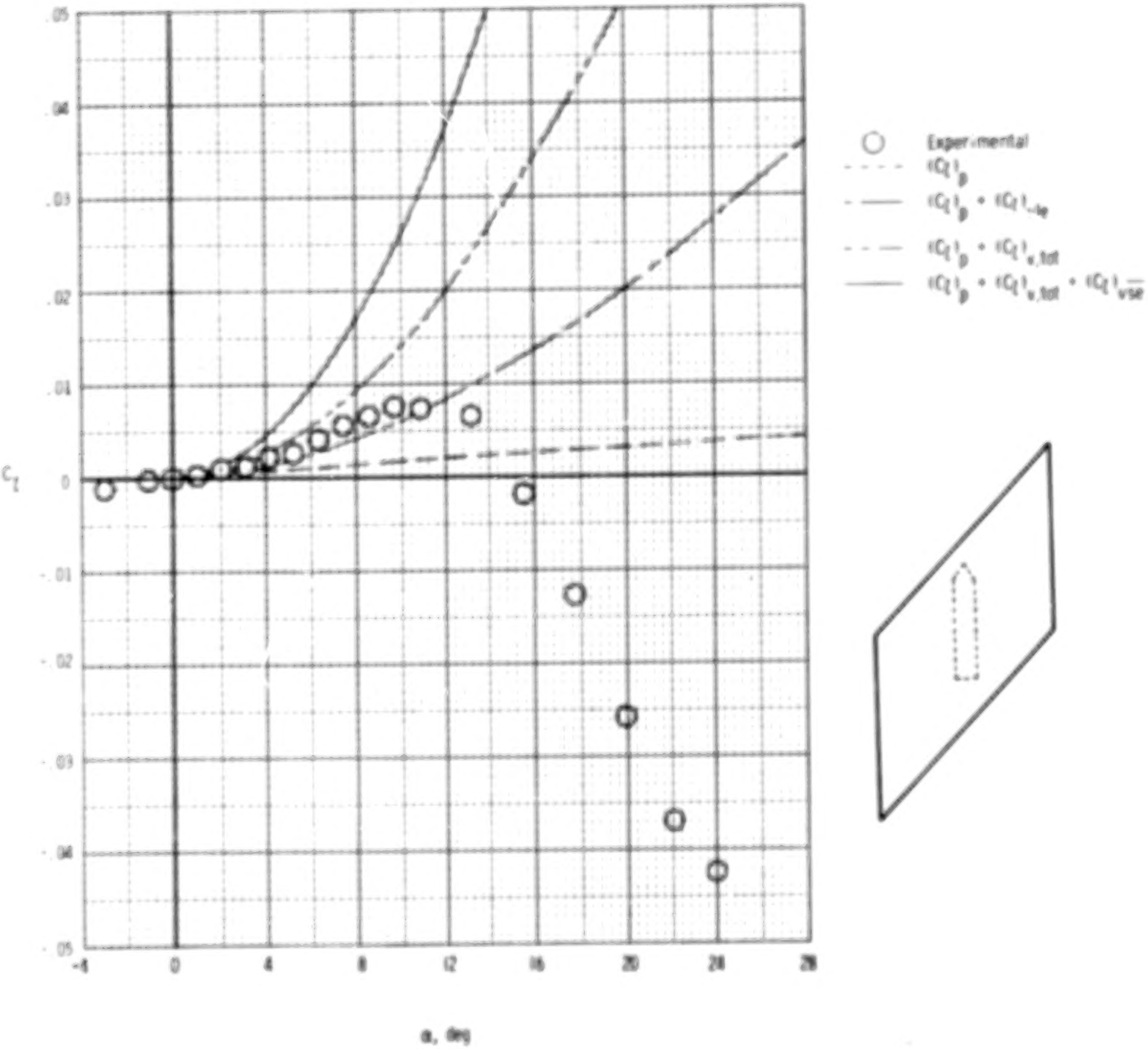

(b) Λ = 45°, A = 1.0.

Figure 26.- Continued.

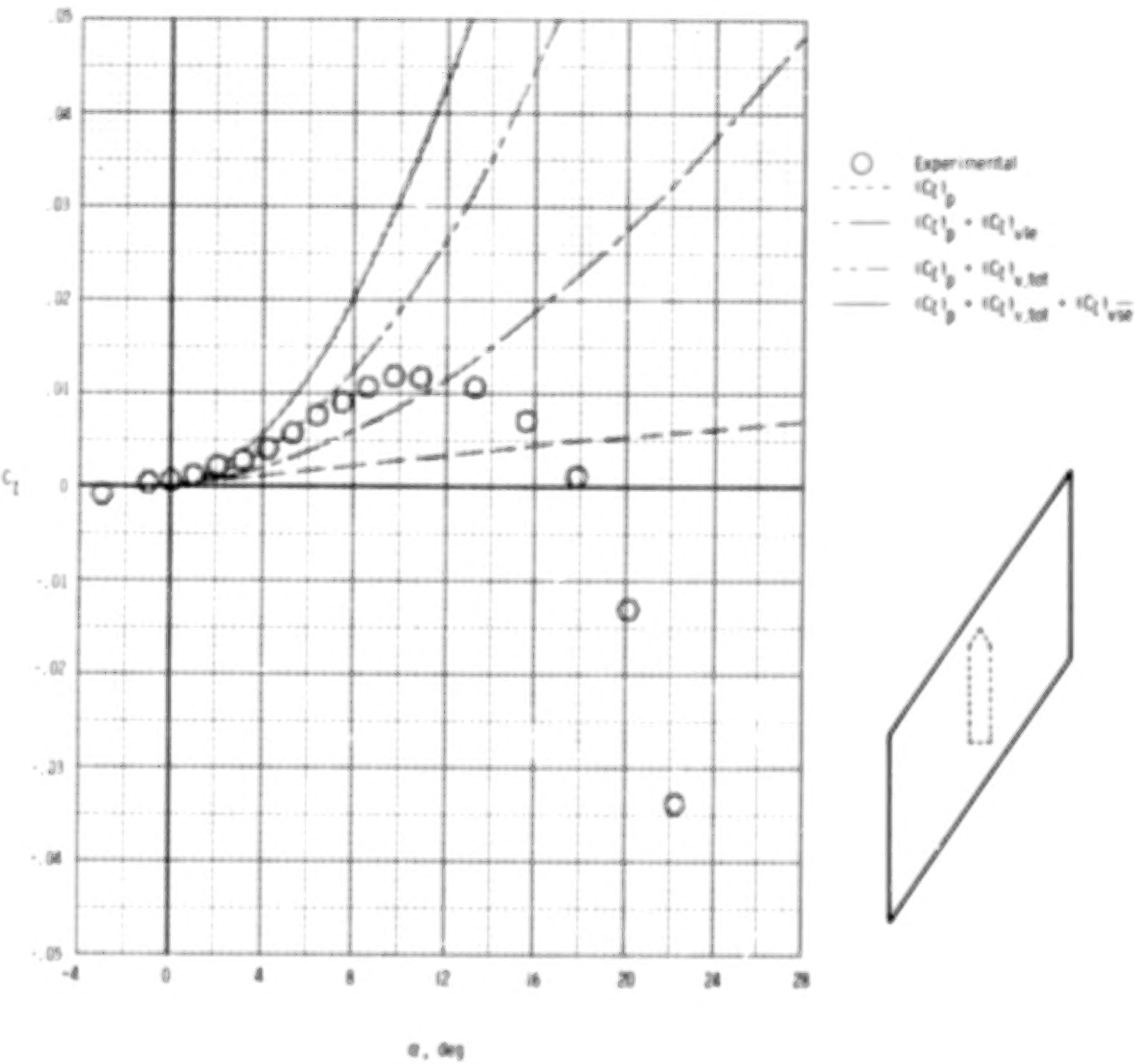

(c) $\Lambda = 55^{\circ}$, $A = 1.0$.

Figure 28.- Continued.

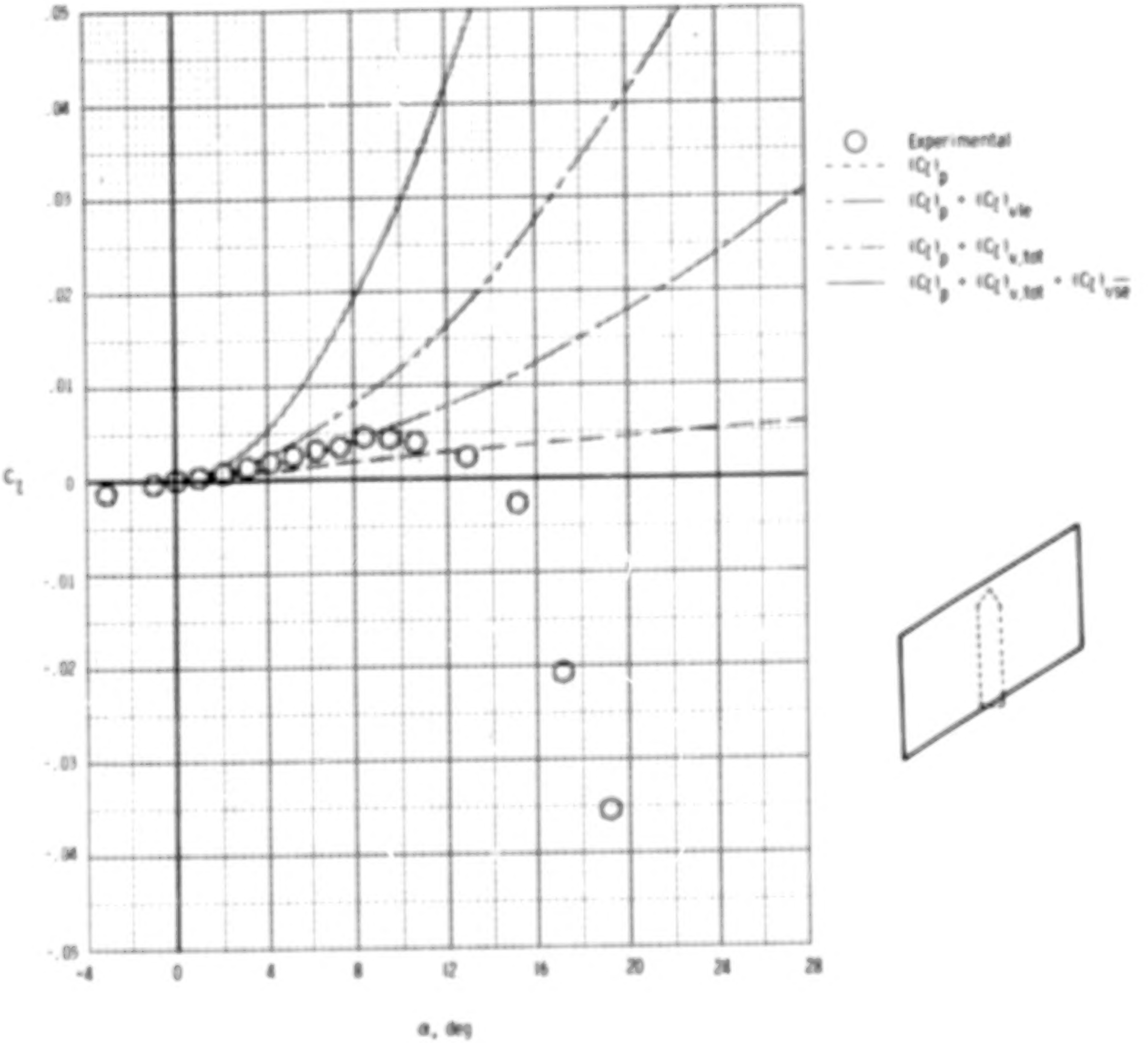

(d) $\Lambda = 30^\circ$, $A = 1.5$.

Figure 28.- Continued.

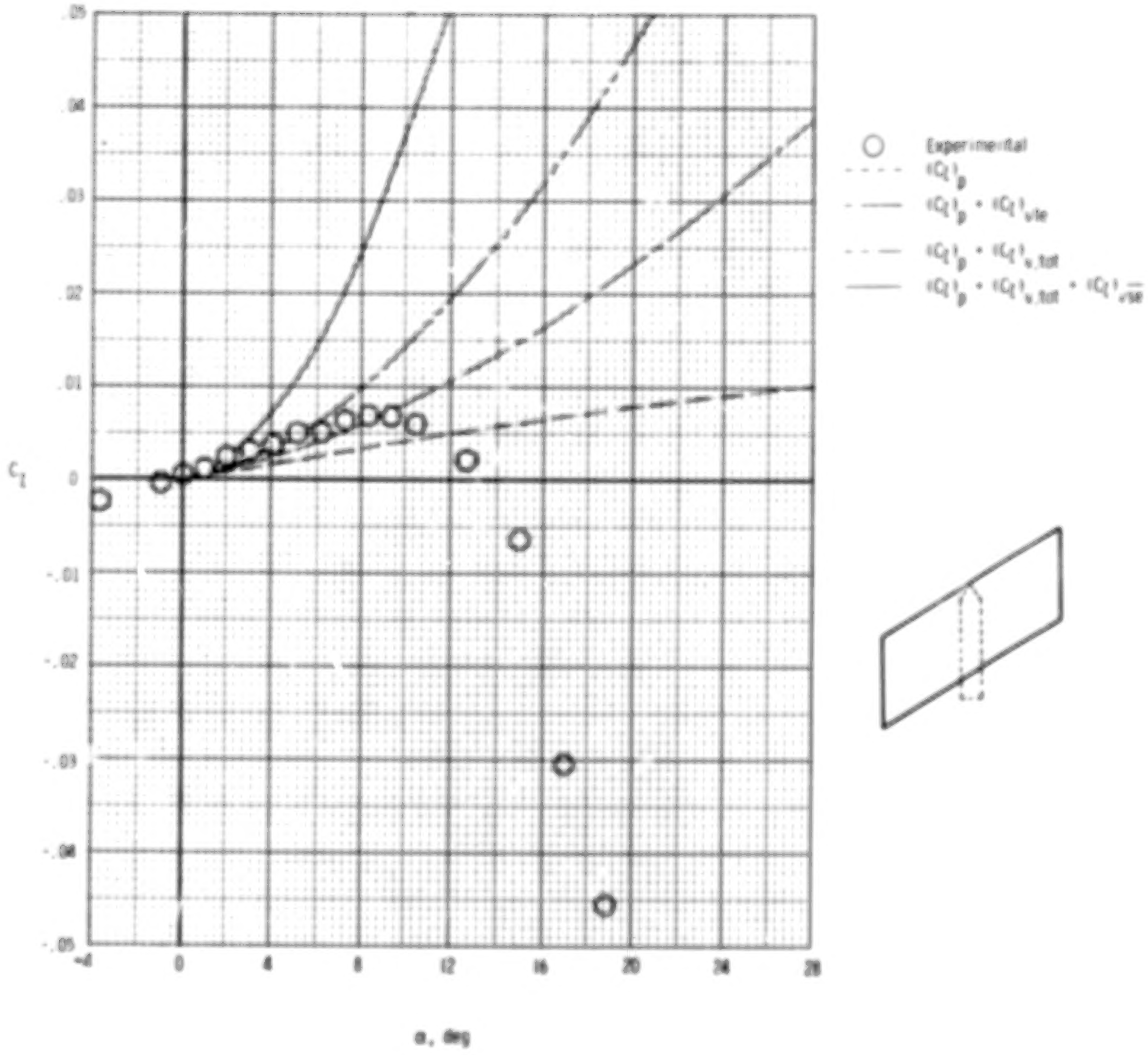

(e) $\Lambda = 30^{\circ}$, $A = 2.0$.

Figure 28.- Concluded.

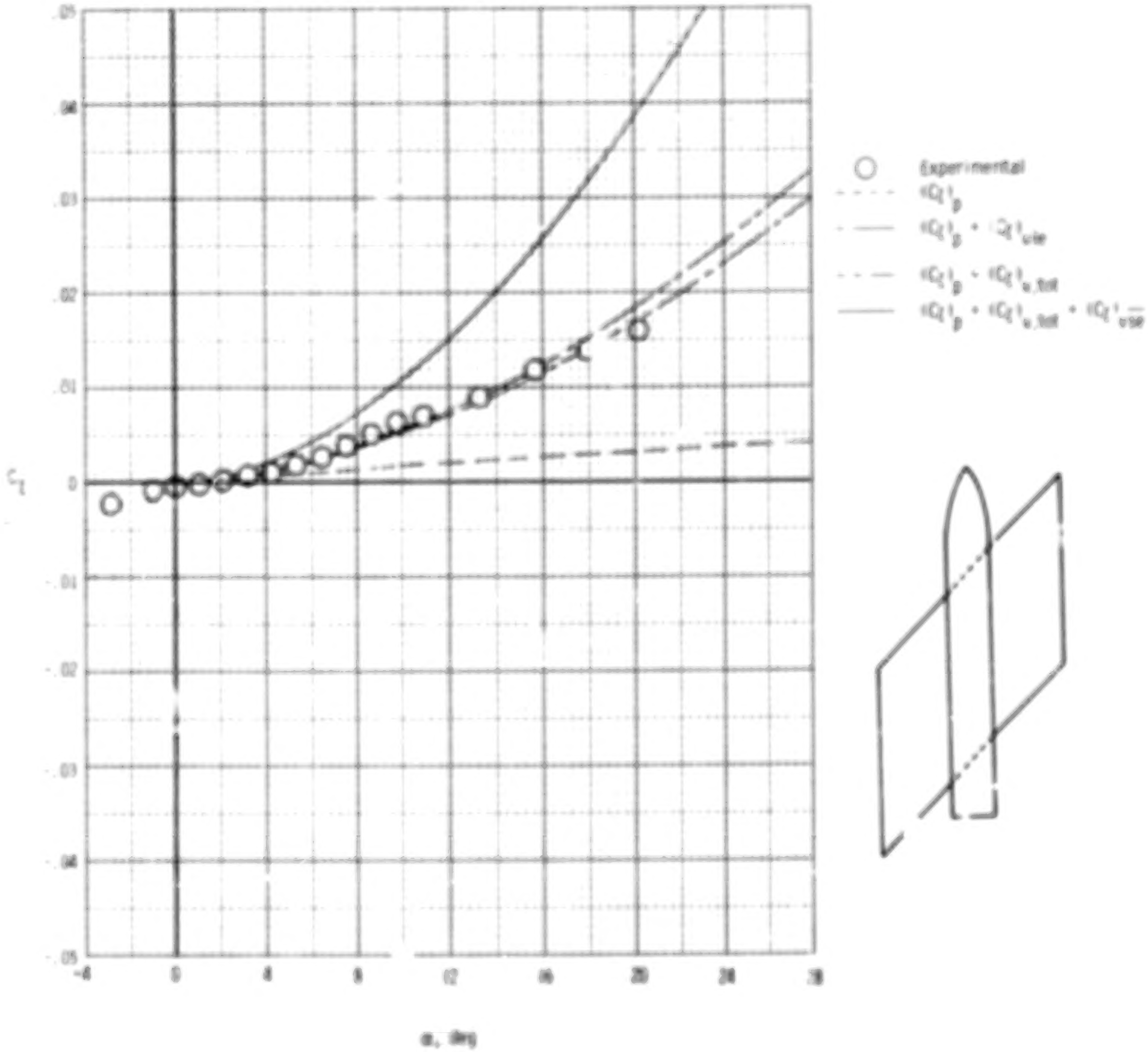

Figure 29.- Comparison of theoretical and experimental rolling-moment characteristics for wing-fuselage configuration. $\Lambda = 45^\circ$; $A = 1.0$; $M_\infty = 0.12$.

NASA-Langley, 1977 L-11230